Abstract

Anthropogenic and Natural Emissions of Mercury (Hg) in the northeastern United States

Jeffrey MacAdam Sigler
May 2006

Mercury (Hg) is a potentially dangerous contaminant. The public health impact may depend on the emission rate. Anthropogenic Hg emissions in the United States are poorly characterized. Natural Hg emissions are poorly understood worldwide, due to lack of data or measurement systems.

This study sought to enhance understanding of Hg emissions to the atmosphere, with emphasis on the northeastern U.S. The research focused on three areas: (1) anthropogenic Hg emission in the northeast, (2) gaseous Hg in soils, and (3) Hg emissions from forest fires.

In (1), measurements of Hg and carbon dioxide in Connecticut were combined to quantify regional Hg emission during 1999/2000 – 2003/2004. Emissions showed significant interannual variation. Trajectory analysis revealed a source region of Hg that showed little interannual variation, suggesting that annual changes in emission cannot be explained by climatology. Hg fluxes from the electric power sector were correlated with emissions derived from atmospheric measurements, illustrating the importance of regional power plant emissions. However, the power sector flux was lower than expected relative to the atmospheric measurement, suggesting that emissions from sources outside the power sector may be underestimated.

In (2), a flask sampling system for measuring gaseous Hg in soil was developed and deployed in background forest soil in Connecticut during 2003-2004.

This was the first detailed study of soil gaseous Hg. Observed gradients in soil gaseous Hg strongly resembled gradients in bound Hg. Soil Hg flux was correlated with gaseous Hg at 2-cm depth. The upper organic layers may act as a source of gaseous Hg that is emitted to the atmosphere. Gradients in gaseous Hg over shallow layers underscore the importance of fine vertical resolution, and therefore the utility of flask sampling.

In (3), measurements of Hg within a smoke plume from forest fires in Canada were used to determine mean Hg flux density for boreal forest fires, annual Hg emissions from Canadian fires and global Hg emissions from boreal fires. Annual Hg emissions from fires typically equal 30-100% of Canadian anthropogenic emissions. Hg emission from biomass burning is dependent on biome/species, so extrapolation from a single fire to the globe is speculative.

Anthropogenic and Natural Emissions of Mercury (Hg) in the northeastern United States

A Dissertation
Presented to the Faculty of the Graduate School
of
Yale University in Candidacy for the Degree of
Doctor of Philosophy

By
Jeffrey MacAdam Sigler

Yale School of Forestry & Environmental Studies
New Haven, Connecticut

Dissertation Director: Xuhui Lee

May, 2006

Table of Contents

Appendices

List of Tables

List of Figures

Acknowledgements

First and foremost, my thanks to Prof. Xuhui Lee, who served as my faculty advisor. He is a man of ideas, and I believe his greatest virtue is his patience. This has served me, and no doubt him, very well, as I knew nothing of the subject of mercury when I arrived at Yale. He has indulged – and hopefully somewhat lessened – my ignorance for 4+ years. Though probably a struggle for him, it was a great opportunity for me. I have been interested in science since I was a young boy, gazing at stars through binoculars in my backyard, but never once did I believe I would have an opportunity to actually study science from a novel perspective at a place like Yale.

Few people from Lynchburg, Virginia end up doing that. So, thanks to Xuhui for taking a chance on me and giving me this opportunity.

I also thank my two committee members, Thomas Graedel and Gaboury Benoit. I regret that my time here was too short, and my research perhaps too focused, to work with them a bit more closely. I took independent studies with both of them. Although the papers I turned in were probably met with something short of applause, I used them as an opportunity to simply learn more about Hg – this was highly valuable, as I knew nothing when I arrived at Yale. I took Gabe's course, "Biogeochemistry and Pollution," my first semester at Yale and it turned out to be among the most informative courses I have ever taken. I also specifically thank Tom for putting me in touch with some very helpful colleagues, notably Nik Themelis of Columbia University, and Gabe for very helpful suggestions during our Spring 2004 committee meeting which aided my ensuing field experiment tremendously.

Many additional people have aided this study in some way, and they are thanked in the acknowledgements in the individual chapters. I have to thank Professors Jose D. Fuentes and Michael Garstang of the University of Virginia for continued friendship and guidance, and for allowing me to gain experience in atmospheric studies as a masters student, and setting me on this path. I give special thanks to the Yale School of Forestry and Environmental Studies for financial aid for conference travel as well as a Yale Institute for Biospheric Studies fellowship. I also thank Elisabeth Barsa and Prof. Os Schmitz for really welcoming me to Yale, helping me get started in formulating a research prospectus, and in Elisabeth's case, always being available to answer any random question I've had since I've been here. I would be remiss in not singling out Prof. David R. Miller of the University of Connecticut. He not only allowed us to use his forest research site in Coventry, CT, for the soil Hg study, but even went out of his way to accommodate us in any way possible, whether it be towing stuck vehicles out of the mud or, most notably, opening up his home to me as a place to occasionally spend the night between site visits.

Many people have provided moral, and other, support during my time at Yale. I am thankful to have made some unforgettable friends in the FES program, including Hui-Ju Wu, David Ellum and Shane Duigan. Andrew Richardson and Ellen Denny befriended me when I arrived here and without them, I fail to see how I ever would have acclimated to Yale and New Haven. My parents, Janet and Julius Sigler, have gently but staunchly encouraged and supported my endeavors, whatever and wherever they may be, and although it sounds like a ridiculous cliché, I'd never have gotten here without them. And last but not least – no offense to the FES program, but the best thing to befall me during my time here was meeting the unexpected acquaintance of Veronica Brooks, now Veronica Brooks-Sigler. I am most grateful for her support, tolerance, encouragement and indulgence.

Chapter 1:

Introduction

Abstract

This chapter briefly outlines the role of Hg as an environmental contaminant, the status of knowledge of Hg emissions and some of the more important uncertainties in our understanding of global Hg emissions. The ecological and public health impacts of anthropogenic Hg emissions are briefly considered. A synopsis of the more important natural and anthropogenic sources of Hg in the United States is given, in addition to a source by source breakdown of anthropogenic in the northeastern U.S. The chapter concludes with an overview of the research problems and purposes of the study.

1.1. Introduction

During the 1950s, dumping of mercury-laden industrial waste into Minamata Bay, Japan, led to a public health disaster [*Kurland et al.*, 1960]. Since this seminal event, the role of mercury (Hg) as a highly toxic environmental pollutant has become of increasing concern to scientists and policymakers.

Annual global emission of anthropogenic Hg has been estimated at approximately 2200 Mg [*Poissant*, 1999] and may vary from 2000 to 4000 Mg [*Mason et al.*, 1994]. Worldwide geological data indicate that anthropogenic Hg emissions have increased dramatically relative to natural sources since the onset of the industrial revolution. After Minamata Bay, the direct disposal of Hg-laden waste into bodies of water was virtually eliminated in most developed countries. Still, bioaccumulation of Hg to alarmingly high levels in aquatic and terrestrial environments has persisted in many ecosystems, even those far-removed from industrial sources.

Elemental Hg (Hg^0) makes up the bulk of the background global atmospheric concentration of Hg (~98%), is not readily absorbed by bare terrain, water or vegetation, has a residence time in the atmosphere of 0.5 – 2 years [*Munthe and McElroy*, 1992] and can therefore be transported over long distances [*Lindqvist and Rodhe*, 1985; *Bullock*, 2000b]. Long-range transport and eventual deposition of Hg emitted into the atmosphere by anthropogenic means is believed to be the primary culprit of the high levels of Hg which have been observed in aquatic environments, even in remote areas [*Mason et al.*, 1994; *Fitzgerald et al.*, 1998; *Allan*, 1999; *Mason et al.*, 2000]. Daytime turbulent mixing in the boundary layer may carry Hg emitted from point sources at the Earth's surface to the deeper troposphere, and thence potentially across the globe. Subsequent vertical mixing and transformation processes lead to deposition in remote areas far from the point source [e.g., *Xu et al.*, 2000b].

Hg can be considered both a global and local pollutant, as local or regional-scale impacts from anthropogenic point sources are also of concern. The oxidized forms of Hg – generally referred to as Reactive Gaseous Mercury (RGM) and comprised primarily of divalent Hg (Hg^{2+}), are generally believed to have a residence time of a few days or less. Particulate forms of Hg (Hg_p) are equally short-lived in the atmosphere [e.g., *EPA*, 1997]. This is attributable to the high solubility of these species, making them more susceptible to removal from the atmosphere via wet deposition [*Lindberg and Stratton*, 1998]. RGM is likely to be deposited to the surface within 1-10 km of its emission source [*Lindqvist and Rodhe*, 1985].

RGM that is wet-deposited locally or regionally is perhaps of highest concern for public health. Wet-deposited Hg tends to be almost exclusively Hg^{2+} [*Lindberg and Stratton*, 1998], particularly in areas with a high density of coal and waste combustion sources which emit a high percentage (likely greater than 50%; [*EPA*, 1997]) of RGM, as in the northeastern United States [*Xu et al.*, 2000b]. Quantifying the rate of local or regional-scale emissions and tracking the degree to which they may change over time is therefore critical to gauging the regional public health impact as well as the impact of legislation implemented to minimize risk.

1.2. Ecological and public health impacts of Hg emissions

Mercury has gained attention in both the environmental sciences and the public policy sphere because of its potentially negative environmental and public health impacts. Birds and mammals may experience reproductive failure, impaired growth and development or even death from Hg exposure. Impacts on vegetation include leaf and root injury, decreased chlorophyll content and inhibition of growth. Of particular concern to humans is the neurotoxicity of methyl Hg, which readily passes into the bloodstream, brain or through the placenta upon ingestion. Hg is present in water primarily as inorganic Hg^{2+}, but is often converted to methylated forms by sediment bacteria [*EPA*, 1997]. Most methyl Hg in aquatic systems is produced in situ, with atmospheric Hg from deposition serving as a substrate for methylation [*Fitzgerald et al.*, 1991; *Mason et al.*, 1994; *Mason et al.*, 2000]. The methylated forms, particularly the more toxic monomethyl Hg, are highly bioaccumulated and account for most of the Hg content in fish [*Fitzgerald*, 1989], which assimilate Hg both directly from the water through gills, and through ingestion of food. Consistent ingestion of methyl Hg by humans in excess of a reference dose of $0.1\ \mu g\ kg_{bw}^{-1}\ day^{-1}$ may cause brain damage, as well as damage to the liver, kidneys, pancreas and central nervous system (i.e., impairment of motor skills and sensory ability). Ingestion of mercuric salts can cause damage to the intestinal tract, liver and kidneys [*EPA*, 1997].

Fish consumption is the dominant Hg exposure pathway for humans and some studies have suggested a plausible link between anthropogenic emissions of Hg and methyl Hg levels in fish [e.g., *Kehrig and Malm*, 1999]. Hg advisories for fish consumption have been issued in 45 U.S. states [*EPA*, 2004] and between one and three percent of women of child-bearing age in the U.S. are at risk of methyl Hg exposure from fish consumption [*EPA*, 1997].

Impacts of anthropogenic Hg emissions vary regionally. Currently, Hg emission in the northeastern U.S. is of high concern since this region had the highest Hg emission rate in the country according to the EPA inventory assessment released in 1997 [*EPA*, 1997; *Pai et al.*, 1998] and may therefore experience a high level of Hg-related environmental stress. Analytical methods for determining Hg emissions and extrapolating them to a regional scale are controversial and sensitive to speciation of Hg within emission plumes.

The severity and extent of environmental and human health impacts of Hg emission is currently difficult to assess, as it may depend on the regional emission rate and chemical form of the emitted species. Estimates of Hg emission are most commonly obtained using the inventory approach, which combines an emission factor (a mass of Hg emitted per mass of fuel burned) with a facility-specific operating, or firing, rate. The most recent, thorough and best assessments of anthropogenic Hg emissions in the United States used the inventory approach [*EPA*, 1997; *Pai et al.*, 1998; *Pai et al.*, 2000 (for all of North America)]. Inventory data are often incorporated in modeling studies of atmospheric Hg transport and deposition to land and water. Results of these studies show that the regional health impact of Hg deposition is extremely sensitive to the emission rate [*EPA*, 1997; *Bullock et al.*, 1998; *Bergen et al.*, 1999; *Xu et al.*, 2000a/b].

Because prolonged or acute Hg exposure can pose great risks to human, plant and animal health, and the health risk is dependent upon the regional emission rate, accurate and timely characterization of temporal trends in atmospheric Hg, its emission rate, as well as spatial variability of emissions are critical. This is especially true in the northeastern United States, which is not only characterized by a high anthropogenic emission rate (50-75% of total Hg emissions may be anthropogenic according to *Xu et al.*, [2000b]), but more than 90% of anthropogenic emissions is contributed by combustion sources that emit a high percentage of oxidized Hg [*EPA*, 1997].

1.3. Overview: Sources of atmospheric mercury in the United States

This section provides a brief overview of the most important anthropogenic and natural sources of Hg emission in the United States. The 1997 Mercury Study Report to Congress [*EPA*, 1997] is the most up-to-date study of anthropogenic Hg emissions and source strengths in the United States. However, Hg emissions from most major source categories have proven difficult to determine, and the state-of-the-science for Hg is rapidly evolving. The 1997 report to Congress was subject to substantial uncertainty in emission factors for certain source types, as EPA claimed an accuracy of only ± 30% for the estimated anthropogenic emission of Hg in the U.S. This is primarily due to the lack of extensive and reliable data on emission factors [*EPA*, 1997] as well as the varying Hg content in various fuels and the large number of diffuse sources [*Sloss*, 1995]. Nonetheless, the report to Congress is the most comprehensive compendium of Hg emissions in the U.S. to date and much of the specific information on anthropogenic Hg emissions in this section was gathered from that document.

1.3.1. Natural sources of Hg

Mercury vapor may be emitted naturally by the volatilization of (primarily elemental) Hg from soils, water, vegetation and rocks. The total contribution of natural source emissions to atmospheric Hg concentrations is not known with certainty, although it is believed that they amount to approximately 2000-3000 Mg annually [*Nriagu*, 1989; *Mason et al.*, 1994; *Schroeder and Munthe*, 1998] and may comprise anywhere from 40 to 67% of total, global Hg emissions to the atmosphere [*Mason and Sheu*, 2002 and references therein]. Oceanic sources of Hg (i.e., evasional flux from the sea surface) are thought to comprise the majority of the natural Hg budget [*Fitzgerald*, 1989]. Other natural sources include geothermal emissions of gaseous or particulate Hg (i.e., volcanoes), entrainment of dust by wind, and forest fires. Typically, these processes contribute little to the global atmospheric load of Hg but are highly stochastic (volcanic activity could account for up to 50% of global natural emissions during a geologically active year).

In terrestrial systems, the most important natural source of Hg is typically emission from soils. However, several recent studies have shown that emissions from biomass burning are more significant than previously believed. An overview of those sources is provided in this section.

1.3.1.1. Soil mercury emission

Recent studies suggest that natural flux of Hg from soil, especially from naturally enriched substrates, may be more important than previously believed [*Gustin and Lindberg*, 2000; *Engle et al.*, 2001; *Coolbaugh et al.*, 2002]. Background Hg flux from temperate forest soils in the southeastern U.S. has been estimated at approximately 7 ng

m^{-2} h^{-1} [*Kim et al.*, 1995; *Carpi and Lindberg*, 1998]. Hg fluxes from slightly contaminated open field soils in the southeastern U.S. may range from 12 to 45 ng m^{-2} h^{-1} [*Carpi and Lindberg*, 1998]. Fluxes from naturally enriched substrates may range from 13 to 19 ng m^{-2} h^{-1} [*Engle et al.*, 2001; *Engle and Gustin*, 2002], and fluxes from contaminated floodplain soils may be as high as 43 ng m^{-2} h^{-1} [*Wallschläger et al.*, 2001]. In background soils, fluxes are typically in the range of 1-3 ng m^{-2} h^{-1}. However, this estimate is based on a very small number of studies [*Schroeder et al.*, 1989; *Poissant and Casimir*, 1998; *Zhang et al.*, 2001] which represent our knowledge of Hg emission from background soils. Currently, no estimates exist for natural Hg fluxes from background soils in the northeastern U.S.

Although soil Hg flux is known to correlate positively with soil temperature, wind speed, vertical mixing in the boundary layer, the soil-air TGM gradient and negatively with soil moisture [e.g., *Kim et al.*, 1995; *Gillis and Miller*, 2000a], little is known of the dynamics of gaseous Hg in soils, the location of desorption sites of Hg within the soil profile, and the mechanisms that control desorption and ultimate release from the surface. This is a key shortcoming as the pool of available gaseous Hg within the soil is obviously an important component in the overall soil emission process, and is ultimately owed to the lack of a widely accepted measurement system.

In order to assess with certainty the contribution of natural sources to atmospheric Hg concentrations, accurate means of measuring natural fluxes are needed. A number of methods have been used to quantify natural flux of Hg from soils. Among these are micrometeorological methods [*Kim et al.*, 1995; *Poissant and Casimir*, 1998] and, more commonly, various types of field flux chambers (*Carpi and Lindberg*, 1998; *Gustin and*

Lindberg, 2000; *Coolbaugh et al.*, 2002; *Engle and Gustin*, 2002; *Lindberg et al.*, 2002; *Zhang et al.*, 2002].

The most common micrometeorological approach for determining natural Hg flux is the Modified Bowen Ratio (MBR) technique, which is designed to overcome the limitation of the eddy correlation method that fast response sensors must measure the contribution of all eddies to the flux [*Kim et al.*, 1995]. The MBR method assumes that if the gradient (ΔC_1) and flux (F_C) of a reference scalar are known, the flux of any other (F) can be determined from the gradient of that constituent over the height interval (ΔC_2):

$$F = \frac{F_c}{\Delta C_1} \Delta C_2 = K \Delta C_2 \qquad [1.1]$$

where K is the eddy diffusivity. To determine Hg flux with the MBR method, *Kim et al.* [1995] measured at two heights (25 cm and 165 cm) and used CO_2 (flux measured by eddy correlation with a sonic anemometer) as the reference constituent.

Flux chambers do not require the experimental effort and monetary expense of micrometeorological methods, and have lower detection limits [*Wallschläger et al.*, 2002]. Chambers are typically made of plexiglass or Teflon and are rectangular (~0.6 × 0.2 × 0.2 cm). As a general description of the experimental approach for using flux chambers, the open-bottom container is first placed over the soil and sealed. Six to nine holes (~2 cm) are drilled into the sides to maintain ambient conditions inside the chamber. A Teflon tube connected to a T-junction is connected to a port at the exhaust end of the chamber. Two tubes emanate from the T-junction, one leading to a small pump (1-10 l min-1) and the other leading to a mercury vapor analyzer via a 3-way valve. A Teflon tube also leads from this valve to the inlet end of the chamber, so that the Hg gradient (ΔC) between the inlet and outlet of the chamber is measured. Soil Hg flux (F) is calculated as

$$F = R\left[\Delta C\right]A^{-1} \qquad [1.2]$$

where R is the rate at which air is drawn through the chamber and A is the surface area of the soil inside the chamber.

No single method is explicitly endorsed by the scientific community. Flux chambers are subject to a range of potential errors, most notably uncertainty regarding the appropriate airflow rates through the chamber and effects of ambient wind exposure which underestimate flux [*Gillis and Miller*, 2000b]. Flux chamber estimates may be approximately 3 times lower than those derived with micrometeorological methods, and co-located flux chambers of different type may produce fluxes that differ by an order of magnitude. Ideally, research efforts should be directed towards developing methods and equipment that will measure fluxes that are more comparable to those derived using micrometeorological methods [*Gustin and Lindberg*, 2000].

1.3.1.2. Hg emission from biomass burning

Hg is emitted naturally by forest fires. Two recent studies, one of a mixed-vegetation fire in the southern Cape Peninsula in Africa by *Brunke et al.* [2001] and the other of a temperate forest fire in southern Ontario [*Friedli et al.*, 2003] suggest that Hg emissions from biomass burning may be a much more significant pathway of Hg exchange between the biosphere and atmosphere than was previously believed, potentially accounting for 12-28% of global TGM per year. Laboratory experiments by *Friedli et al.* [2001] suggest that burning of litter and green vegetation results in nearly complete release of Hg (almost entirely in the elemental form) contained in the fuel, and that release of Hg from biomass fires may be 104-526 Mg y^{-1}, or 3.5-17.5% of natural Hg emissions and 1.6-8.0% of all emissions. Comparison of these studies suggests that boreal fires do not comprise a significant percentage of global emission of Hg from biomass burning. However, direct measurements of Hg release from actual fires indicate that laboratory measurements significantly underestimate Hg release from fires, primarily due to the inability to account for Hg release from fire-heated soil [*Friedli et al.*, 2003]. Therefore, more measurements of Hg release from fires in situ would add confidence to our understanding of the role of this source in the global Hg budget.

There is no published record of Hg emission from natural fires in Canadian boreal forests, much less subsequent long-range transport to the United States. However, large natural fires in this region have been linked to enhancements in carbon monoxide (CO) and volatile organic compounds (VOCs) in the mid-latitudes [*Wofsy et al.*, 1994]. These species as well as ozone (O_3) and aerosols may be transported in Canadian forest fire plumes as far as the southeastern United States, causing local enhancements in their concentrations [*Wotawa and Trainer*, 2000]. This raises questions regarding the role of fire in the annual Hg budget in North America, especially in Canada where anthropogenic emissions of Hg are significantly lower than in the United States [*EPA*, 1997; *Environment Canada*, 2000].

1.3.2. Anthropogenic Sources

Globally, anthropogenic sources emit approximately 3500 Mg of Hg per year [*Schroeder and Munthe*, 1998]. Anthropogenic sources of Hg can be subdivided into point and non-point, or area, sources. Point sources are fixed in a readily identified geographic location. Area sources are often mobile, numerous and difficult to pinpoint geographically.

Annual anthropogenic emission of Hg in the U.S. has been estimated at approximately 146 Mg, with fossil fuel combustion, medical and municipal waste incineration and manufacturing and smelting emissions accounting for 41.7%, 38.9% and 18.4%, respectively [*EPA*, 1997; *Pai et al.*, 1998; these two studies showed similar total emissions and slight variations in source-by-source emissions]. These are point source emissions of Hg. Area source emissions (e.g., fluorescent lamps, latex paint residue, dental amalgams, pesticides, automobile exhaust etc) are more difficult to quantify but have been estimated at 43 Mg yr^{-1} in North America [*Pirrone et al.*, 1996]; however, the brunt of U.S. emissions are from point combustion sources

1.3.2.1 Point combustion sources

Combustion is by far the most significant anthropogenic source of Hg in the United States, accounting for 86% (~125 Mg) of annual emissions [*EPA*, 1997]. Mercury exists in trace amounts in fossil fuels and easily volatilizes at the high temperatures reached in combustion stacks, and is therefore released into the air in significant amounts. A small amount may also escape as particulate matter during storage and handling.

Utility boilers account for approximately 33% of annual anthropogenic emissions in the U.S. [*EPA*, 1997]. Utility boilers burn coal, oil or natural gas to generate electricity (i.e., typical power plants). Coal-fired boilers are most common and tend to be located in the Midwest, the Ohio River Valley, Pennsylvania and the northeast corridor (Delaware, Maryland, New York, New Jersey and lower New England). A vast majority of American oil-fired plants are clumped along the East Coast between Maryland and Massachusetts.

Additionally, approximately 18% of U.S. Hg emissions are from non-utilities – commercial and industrial boilers – which also burn coal, oil or natural gas. Therefore, electricity generators accounted for approximately 50% of all U.S. anthropogenic Hg emissions in 1994-95.

Municipal waste combustors (MWC), located abundantly along the East Coast, reduce by 90% the mass and volume of municipal solid waste (garbage, commercial, and industrial solid waste, etc) that must be deposited in landfills. Mercury emissions from this source may derive from discarded florescent light bulbs, batteries, paint residues and electrical equipment. The three major types of municipal waste combustors are mass burn, modular, and refuse-derived fuel-fired combustors. Mass burn and modular combustors require no pre-processing of the waste, while waste is pre-processed (and thus has a higher heating value) in the case of the refuse-derived fuel combustors.

Emissions from municipal waste combustors in the United States were approximately 27 Mg in 1995, nearly a 50% reduction from the 1990 level [*EPA*, 1996]. Currently, emissions from this category are believed to be >90% lower than the 1994 level [*N.J. Themelis*, personal communication]. The reduction is due to the closing of a number of facilities, air pollution control measures and decreased levels of Hg in municipal waste due to state and national-level legislation [EPA New Source Performance Standards (NSPS)].

Medical waste incinerators (MWI), which burn infectious and non-infectious waste materials from hospitals, clinics, veterinary and dental offices as well as medical research facilities, accounted for 15 Mg, or 10% of the total anthropogenic emissions, of Hg in 1994-95. Medical waste may contain a number of items containing Hg, including thermometers, lamps, batteries, antiseptics, diuretics, skin preparation paper and CAT scan paper. Similar to MWC, the EPA NSPS of 1997 were expected to reduce emissions from medical waste incineration by more than 90%.

Nationally, electricity generators, municipal and medical waste incinerators accounted for 91.4% of total Hg emissions from combustion sources (and nearly 80% of all anthropogenic emissions). The remaining 8.6% was emitted by hazardous waste combustors (HWC; 5%), residential boilers (2.6%), sewage sludge incinerators (SSI; 0.7%), wood-fired boilers (0.1%) and crematories (<0.1%).

In order to assess local and regional environmental and public health impacts of Hg emission from combustion sources, quantifying not only bulk emissions, but speciation of Hg within the emission plume is critical. Reactive species of Hg are likely to be deposited within 10-km of the source. Reliable chemical discrimination of Hg in collected air samples is a relatively recent development [*Lindberg and Stratton*, 1998] and we will not have an adequate understanding of Hg deposition and biogeochemical cycling until we achieve a better capability to predict the speciation of Hg in point source emission plumes and during atmospheric transport. Efforts to model atmospheric transport of Hg tend to be highly sensitive to speciation of Hg within emission plumes. Lack of understanding of emission strengths and the relative proportions of Hg species from typical sources therefore has a significant impact on results from modeling techniques [*EPA*, 1997; *Bullock et al.*, 1998; *Pai et al.*, 1999].

Our ability to estimate the relative abundance of various chemical and physical forms of Hg in emissions plumes is also crucial for developing a clear understanding of atmospheric transformation and deposition of Hg [*Bullock*, 2000a]. The speciation of

Hg emissions from combustion sources is a complex function of Hg concentration in feed material (fuel), the concentration of other pollutants (such as HCl) in the exhaust stream, the carbon content of the exhaust stream, the temperature of the flue gas and the type of air pollution control devices used [*Carpi*, 1997]. Data presented by *Galbreath and Zygarlicke* [1996] indicate that flue gas Hg emissions from coal combustion systems are equally divided between Hg^o and Hg^{2+}. *Carpi* [1997] suggests that the proportions are actually much more variable but in the range of 20-50% Hg^o and 50-80% Hg^{2+}, while emissions from municipal waste combustors are 10-20% Hg^o and 65-85% Hg^{2+} [*Carpi*, 1997].

1.3.2.2. Point manufacturing sources

Manufacturing sources accounted for approximately 10% of the total anthropogenic emissions of Hg (~14 Mg according to the EPA inventory) in 1995. The most important manufacturing sources are chlor-alkali plants that use Hg cells as an electrolyzer in the production process. This process accounted for 6.5 Mg, or 4.5% of the total inventory, in 1995. Each plant contains over 100 cells containing at least 3 tons of Hg. However, the chlorine industry has been actively replacing Hg cells with alternative technologies, and the number of chlor-alkali plants using Hg cells declined from 25 to 14 facilities between 1975 and 1995. The second-largest manufacturing source is Portland cement plants, which are spread throughout the country with the highest number of facilities located in Pennsylvania. Hg may be present in both the raw material (limestone, silica and other minerals) and the coal/oil used in pyroprocessing inside the kiln. Portland cement manufacturing accounted for 4.4 Mg of Hg emitted, or 1.2% of the total inventory, in 1995.

Some additional manufacturing sources of Hg exist but emit only 2.4% of the total Hg emissions inventory. These include pulp and paper manufacturing, thermometer manufacturing, secondary production (processing/recycling industrial waste and scrap which may contain Hg), manufacturing of electrical switches, thermal sensing instruments, florescent lamps, carbon black production (produced by hydrocarbon combustion; facilities located primarily in Texas and Louisiana), lime manufacturing, lead smelting (two facilities nationwide), copper smelting (8 facilities, 7 in New Mexico and Arizona), florescent lamp recycling, battery production, primary Hg production (i.e., mining, although Hg is no longer mined as an ore in the U.S., only as a byproduct of a small number of gold mines), Hg compounds production (4 locations), byproduct coke production (Ohio and Pennsylvania) and petroleum refining.

1.3.2.3. Area (non-point) sources

Area sources accounted for only 2.2% of total anthropogenic Hg emissions in the U.S. in 1995. The most significant non-point source is electric lamp breakage (1.4 Mg, or 1% of the total Hg inventory, in 1995). Florescent, metal halide, vapor and high-sodium lamps may all contain Hg that may be emitted to the atmosphere upon breakage during use or disposal. Emissions from this source should become almost negligible since recycling programs and efforts to reduce Hg in lamp manufacturing are on the rise. Other non-point sources include laboratory use (in instrumentation or as reagents/catalysts), dental amalgams, landfills and sludge allocation. Also, vehicular emissions, paint use and agricultural burning are non-point sources of Hg but limited information on these sources prohibits a reliable determination of emissions.

1.3.2.4. Hg sources in the northeast

In the northeastern and mid-Atlantic states (New England, NY, NJ and PA), combustion sources are even more significant than they are nationally, accounting for ~96% of anthropogenic emissions [based on *EPA*, 1997]. In 1994-95, municipal waste combustors and utility boilers were the largest Hg emitters, and PA, NY and MA were the area's largest statewide emitters of anthropogenic Hg (see Table 1.1 – 1994/95 EPA data are used, as this is the most up-to-date inventory). However, despite the preponderance of municipal waste combustion facilities on the east coast, the combined electric power sector (utility and independently-run (commercial and industrial) boilers) accounted for a larger fraction of total Hg emissions in the northeast (42%, versus 38% from municipal waste combustion). Also, as noted previously, emissions from municipal and medical waste combustion are currently believed to be emitting <10% of their 1995 totals. A categorical breakdown of anthropogenic Hg emissions in the northeast, based on inventory data [*EPA*, 1997], is provided in Table 1.1.

Table 1.1: Combustion and manufacturing source emissions (Mg yr^{-1}) among northeastern states in 1994-95 (based on 1997 EPA raw data/emission factors).

Source	**PA**	**CT**	**NJ**	**NY**	**ME**	**RI**	**MA**	**NH**	**VT**	**Total**
Combustion										
coal utility boilers	4.66	0.07	0.82	1.18	0.00	0.00	0.29	0.13	0.00	7.14
nat. gas utility boilers	0.00	0.00	0.02	0.00	0.00	0.00	0.00	0.00	0.00	0.02
oil utility boilers	0.01	0.09	0.03	0.00	0.00	0.00	0.09	0.00	0.00	0.22
MWC	2.81	1.09	1.03	3.18	0.54	0.18	3.18	0.45	0.00	12.47
coal comm./ind. boilers	2.99	0.00	0.44	0.64	0.18	0.00	0.00	0.00	0.73	4.97
oil comm./ind. boilers	0.34	0.10	0.00	0.71	0.05	0.04	0.24	0.07	0.03	1.57
MWI	0.65	0.23	0.34	0.16	0.33	0.10	1.00	0.15	0.03	2.99
coal residential boilers	0.13	0.00	n/a	0.02	0.00	0.00	0.00	0.00	0.00	0.15
oil residential boilers	0.37	0.24	n/a	0.51	0.11	0.06	0.37	0.07	0.05	1.78
SSI	0.16	0.07	0.00	0.25	0.00	0.01	0.02	0.01	0.01	0.53
wood boilers	0.00	0.00	0.00	0.00	0.00	0.00	0.00	0.00	0.00	0.00
total	12.11	1.88	2.67	6.63	1.22	0.40	5.19	0.90	0.83	31.83
Manufacturing										
chlor-alkali plants	0.00	0.00	n/a	0.00	0.27	0.00	0.00	0.00	0.00	0.27
cement manufacturing	0.27	0.00	n/a	0.18	0.03	0.00	0.00	0.00	0.00	0.48
pulp/paper manufacturing	0.04	0.00	n/a	0.00	0.09	0.00	0.00	0.00	0.00	0.13
secondary production	0.01	0.00	n/a	0.09	0.00	0.00	0.00	0.00	0.00	0.10
battery production	0.00	0.00	n/a	0.00	0.00	0.00	0.00	0.00	0.09	0.09
byproduct coke	0.13	0.00	n/a	0.02	0.00	0.00	0.00	0.00	0.00	0.15
total	0.44	0.00	0.13	0.29	0.39	0.00	0.00	0.00	0.09	1.34

1.4 Overview of study

1.4.1. Research Problems

Mercury (Hg) is a toxic and dangerous environmental contaminant. The degree to which anthropogenic Hg emissions impact human health is dependent on the emission rate, as well as the chemical form, of the emitted species. At present, there is no up-to-date, accurate assessment of the Hg emission rate in the northeast U.S., as the last inventory-based estimate [*EPA*, 1997] was made in 1995 and within only 30% accuracy [*EPA*, 1997; *Pai et al.*, 1998]. Since then, researchers and policy makers alike have had little indication as to whether emissions change seasonally or annually, or, aside from a few revealing studies [*Themilis and Gregory*, 2002; *MA DEP*, 2002], little understanding of the impact of the 1997 EPA New Source Performance Standards, which sought to reduce emissions from municipal and medical waste combustion by >90%. The impossibility of obtaining inventory emission estimates with high time resolution, the changing nature of feed materials and control technologies, and lack of extensive, reliable data on emission factors renders the inventory approach unsuitable for obtaining a timely and accurate understanding of Hg emissions. Accurate quantification of emissions on short time scales may especially be a concern for the northeastern U.S., which possesses the highest regional anthropogenic Hg flux density in the country [*EPA*, 1997]. Therefore, a clear need exists to refine our ability to determine trends in Hg emissions if we are to address legislative strategies for reducing environmental impacts, or gauge the progress of existing abatement policies and control technologies. A more accurate methodology with higher (annual or seasonal) time resolution should be applied to the study of emissions in the northeast in order to determine how emissions have changed in magnitude since the EPA study, whether they vary seasonally or annually, and if so, whether this is in response to climatological variables, or to changes in the anthropogenic sources themselves.

In addition to anthropogenic source emissions, this study will consider several natural sources of Hg. No detailed field studies of natural (soil) fluxes of Hg in the northeast have been undertaken. More generally, little is known of the behavior of gaseous Hg within soil. Better characterization of background forest soil emissions and the environmental variables that influence them as well as the physical and chemical behavior of Hg within soils in general is essential to a full understanding of regional and global Hg budgets as well as the biogeochemical cycling of Hg. Relatively little experimental evidence exists to confirm modes of Hg transport within and evasion from soil or the exact desorption sites of oxidized Hg. To this point, although some studies have estimated gaseous Hg concentrations within soil, there are essentially no detailed studies of this parameter due to the lack of a widely accepted measurement method.

Some recent studies [e.g., *Brunke et al.*, 2001; *Friedli et al.*, 2003] suggest that Hg emissions from biomass burning may be a more significant pathway of Hg exchange between the biosphere and atmosphere than was previously believed. The magnitude of Hg emission from boreal forest fires is poorly quantified and there is no published record of Hg emission from a large-scale natural fire in the Canadian boreal forests. Direct measurements of Hg release from actual boreal fires would add confidence to our understanding of the contribution of this source to the global Hg budget. Also, long-range transport from Canadian boreal fires have been linked to enhancements in carbon monoxide (CO), ozone (O_3), aerosols and volatile organic compounds (VOCs) in the mid-latitudes and southeastern U.S. [*Wofsy et al.*, 1994; *Wotowa and Trainer*, 2000]. This raises questions regarding both the short-term impact of Canadian boreal fires on ambient Hg concentrations in the U.S. and the role of fire in the annual Hg budget in North America, especially in Canada where anthropogenic emissions of Hg are significantly lower than in the United States [*EPA*, 1997; *Environment Canada*, 2000].

1.4.2. Purposes of study

This project was both regional and global in scope, and was designed to improve our ability to measure Hg in natural environments, analyze the Hg data we collect, and to contribute significantly to the body of knowledge of Hg emissions, especially in the United States. One purpose was to use long-term measurements of Hg concentrations at a background site in New England (Great Mountain Forest, Norfolk, CT) to examine the magnitude of and recent trends in the regional anthropogenic Hg emission rate in the northeastern U.S. This was achieved by combining measurements of ambient Hg and carbon dioxide (CO_2) over five winters (1999/2000 through 2003/2004). CO_2 is emitted strongly by combustion sources and has a better-characterized inventory flux than Hg and is therefore considered to be a "tracer" for Hg emission. The goal here was to provide a more accurate estimate of the rate and temporal variability of anthropogenic Hg emissions in the northeast. An additional goal was to combine these data with backward trajectory analysis in order to assess spatial variability of emissions (i.e., annual source regions) impacting the Hg measurements at Great Mountain and therefore elucidate possible climatological influences. This was achieved by using an on-line NOAA (National Oceanic and Atmospheric Administration) trajectory model [HYSPLIT-4, *Draxler and Hess,* 1997] and incorporating trajectory data into a potential source contribution function. This is the first study to employ tracer analysis over a multi-year time period, and in tandem with long-term air trajectory modeling. In addition to estimating recent trends in Hg emission in the northeast, determining typical geographic source areas which impact the atmospheric Hg signal and thereby assessing the extent to which climatology or changes in anthropogenic sources impact emission estimates, the combination of long-term monitoring and trajectory analysis will provide a new framework for interpretation of regional Hg emissions at any location.

To improve the general body of knowledge of natural Hg emissions, a primary goal of the study was to develop a new measurement methodology for the study of gaseous Hg in soil. The method involves removing air from the soil profile at a very low flow rate, collecting it in a flask and removing it from the field for sampling. After the system was assembled and tested in both the laboratory and the field, it was used to measure gaseous soil Hg concentrations at a background forest site in the northeast (Coventry, CT) over two field campaigns (July-November 2003, May-October 2004). Gaseous Hg concentrations were analyzed in order to examine their relationship with environmental variables and their role in emissions from soil. Soil gaseous Hg data will further our understanding of the processes that control the pool of gaseous Hg within soil pores that is available for emission, as well as the ultimate release from the surface. This set of field experiments represents not only the first detailed study of gaseous Hg in soil, but also provides the first measurement of Hg flux from background forest soils in the northeast U.S. The measurement methodology is intended to have general applicability to the study of Hg and other trace gases in soil.

This study also explored Hg emissions from biomass burning. During the summer of 2002, ambient Hg was measured at a background site in Massachusetts (Harvard Forest) and the impact of a large smoke plume emitted by a series of widespread Canadian boreal forest fires was detected. These data were combined with correlated measurements of another combustion tracer [carbon monoxide (CO)] during the event to assess typical Hg emissions from boreal fires and postulate their regional and global contributions to the atmospheric Hg budget. This phase of the study will provide valuable data for a natural source of Hg that has been rarely studied and is therefore poorly understood. This analysis as well as the soil Hg study will improve our knowledge of natural source contributions to the global Hg budget.

Detailed methodologies and further literature review will be found in Chapters 2-4 of this dissertation. These chapters are, with slight modification, presented in the form of manuscripts published in or, at the time of this writing, under peer review by journals. Chapter 2 presents the results of the regional Hg emission study. Chapter 3 outlines the methodology of the flask sampling system for soil gas, important results of the laboratory testing, and the methodology and results of the two field experiments in which gaseous Hg concentrations within and flux from background forest soil in Connecticut were measured. In Chapter 4, measurements of Hg within a smoke plume from a large boreal forest fire in Canada are presented, and estimates of Hg emission from boreal fires are discussed and placed in global context. Chapter 5 includes a summary of the main conclusions and overall implications of this work.

1.5. References

Allan, R.J. (1999), Atmospheric mercury contamination of remote aquatic ecosystems in Canada, *Wat. Sci. Tech.*, 12, 173-177.

Bergen, T., Gallardo, L., and Rodhe, H. (1999), Mercury in the global troposphere: A three-dimensional model study, *Atmos. Env.*, 33, 1575-1585.

Brunke, E-G., Labuschagne, C., and Slemr, F. (2001), Gaseous mercury emissions from a fire in the Cape Peninsula, South Africa, during January 2000, *Geophys. Res. Lett.*, 28, 1483-1486.

Bullock, O.R., Brehme, K.A., and Mapp, G.R. (1998), Lagrangian modeling of mercury air emission, transport and deposition: An analysis of model sensitivity to emissions uncertainty, *Sci. Total Env.*, 213, 1-12.

Bullock, O.R. (2000a), Current methods and research strategies for modeling atmospheric Mercury, *Fuel Proc. Tech.*, 65-66, 459-471.

Bullock, O.R. (2000b), Modeling assessment of transport and deposition patterns of anthropogenic mercury air emissions in the United States and Canada, *Sci. Tot. Env.*, 259, 145-157.

Carpi, A. (1997), Mercury from combustion sources: A review of the chemical species emitted and their transport in the atmosphere, *Water Air Soil Poll.*, 98, 241-254.

Carpi, A., and Lindberg, S.E. (1998), Application of a Teflon dynamic flux chamber for quantifying soil mercury flux: Tests and results over background soil, *Atmos. Env.*, 32, 873-882.

Coolbaugh, M.F., Gustin, M.S., Rytuba, J.J. (2002), Annual emissions of mercury to the atmosphere from natural sources in Nevada and California, *Env. Geol.*, 42, 338-349.

Draxler, R.R., and Hess, G.D. (1997), Description of the HYSPLIT_4 Modeling System, NOAA Technical Memorandum ERL ARL-224, 24 pp.

Engle, M.A., Gustin, M.S., and Zhang, H. (2001), Quantifying natural source mercury emissions from the Ivanhoe Mining District, north-central Nevada, USA., *Atmos. Env.*, 35, 3987-3997.

Engle, M.A., and Gustin, M.S. (2002), Scaling atmospheric mercury emissions from three naturally enriched areas: Flowery Peak, Nevada; Peavine Peak, Nevada; and Long Valley Caldera, California, *Sci. Tot. Env.*, 290, 91-104.

Environment Canada (2000), The Status of Mercury in Canada, http://www.cec.org/Programs_projects/pollutants_health/smoc/pdfs/hgcan-e.pdf.

EPA (United States Environmental Protection Agency) (1997), Mercury Study Report to Congress, http://www.epa.gov/mercury.html.

EPA (2004), National Listing of Fish Advisories, http://www.epa.gov/waterscience/fish/advisories/factsheet.pdf

Fitzgerald, W.F. (1989), Atmospheric and oceanic cycling of mercury.In Chemical Oceanography Series, Ch. 57, Volume 10, Riley, J.P., Chester, R. (Eds.), Academic Press, New York, pp. 151-186.

Fitzgerald, W.F., Vandal, G.M., and Mason, R.P. (1991), Atmospheric cycling and air-water exchange of Hg over mid-continental lacustrine regions, *Water Air*

Soil Poll., 56, 745-767.

Fitzgerald, W.F., Engstrom, D.R., Mason, R.P., and Nater, E.A. (1998), The case for atmospheric mercury deposition in remote areas, *Env. Sci. Tech.*, 32, 1-7.

Friedli, H.F., Radke, L.F., and Lu, J.Y. (2001), Mercury in smoke from biomass fires, *Geophys. Res. Lett.*, 28, 3223-3226.

Friedli, H.F., Radke, L.F., Lu, J.Y., Banic, C.M., Leaitch, W.R., and McPherson, J.I. (2003), Mercury emissions from burning of biomass from temperate North American forests: laboratory and airborne measurements, *Atmos. Env.*, 37, 253-267.

Galbreath, K.C., and Zygarlicke, C.J. (1996), Mercury speciation in coal combustion and gasification flue gases, *Env. Sci. Tech.*, 30, 2421-2426.

Gillis, A., and Miller, D. (2000a), Some local environmental effects on mercury emission and absorption at a soil surface, *Sci. Tot. Env.*, 260, 191-200.

Gillis, A., and Miller, D. (2000b), Some potential errors in the measurement of mercury gas exchange at the soil surface using a dynamic flux chamber, *Sci. Tot. Env.*, 260, 181-189.

Gustin, M.S., and Lindberg, S.E. (2000), Assessing the contribution of natural sources to the global mercury cycle: The importance of intercomparing dynamic flux measurements, *Fresenius J. Anal. Chem.,* 366, 417-422.

Kehrig, H.D., and Malm, O. (1999), Methylmercury in fish as a tool for understanding the Amazon mercury contamination. *App. Organomet. Chem.*, 13, 689-696.

Kim, K-H., Lindberg, S.E., and Meyers, T.P. (1995), Micrometeorological measurements of mercury vapor fluxes over background forest soils in eastern Tennessee, *Atmos. Env.*, 29, 267-282.

Kurland L, Faro S, and Siedler H. (1960), Minamata disease: the outbreak of a neurologic disorder in Minamata, Japan, and its relationship to the ingestion of seafood contaminated by mercuric compounds, *World Neurol.,* 1, 370-95.

Lindberg, S.E., and Stratton, W.J (1998), Atmospheric mercury speciation: Concentrations and behavior of reactive gaseous mercury in ambient air, *Env. Sci. Tech.*, 32, 49-57.

Lindberg, S.E., Zhang, H., Vette, A.F., Gustin, M.S., Barnett, M.O., and Kuiken, T. (2002), Dynamic flux chamber measurement of gaseous mercury emission fluxes over soils: Part 2 – effect of flushing flow rate and verification of a two-resistance exchange interface simulation model, *Atmos. Env.*, 36, 847-859.

Lindquist, O., and Rodhe, H. (1985), Atmospheric mercury – a review, *Tellus*, 37B, 136-159.

Mason, R.P., Fitzgerald, W.F., Morel, F.M.M. (1994), The biogeochemical cycling of elemental mercury: anthropogenic influences, *Geochem. et Cosmochem. Acta,* 58, 3191-3198.

Mason, R.P., Lawson, N.M., and Sheu, G.R. (2000), Annual and seasonal trends in mercury deposition in Maryland. *Atmos. Env.*, 34, 1691-1701.

Mason, R.P., and Sheu, G.R. (2000), Role of the ocean in the global mercury cycle, *Global Biogeochem. Cycles*, 16, 1093.

Massachusetts Department of Environmental Protection (MA DEP) (2002), Municipal Waste Combustor Facility and Trend Reports, www.mass.gov/dep/mwc/mwcfr.htm.

Munthe, J., and McElroy, W.J. (1992), Some aqueous reactions of potential importance in the atmospheric chemistry of mercury, *Atmos. Env.*, 26A, 553-557.

Nriagu, J.O. (1989), A global assessment of natural sources of atmospheric trace metals, *Nature*, 338, 47-49.

Pai. P., Karamchandani, P., and Seigneur, C. (1998), Simulation of the regional atmospheric transport and fate of mercury using a comprehensive eulerian model, *Atmos. Env.*, 31, 2717-2732.

Pai, P., Karamchandani, P., Seigneur, C., and Allan, M.A. (1999), Sensitivity of simulated atmospheric mercury concentrations and deposition to model input parameters, *J. Geophys. Res.*, 104, 13855-13868.

Pai, P., Niemi, D., and Powers, B. (2000), A North American inventory of anthropogenic mercury emissions, *Fuel Proc. Tech*., 65-66, 101-115.

Pirrone, N., Keeler, G., Nriagu, J.O. (1996), Regional differences on world-wide emissions of mercury to the atmosphere, *Atmos. Env.*, 30, 2981-2987.

Poissant, L., and Casimir, A. (1999), Water-air and soil-air exchange rate of total gaseous mercury measured at background sites. *Atmos. Env.*, 32, 883-893.

Poissant, L. (1999), Potential sources of atmospheric total gaseous mercury in the St. Lawrence River valley, *Atmos. Env.*, 33, 2537-2547.

Schroeder, W.H., Munthe, J., and Lindquist, O. (1989), Cycling of mercury between water, air and soil compartments of the environment, *Water Air Soil Poll.*, 48, 337-347.

Schroeder, W.H., and Munthe, J. (1998), Atmospheric Mercury – An Overview, *Atmos. Env.*, 32, 809-822.

Sloss, L.L. (1995), Mercury emissions and effects – the role of coal, International Energy Agency (IEA) Coal Research, London, 38 pp.

Wallschläger, D., Kock, H.H., Schroeder, W.H., Lindberg, S.E., Ebinghaus, R., and Wilkin, R.-D. (2002), Estimating gaseous mercury emission from contaminated floodplain soils to the atmosphere with simple field measurement techniques. *Water Air Soil Poll.*, 135, 39-54.

Wofsy, S.C., Fan, S-M., Blake, D.R., Bradshaw, J.D., Sandholm, S.T., Singh, H.B., Sachse, G.W., and Harriss, R.C. (1994), Factors influencing atmospheric composition over subarctic North America during summer, *J. Geophys. Res.*, 99, 1887-1897.

Wotawa, G., and Trainer, M. (2000), The influence of Canadian forest fires on pollutant concentrations in the United States, *Science*, 288, 324-328.

Xu, X., Yang, X., Miller, D.R., Helble, J.J., and Carly, R.C. (2000a), A regional scale modeling study of atmospheric transformation of mercury. I. Model development and evaluation, *Atmos. Env.*, 34, 4933-4944.

Xu, X., Yang, X., Miller, D.R., Helble, J.J., and Carly, R.C. (2000b), A regional scale modeling study of atmospheric transformation of mercury. II. Simulation results for the northeast United States, *Atmos. Env.*, 34, 4945-4955.

Zhang, H., Lindberg, S.E., Marsik, F.J., and Keeler, G.J. (2001), Mercury air/surface exchange kinetics of background soils if the Tahquamenon river watershed in the Michigan upper peninsula, *Water Air Soil Poll.*, 126, 151-169.

Zhang, H., Lindberg, S.E., Barnett, M.O., Vette, A.F., and Gustin, M.S. (2002), Dynamic flux chamber measurements of gaseous mercury emission fluxes over soils. Part 1: simulation of gaseous mercury emissions from soils using a two-resistance exchange interface model, *Atmos. Env.*, 36, 835-846.

Chapter 2:

[1]Recent trends in anthropogenic mercury emission in the northeast United States

---

[1] Submitted to *Journal of Geophysical Research-Atmospheres,* 10-2005.

Abstract

The northeastern U.S. is characterized by the highest anthropogenic mercury (Hg) flux in the nation. Wintertime measurements of total gaseous mercury (TGM) were combined with a combustion tracer (carbon dioxide) at a background site in Connecticut to investigate changes in regional Hg emission from 1999/2000 through 2003/2004. This method allows timelier flux estimates than inventory approaches. A 20% decrease in emission between 1999/2000 and 2003/2004 was observed, although the rate has increased since 2001/2002. Air trajectory analysis reveals a source region of Hg influencing the site that encompasses most of the mid-Atlantic and New England states, and Maryland and Delaware, with small interannual variation. The significant interannual changes in Hg emission therefore cannot be fully explained by climatological changes. Inventory calculations of Hg flux from the regional electric power sector show significant correlation with the emission trend derived from the atmospheric measurements, suggesting that the power sector strongly influences the regional Hg flux to the atmosphere. However, averaged over the five winters, the Hg flux from the power sector was 75% of the atmospheric flux, which is assumed to be >95% elemental Hg. If 50% or more of Hg emitted by power sources is reactive and deposits locally, the power sector can account for only 40% of the observed elemental Hg flux to the atmosphere. This may suggest that emissions from sources outside the power sector are underestimated, or that emissions from municipal and medical waste combustion have not been curbed to the EPA targeted level.

2.1. Introduction

Mercury (Hg) is dangerous environmental contaminant. The degree to which anthropogenic Hg emissions impact human health is dependent on the emission rate, as well as the chemical form, of the emitted species. The northeastern United States is characterized by the highest regional anthropogenic Hg flux density in the nation, due primarily to combustion of coal and municipal waste in urban areas [*EPA,* 1997]. The emissions reported by the EPA were based on an inventory approach, which combines facility-specific emission factors, activity levels, fuel characteristics and control technology. Lack of emission test data renders the accuracy of the EPA's emission inventory to no better than 30%. Moreover, timely assessment of temporal trends in Hg emission using the inventory approach is nearly impossible given the sheer number of point sources, the complexity of source categories, ever-changing trends in mercury consumption, advancements in control technologies and state and national legislation advanced since the EPA study. The need for an alternate approach is underscored by additional, recent studies that show that Hg sources in urban areas are diverse and can change rapidly across time scales. Therefore long-term measurements, preferably at multiple locations, are important [*Kim and Kim*, 2001; *Nadim et al.*, 2001; *Landis et al.*, 2002; *Chen et al.*, 2004].

An alternative technique for deriving the regional Hg emission rate is the correlation of ambient Hg with an atmospheric tracer. This technique provides an estimate of emission on a fine time resolution (<1 year) and can be based on a chemical species characterized by inventory data that are more reliable and timely than Hg inventories. Furthermore, the derived emissions ratio is understood to have a footprint representative of a large area (on the order of 500 km) when established with data over time scales of weeks or longer [*Potosnak et al.*, 1999].

Tracer analysis has been used extensively in atmospheric chemistry and transport studies. For example, *Wofsy et al.* [1994] used CO and hydrocarbons as tracers to estimate the contribution of chemicals released from biomass burning to the subarctic. *Wang et al.* [2002] used emission ratios of CO and SO_2 with NO_y and other industrial tracers to infer combustion fuel type and sources of elevated CO in rural eastern China. CO_2/CO correlation analyses have been used to infer combustion source types and regions [*Suntharalingam et al.*, 2004]. CO and CO_2 have also been used as tracers for determining Hg emission from biomass burning events [*Brunke et al.*, 2001; *Friedli et al.*, 2003; *Sigler et al.*, 2003].

Wintertime CO_2 has been demonstrated to be a viable tracer for combustion sources in the northeast U.S. [*Bakwin et al.*, 1994; *Potosnak et al.*, 1999]. Combustion sources are responsible for more than 90% of regional Hg emissions and tend to be located near non-combustion (e.g., area and manufacturing) sources of Hg [*EPA*, 1997]. The fact that the sources that emit both gases are co-located geographically makes CO_2 an excellent tracer for Hg. For example, *Lee et al.* [2001] used Hg and CO_2 atmospheric concentration data for winter 1999/2000 collected at the same site to determine a regional anthropogenic elemental Hg (Hg°) flux of 41(±2) g km^{-2} yr^{-1} for the northeast U. S.

In this study, measurements of ambient TGM (total gaseous mercury) and wintertime CO_2 at a background site in northwest Connecticut were used to determine interannual variability in the TGM emission rate in the northeast United States during the winters of 1999/2000 to 2003/2004. This study appears to be the first that applies the tracer technique to a multi-year time period. Utilizing wintertime air mass trajectory data, a potential source contribution function (PSCF) was created for each year in order to identify potential geographical source regions and dominant flow pathways that contributed the most to ambient TGM concentrations at our measurement site. Also, changes in the consumption of fuels by electric power producers were analyzed in order to explain changes in regional Hg emissions.

2.2. Data and Methodology

2.2.1. Ambient measurements and tracer analyses

TGM was monitored at Great Mountain Forest in northwest Connecticut (41º58´N, 73º14´W) from the summer of 1999 through the spring of 2004. The measurement was made at 5-minute intervals using a mercury vapor analyzer (Model 2537A, Tekran, Inc.) housed in a temperature-controlled shelter. The analyzer is calibrated daily against an internal permeation source to an accuracy of 5%. TGM data were carefully screened so that low-mercury episodes (TGM<1.0 ng m^{-3}) and periods during which the analyzer malfunctioned were excluded. The instrument cannot distinguish elemental and speciated Hg, but over 95% of TGM is assumed to be in elemental form [*Lindberg and Stratton*, 1998].

Although measurements of ambient TGM concentrations may suggest influences from local or regional pollution sources, such measurements by themselves do not indicate actual emission rates. Rather, they must be correlated with measurements of a tracer species that is emitted by the same sources or sources that are co-located with Hg emissions. In this study CO_2 was used as a tracer species for TGM emissions. CO_2 was measured at Great Mountain concurrently with TGM using a Licor infrared gas analyzer, calibrated weekly to an accuracy of 1%.

The tracer analyses were limited to daytime conditions (10:00-16:00 LST) when the atmospheric boundary layer is well-mixed. Where CO_2 data are concerned, only the colder months as defined by the 5-cm soil temperature less than 3°C were considered, so that biological CO_2 signals were negligible. This condition is typically met at Great Mountain from late December to the end of April. For convenience, the atmospheric measurements were compared with inventory data reported for the four winter calendar months (January to April).

Tracer analysis assumes that the slope of a regression line between TGM and CO_2 concentrations is equivalent to the regional emission ratio of the two species [*Bakwin et al.*, 1994; *Stehr et al.*, 2000; *Lee et al.*, 2001). Rather than ordinary least square regression, orthogonal or geometric mean regression as outlined in *Draper* [1997] and *Richardson* [2000] was used. Combining the emission ratios with an inventory carbon flux yields the annual regional TGM flux. Methods and data described in *Andres et al.* [1996] were used to derive an inventory carbon (C) emission rate of 529 t of C per km^2 $year^{-1}$ over the potential source region for the period 1994-1995. This includes most New England and mid-Atlantic states (CT, MA, RI, NY, NJ, PA) as well as Maryland (MD) and Delaware (DE). The total carbon emissions from fossil fuel burning in the northeastern states changed on average by no more than 2% during the period of 1990-2001 [*Blasing et al.*, 2004]. The state-by-state CO_2 inventory activity was terminated after 2001. However, total CO_2 emissions within the source region have been known to consistently comprise the same percentage (approximately 15%) of national emissions each year [*Blasing et al.*, 2004], and national emissions changed by less than 2.5% between 1999 and 2003 [*EIA*, 2004c]. For these reasons, the same total CO_2 emission rate (529 t of C per km^2 $year^{-1}$) was used for the entire study period. Wintertime (January to April) monthly C flux is given as 1/12 of the annual flux, which represents the typical fraction of annual CO_2 emissions from fossil fuel burning in the U.S. [*Blasing et al.*, 2005].

2.2.2. Air trajectory analysis

The TGM and CO_2 measurements were combined with air trajectory analysis to determine the source region impacting the measurement site and the potential influence of interannual variation in climatology and air transport patterns on the tracer correlation result. Trajectory analysis is commonly used to identify air mass source regions, transitions and atmospheric transport history [e.g., *Moody et al.*, 1998; *Cooper et al.*, 2001]. In this study, NOAA HYSPLIT-4, an on-line air trajectory model [*Draxler and Hess*, 1997], was used to build a trajectory database for each winter of TGM observation. Three 48-hour backward trajectories were simulated per day, at 15:00, 18:00 and 21:00 GMT (10:00, 13:00 and 16:00 LST) for the months of December through April, coinciding with the period considered in the tracer analyses. There were some significant gaps in TGM data during December of 2001 and March of 2002. Trajectories were not simulated for these gaps.

The HYSPLIT model was initialized at 500 m above the surface in a well-mixed boundary layer and uses gridded wind fields from the Eta Data Assimilation System (EDAS). The output of the HYSPLIT model gives the location in latitude and longitude of each hourly endpoint (48 endpoints per trajectory data file).

2.2.3. Potential source contribution function

Backward trajectories calculated during Hg pollution events at Great Mountain may indicate source regions of polluted air masses impacting the site. To identify these source regions, trajectory data can be incorporated into a receptor model that creates a probability field for emission source potential.

Using the trajectory data, a single-layer PSCF was created for each winter. The concept of PSCF has previously been used to determine, for example, sources and transport pathways of aerosols and TGM in the Canadian high Arctic [*Cheng et al.*, 1993; *Cheng and Schroeder*, 2000; *Lin et al.*, 2001] and sources of TGM in the St. Lawrence River valley [*Poissant*, 1991]. Detailed descriptions of the model can be found in these and other studies. In summary, the source region was divided into an array of 0.5° latitude by 0.5° longitude grid cells. If a trajectory endpoint lies in a particular grid cell, the trajectory is assumed to collect material emitted from that grid cell and transport it to the receptor site. Mathematically, the probability that an endpoint lies in a particular cell is $P[A_{ij}] = n_{ij}/N$, where n_{ij} is the number of endpoints falling in the ijth grid cell and N is the total number of endpoints. A certain number m_{ij} of these endpoints corresponds to the observation of TGM concentrations above a criterion value at the receptor site, which is defined as the 85th percentile concentration of all TGM measurements for that winter. The probability of this event is $P[B_{ij}] = m_{ij}/N$. The PSCF value for each grid cell is therefore $\mathrm{PSCF}_{ij} = P[B_{ij}|A_{ij}]$, or m_{ij}/n_{ij}. This value, between 0 and 1, describes probable geographic source regions based on the trajectories arriving at the source site.

PSCF values may be biased in cells where n_{ij} is small. Therefore, a weighting function (W) was introduced to minimize such biases, as

$$W(n_{ij}) = \begin{bmatrix} 1.0 & \dfrac{n_{ij}}{n_{mean}} \geq 1.0 \\ 0 & \dfrac{n_{ij}}{n_{mean}} \leq 1.0 \end{bmatrix} \qquad [2.1]$$

where n_{mean} is the mean of the n-value for those cells with $n_{ij} >= 10$. Choice of a weighting function is somewhat subjective, but Equation 2.1 was determined to give precedence to cells with higher count totals as those cells likely influence the TGM signal at the site most significantly. Other studies use the function $W(n_{ij}) = 0.1\ n_{ij}$ for $n_{ij} \leq 10$ [*Lin et al.*, 2000] or employ weight functions for $n_{ij} \leq 4$ [*Poissant*, 1999], with far fewer typical n-values than in this study. Application of these functions to trajectory data in this study results in physically unrealistic source region maps. For example, rural areas in the midwestern and western U.S. and Canada would be designated as highly probable source regions when only 2-3 trajectories, all of which happen to be polluted, impact them during the entire study period.

2.2.4 Fuel consumption data for the power sector

It is known that combustion sources accounted for more than 85% of all Hg emissions in the United States in the mid-1990s. Nationally, coal-fired power plants are the most important emissions category [*EPA*, 1997]. As recently as 1997, municipal waste combustors (MWC), common along the East Coast of the U.S., were the largest single Hg source category in the northeastern states. However, EPA new source performance standards of 1997 sought to reduce emissions from MWC (as well as medical waste incinerators) by >90% by 2000. There is evidence that these and other state-imposed regulations have been successful and that MWC have ceased to be the most important anthropogenic source category in the northeast. For instance, Hg emissions from this source category were reduced by two-thirds in New Jersey between 1997 and 1999 [*Themelis and Gregory*, 2002] and by more than one-half during the same period in Massachusetts [*MA DEP*, 2002]. Total U.S. emissions from this category are now believed to be approximately 1 ton per year, less than 3% of 1995 emissions [*Themelis*, personal communication].

Given the decline in emissions from municipal and medical waste combustion after 1997, the electric power sector is now thought to be by far the most important Hg source category in the northeastern states. It includes electric utilities, independent power producers (non-utilities) and combined heat and power plants that primarily burn coal, natural gas, or petroleum (usually residual or distillate fuel oil). Despite uncertainty in knowledge of the Hg emission factor, and variation among coal types and geographic origin, coal is known to have the highest Hg emission factor of these three main fuel categories [*EPA*, 1997]. Natural gas is relatively clean, with an emission factor that is several orders of magnitude lower than petroleum or coal [*EPRI*, 1996].

Given the disparity in Hg content and emission factor among coal, natural gas, and petroleum, it is possible that the regional emission rate of Hg from electricity generation may be influenced by the relative percentages of these three fuels that are combusted seasonally or annually in the northeast. Therefore, changes in total wintertime consumption of coal, petroleum, and natural gas for electricity generation were examined among the northeastern states.

Data on total consumption of coal, petroleum and natural gas for electricity generation from the U.S. Department of Energy (DOE) Energy Information Administration (EIA)'s Monthly Energy Review [*EIA*, 2005] were compiled. For each winter, the total consumption of each fuel type was compiled for each state in the source region (CT, MA, RI, NY, PA, NJ, MD, DE; see section 2.3.3) for the four winter months (Table 2.1). An Hg:C emission ratio was also calculated by applying approximate heat contents, CO_2 and Hg emission factors to each fuel consumption total, as shown in Equation 2.2:

$$\frac{Hg}{CO_2} = \frac{(c \times H \times F_m) + (p \times H \times F_m) + (g \times H \times F_m)}{(c \times H \times F_C) + (p \times H \times F_C) + (g \times H \times F_C)} \qquad [2.2]$$

where c is total coal (short tons), p is total petroleum (barrels), g is total natural gas [(thousand cubic feet (Mcf)], H is the heat content of the fuel (expressed as British thermal unit (Btu) per ton coal, barrel petroleum or Mcf natural gas) and F_m and F_C are the Hg (lb Hg/Btu) and CO_2 (lb CO_2/Btu) emission factors, respectively, for the particular fuel. Table 2.2 shows heat contents and emission factors used in the calculation and information on data sources (English units are used here to be consistent with literature and database convention, but the flux calculation was ultimately converted to SI units).

The consumption data included in this study represent the entire energy sector. Nationally, electric utilities are responsible for approximately 60% of total electric generation, down from more than 90% in the mid-1990s [*EIA*, 2004a]. For the northeastern and mid-Atlantic states, electric utilities accounted for only 15% of net

Table 2.1: Total wintertime (January-April) consumption of coal, petroleum and natural gas by the electric power sector within the source region.

	2000	**2001**	**2002**	**2003**	**2004**
Coal (short tons)	3.04×10^7	2.5×10^7	2.66×10^7	2.88×10^7	3.0×10^7
Petroleum (barrels)	2.71×10^7	2.89×10^7	1.33×10^7	2.97×10^7	3.02×10^7
Natural gas (Mcf)	3.6×10^8	2.06×10^8	2.28×10^8	1.8×10^8	1.98×10^8

Table 2.2: Heat content and Hg, CO_2 emission factors (EF) for coal, petroleum and natural gas combustion. The CO_2 EF for coal represents a mean value of subbituminous and bituminous coal and that of petroleum is the emission factor for residual fuel oil, which typically represents >80% of petroleum consumption for electric power in the U.S [*EIA*, 2004a/b]. The Hg EF used for coal represents a median value based on direct measurements from coal-burning power plants by the Electric Power Research Institute (EPRI; *Chu and Porcella* [1995]). The Hg EF for petroleum is based on average values for residual oil combustion [*EPA*, 1997] and the natural gas EF is taken from *EPRI* [1996].

	Coal	Petroleum	Natural gas
Heat Content	2.04×10^{7} (Btu/ton)	6×10^{6} (Btu/barrel)	1.02×10^{6} (Btu/Mcf)
CO_2 emission factor ($\text{lb } CO_2 \text{ Btu}^{-1}$)	2.07×10^{-4}	1.73×10^{-4}	1.17×10^{-4}
Hg emission factor ($\text{lb } 10^{-12} \text{ Btu}$)	10	6.8	0.0008

generation and total coal combustion during 2004 [*EIA*, 2005]. Therefore, this study did not distinguish between utilities and independent power producers.

2.3. Results and Discussion

2.3.1. TGM concentrations

Figure 2.1 presents seasonal statistics of the TGM data. It indicates that Great Mountain is a background site with little interannual variation in TGM concentration. The mean TGM concentration during 1999-2004 was 1.6 ng m^{-3}, which is comparable to other Northern Hemisphere, mid-latitude background sites [*Slemr et al.*, 1985; *Xiao et al.*, 1991; *Kim et al.*, 1995]. Median TGM concentrations varied by only 0.2 ng m^{-3}, between 1.4 and 1.6 ng m^{-3}, and wintertime concentrations tended to be higher than the previous summer. However, it is improper to suggest from the seasonal mean concentration data that the regional TGM emission changed little over the observational period, as TGM data alone cannot discriminate contributions of regional sources from the global background.

A detailed analysis of the TGM time series revealed that the site is frequently impacted by pollution events. These events, during which TGM and CO_2 exhibit significant and well-correlated temporal enhancements, typically for 1-4 hours, are common, occurring approximately once per week during the winter. Comparison of measurements taken at Great Mountain with CO_2 measurements from Harvard Forest near Petersham, MA (42º32´N, 72º11´W, 120 km to the northeast of Great Mountain) shows a high correlation ($r = 0.73$, $p < 0.01$) between CO_2 measurements at both locations (Figure 2.2a). Similarly, a high correlation ($r = 0.81$, $p < 0.01$) was also found

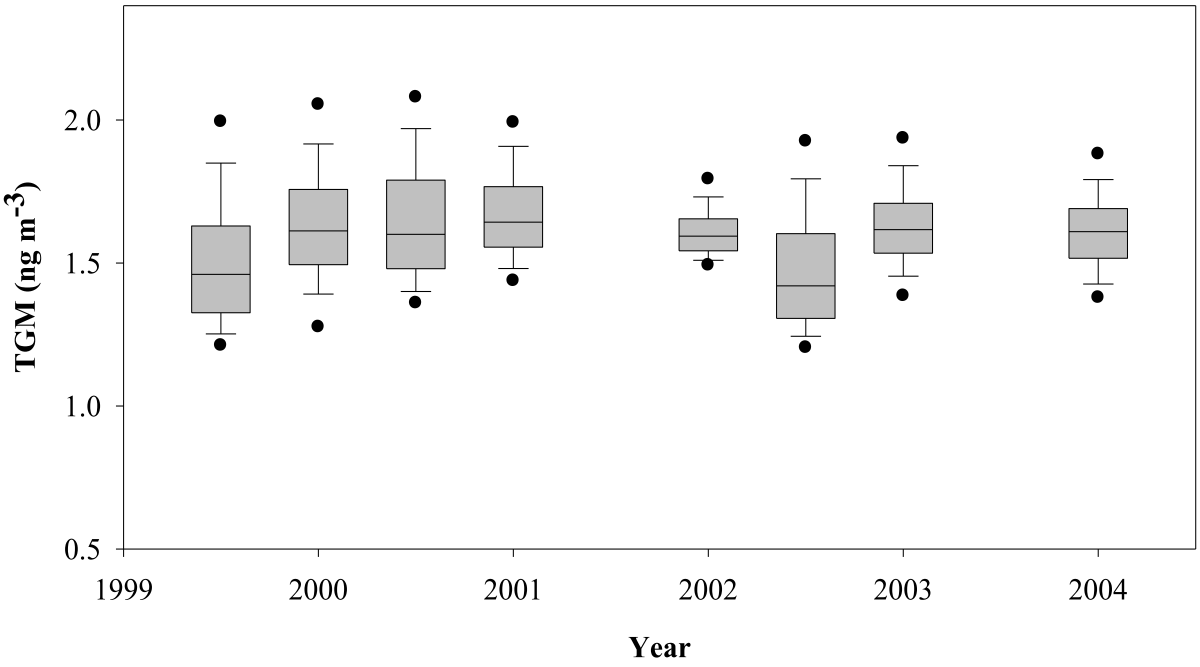

Figure 2.1: Box plots of interannual TGM concentration at Great Mountain Forest, CT, 1999-2004. Median, 10th, 25th, 75th and 90th percentile values are shown. Mid-year data points represent summertime data, and all others are wintertime.

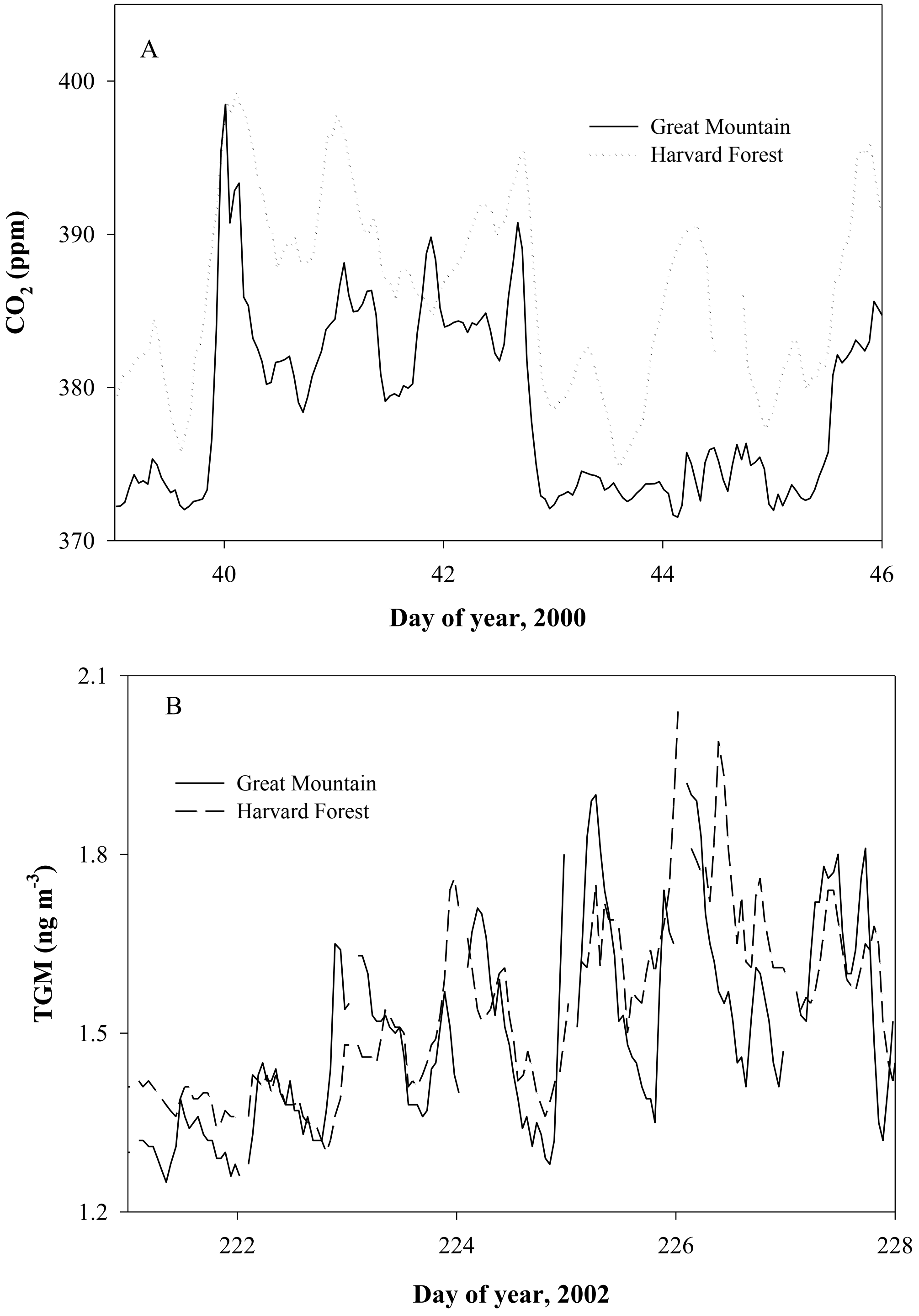

Figure 2.2: (A) Temporal variation in ambient CO_2 measured at Harvard Forest (MA) and Great Mountain Forest (CT) during winter 2000 and (B) TGM at Great Mountain and Harvard Forest during summer 2002. The small difference in CO_2 concentrations at both sites is due to different calibration standards

in TGM during the summer of 2002 when both sites were equipped with TGM monitors (Figure 2.2b). Given the distance between the sites, the elevated TGM concentrations at Great Mountain are caused by regional, rather than local, pollution sources. Therefore, Great Mountain is a site of regional character and suitable for tracer analysis.

2.3.2. Tracer analysis of TGM:C emissions ratio

Wintertime correlation between CO_2 and TGM at Great Mountain showed R^2 values ranging from 0.38 to 0.59 ($p<0.01$), with the number of observations ranging between 800 and 1650 for each winter. The strength of these correlations supports the use of CO_2 as a tracer for Hg as they are generally comparable to other tracer studies [e.g., *Bakwin et al.*, 1997; *Potosnak et al.*, 1999]. Figure 2.3 (open circles) shows the derived TGM:C emissions ratio for each winter. The largest incremental change was observed between the winters of 1999/2000 and 2000/2001, when the emissions ratio declined by more than 40%. However, after a further decline in the winter of 2001/2002, a gradual increase was observed since that year. The tracer analysis suggests that, unlike the trend in mean TGM concentration (Figure 2.1), the regional TGM emission rate in the northeast may vary significantly from year to year.

2.3.3. Potential source regions for TGM

There are two lines of argument for the observed interannual variation in regional TGM emission as revealed by the atmospheric measurements. First, interannual changes in the source region impacting Great Mountain may lead to changes in the measured correlation between Hg and CO_2 irrespective of any actual interannual variation in emissions. For this to occur, the emission source types and hence the resulting Hg:C

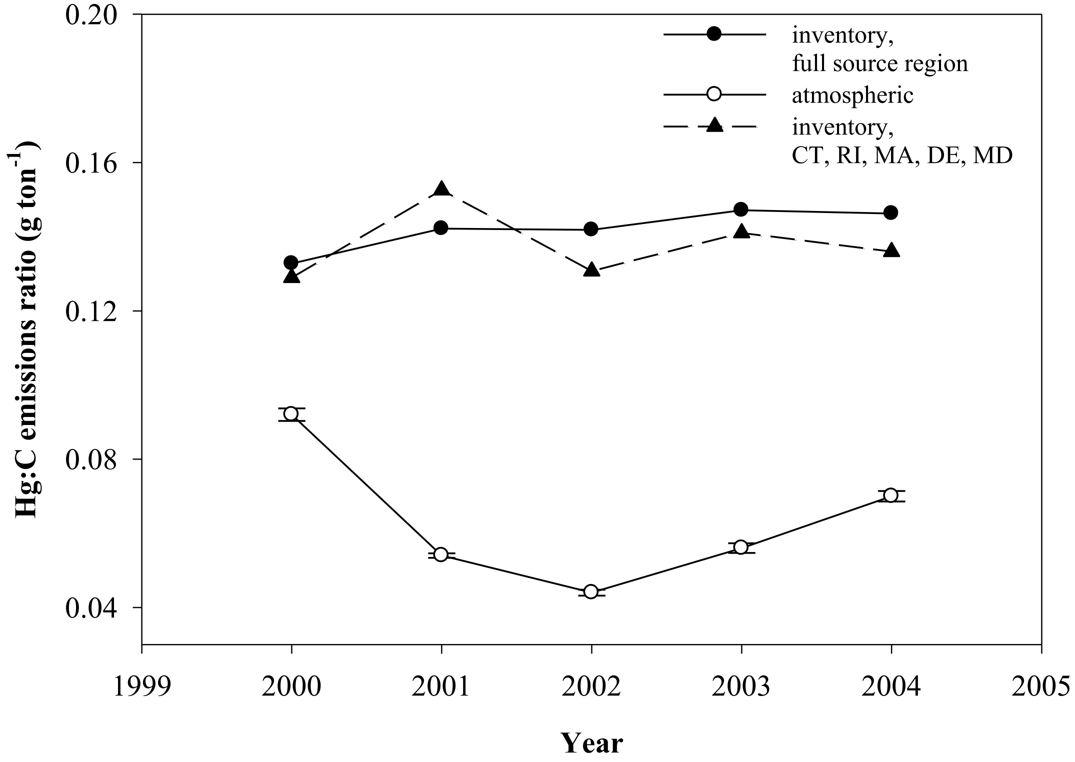

Figure 2.3: Comparison of wintertime Hg:C emission ratios derived from atmospheric measurement and those derived from inventory fuel consumption data for electric power sector. Error bars on atmospheric plot are 95% confidence intervals.

emissions ratio must vary geographically. The second argument is that there are changes in the major anthropogenic sources of Hg (e.g., changes in capacity, activity levels, emission category, fuel type, or control technology) which would lead to actual interannual variation in emission.

The first line of argument was tested by building PSCF maps for each year. The potential source map for 1999/2000, which exhibited the highest TGM:C emissions ratio during the 5-year study period, is shown in Figure 2.4. For comparison, Figure 2.5 shows the potential source region for 2001/2002, when the lowest emissions ratio was observed.

The highest-value cells for 1999/2000, which could be viewed as more likely source regions (Figure 2.4), lie in southeastern Pennsylvania, centered approximately over Philadelphia, with slightly lower though still high values reaching into lower Pennsylvania and central/lower New Jersey. This is an area determined by *EPA* [1997] to have a high anthropogenic Hg emission rate. There were also potential source regions in northern New York State, Delaware and eastern Maryland, as well as western Pennsylvania (Pittsburgh). Coal-burning power plants are the most important point sources of Hg in all of these areas (see section 2.2.4).

The potential source region for 2001/2002 (Figure 2.5) was similar to that derived for 1999/2000, although somewhat less extensive and with generally lower probabilities. As in 1999/2000, most of the source region for 2001/2002 lies in the states of New York, New Jersey and Pennsylvania. There was some similarity in the location of cells with the largest probabilities in both Figures 2.4 and 2.5, as high-value cells are found in lower New York, New Jersey, and eastern Pennsylvania. PSCF maps created for the winters of 2000/2001, 2002/2003 and 2003/2004 (not shown) were similar to those shown in

Figures 2.4 and 2.5. In any given year, the most likely source regions tend to lie in Connecticut, western Massachusetts, lower New York, New Jersey, and eastern and northern Pennsylvania. To further illustrate this point, all trajectory and TGM data (1999/2000 –2003/2004) were combined to create a composite source region during the entire study period (Figure 2.6). According to Figure 2.6, the source region encompasses most New England and mid-Atlantic states (CT, MA, RI, NY, NJ, PA), as well as Maryland and Delaware, with the most likely source regions being lower New York, New Jersey, eastern Pennsylvania, and the upper Chesapeake Bay area (Maryland, Delaware).

The PSCF analysis suggests that interannual, climatological changes in geographic source region are, at the most, mitigating factors affecting the correlation analysis. Visual inspection of Figures 2.4 and 2.5 indicate some differences in probability and size of the total source region and therefore perhaps some degree of climatological influence on the estimate of TGM emission rate. However, there was significant overlap in both total source region (low and high-probability cells combined) and likeliest source regions (high-probability cells) among all winters. Furthermore, regional emissions ratio derived from fuel consumption inventory data did not reveal much sensitivity to change in the geographic size of the source region (Figure 2.3). Thus, it can be concluded that changes in source region cannot explain the observed interannual variation in the emissions ratio, especially the difference of nearly 50% in the Hg:C emissions ratio between 1999/2000 and 2001/2002.

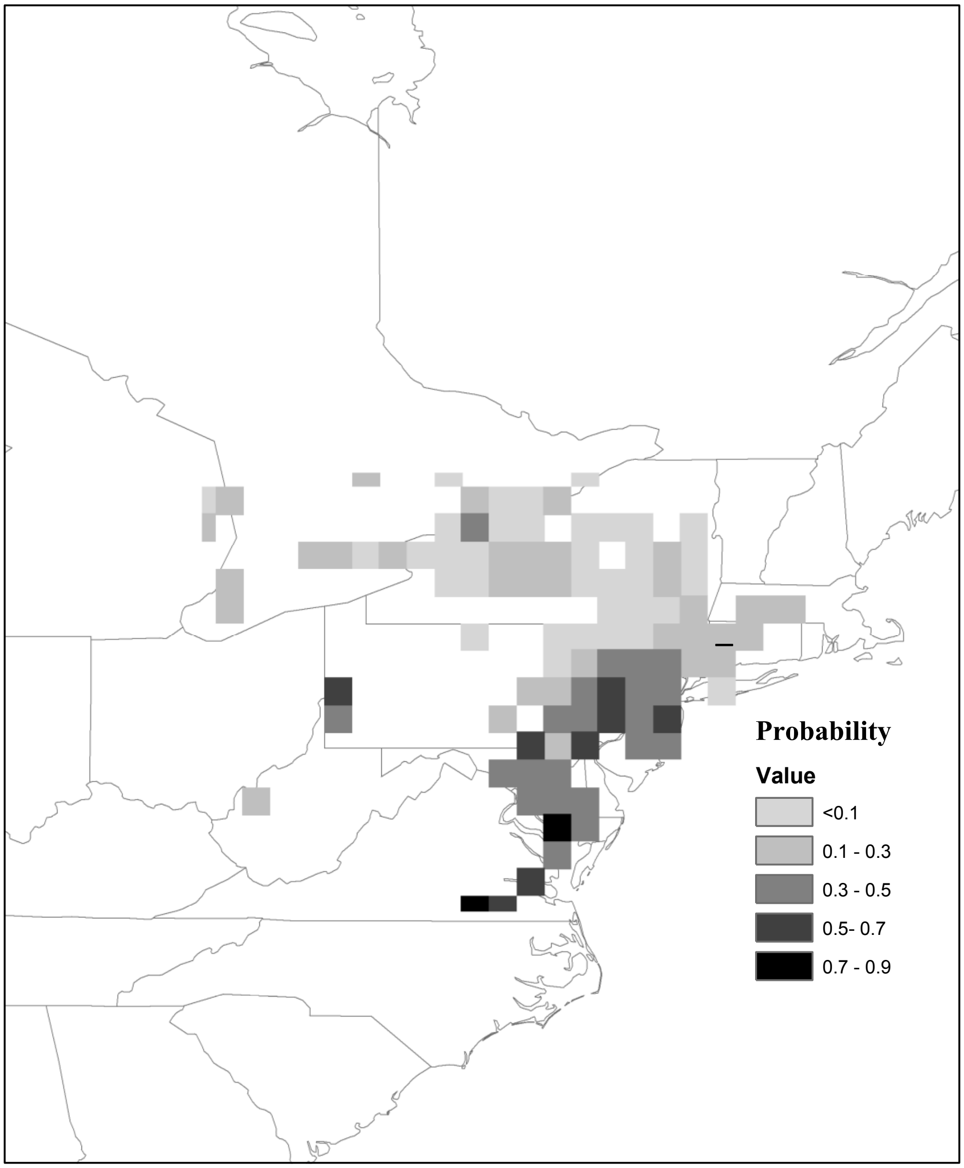

Figure 2.4: Map of the northeast U.S. showing PSCF grid values during winter 1999/2000. The star marks the location of Great Mountain.

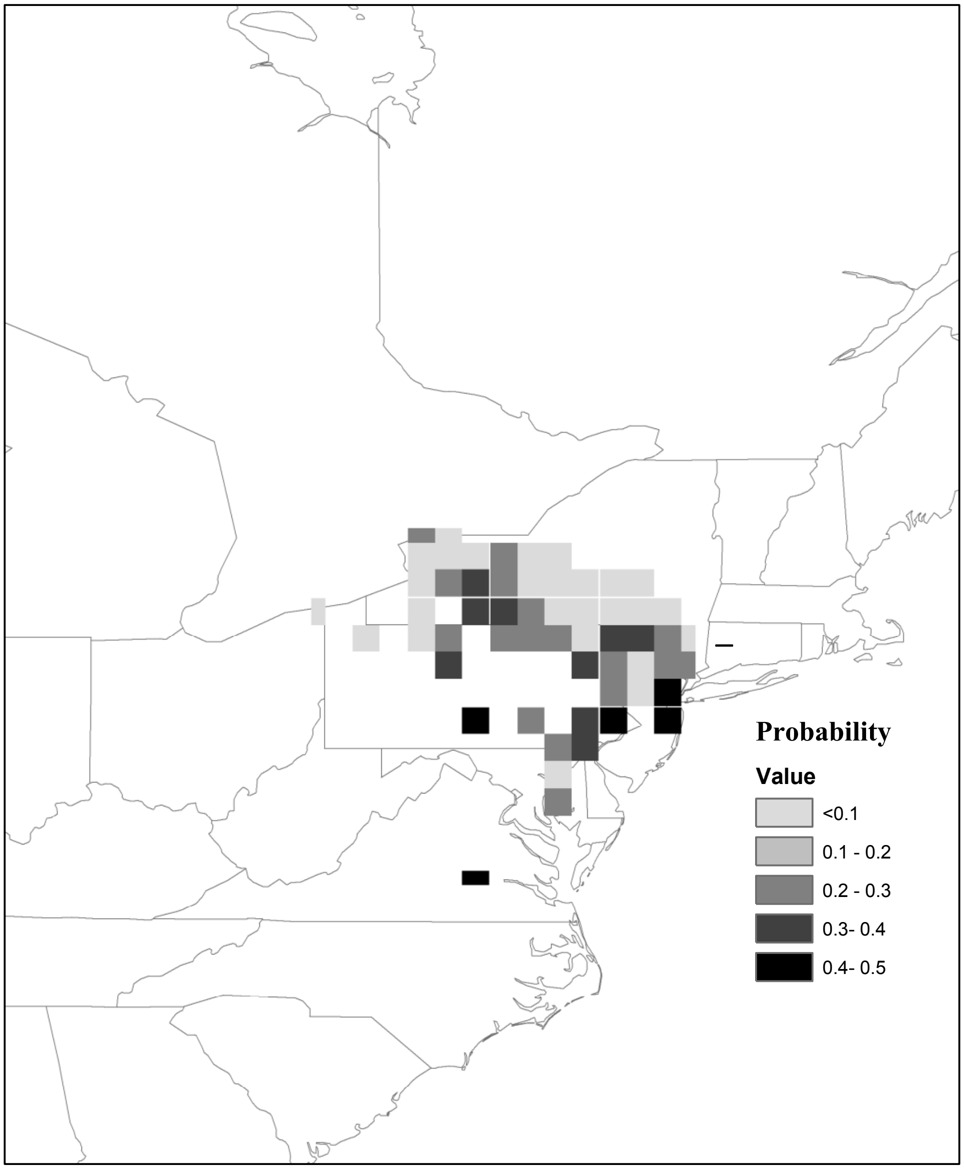

Figure 2.5: As in Figure 2.4, except for 2001/2002.

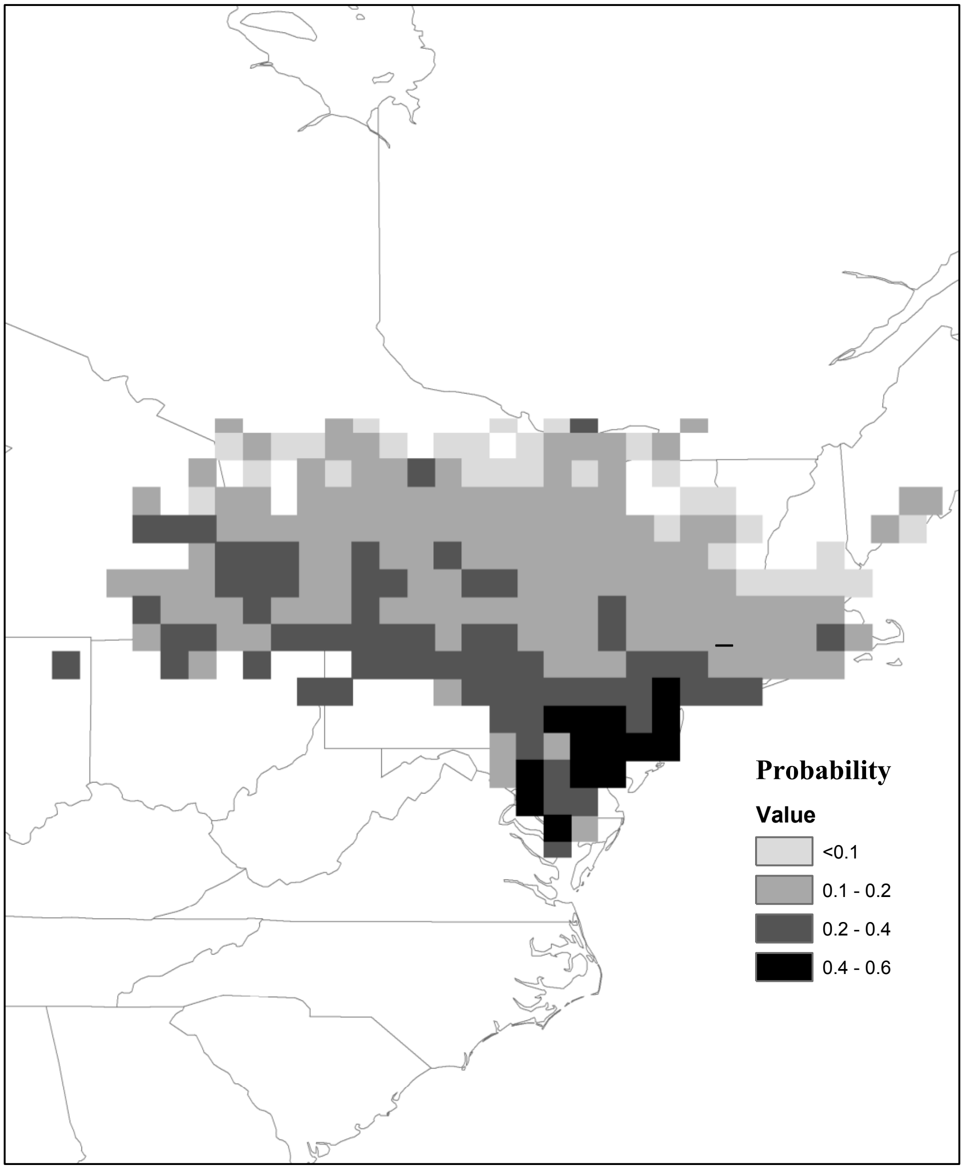

Figure 2.6: As in Figures 2.4 and 2.5, except for the entire study period (1999/2000-2003/2004).

2.3.4. Hg:C emissions ratio based on fuel consumption

The fact that the interannual variation in the source region cannot explain the observed change in the emissions ratio urges testing of the line of argument that the observed changes in the Hg:C emissions ratio, and therefore the regional TGM emission rate, were related to interannual changes in the anthropogenic sources themselves. Emphasis was placed on one factor, change in fuel type in the electric power sector, as the inventory data are more or less complete. Hg:C emission ratios from the electric power sector within the source region depicted in Figure 2.6, and as outlined in section 2.2.4. It should be noted that there is a high level of uncertainty in Hg emission factors and heat content among different types of coal and petroleum, as well as the influence of coal cleaning and Hg control technology, which was ignored here.

Figure 2.3 presents the results along with the observed emissions ratio. In general, the emissions ratio derived from the fuel inventory data was higher than the measured value at Great Mountain, by an average of 0.08 g ton^{-1} over the five year period. This is not surprising since power plants are a mercury-rich point source and should therefore have a higher bulk Hg:C emission ratio than what was observed at Great Mountain, which includes area, combustion and other, cleaner point sources which are relatively dilute with Hg. Exclusion of the mid-Atlantic states (New York, New Jersey, Pennsylvania) from the source region resulted in a slight decrease in the emissions ratio by an average of 0.008 g ton^{-1} over the five year period. The change however was much smaller than the observed interannual variability, supporting the interpretation that interannual variability in source region cannot explain the observed change in the

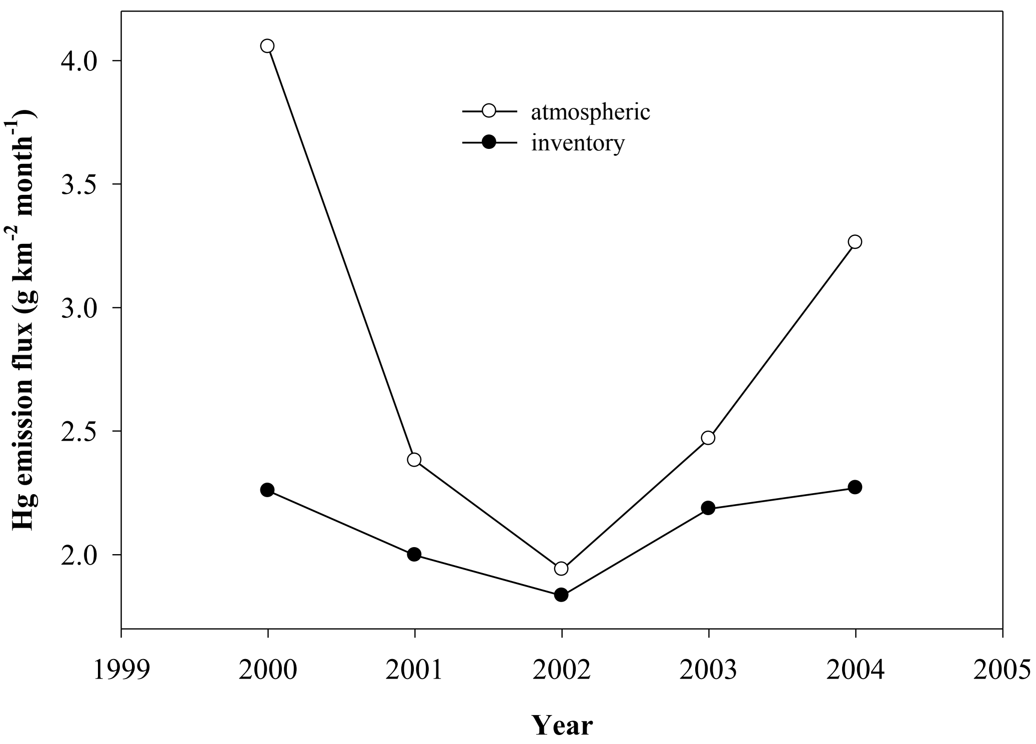

Figure 2.7: Two estimates of wintertime Hg emission flux over the whole source region. The linear correlation coefficient of the two estimates is 0.81.

emissions ratio. Another important point is that the observed interannual variability is absent in the inventory data.

2.3.5. Regional mercury flux

Figure 2.7 presents two estimates of monthly Hg emission flux over the source region for the winter season (January to April). The inventory flux estimate was computed as the product of the C emission flux from the electric power sector and the inventory Hg:C emissions ratio (Figure 2.3). The atmospheric flux estimate was computed as the product of the emissions ratio derived from the tracer correlation analysis and the total C emission flux over the source region. As stated above, the total C flux was held at a constant of 529 Mg C km^{-2} yr^{-1} over the study period, whereas the power sector C flux was computed annually from the inventory data. The total C flux is not sensitive to the interannual variation of the power sector C flux as the latter typically contributes 26-28% to the total annual C flux in the U.S. [*EIA*, 2004c]. For example, the power sector C flux decreased by ~20% from 2000 to 2001, while the state-by-state total C flux over the source region decreased by only ~3% over the same period [*Blasing et al.*, 2004].

The two Hg flux estimates displayed a high degree of correlation (linear correlation coefficient of 0.81), with a clear declining trend from 1999 to 2002 and an increasing trend from 2002 to 2004. Therefore, electricity generation plays a discernable role in the interannual variation of Hg flux to the atmosphere, and makes a significant contribution to the regional atmospheric Hg budget.

Averaged over the five winters, the Hg flux from the power sector was 2.1 g km^{-2} $month^{-1}$ and was only 75% of the flux from the atmospheric tracer analysis (2.8 g km^{-2}

month^{-1}). This result is striking given the perceived reduction in emissions from municipal and medical waste combustion. According to *EPA* [1997], in the mid 1990s emissions from municipal and medical waste combustion were approximately 43% of the total anthropogenic emission to the atmosphere in the northeastern United States, while electric utilities accounted for approximately 25%, commercial and industrial boilers produced approximately 23%, with the remaining 9% from minor sources such as cement manufacturing and sewage sludge incineration. The EPA new source performance standards of 1997 sought to reduce emissions from municipal waste combustion as well as medical waste incinerators by >90% by 2000. If this goal was achieved and emissions from other sources are assumed to have remained unchanged since 1995, the power sector emission would become by far the dominant source category over the study period, contributing no less than ~75% to the total emission over the source region.

TGM measurements used in the tracer analysis are assumed to be >95% Hg^0 [*Lindberg and Stratton*, 1998], while at least half of the power sector emission is thought to be in reactive and particulate form [*Galbreath and Zygarlicke*, 1996; *Prestbo and Bloom*, 1995; *Carpi,* 1997; *EPA*, 1997] and thought to deposit locally near the source [e.g., *Bullock et al.*, 1998]. This means that under the assumption of 50% speciation from electricity generators [*EPA*, 1997], the electric power sector in the source region can account for, on average, approximately 40% of the observed elemental Hg flux to the atmosphere. The disparity is even larger under the consideration that in the inventory calculation, an Hg emission factor for coal that did not account for advanced control technology was used, or that some studies have shown that reactive Hg may comprise significantly more than 50% of total Hg emitted from electricity generators [60-80%; *Prestbo and Bloom*, 1995; *Carpi,* 1997].

Several possible explanations exist for the large disparity between the atmospheric and electric power inventory Hg flux. One possibility is that the percentage of reactive Hg emitted into the atmosphere by coal combustion is much lower than expected. However, if this is the case, essentially all of the Hg emitted by the power sector would need to be elemental in order to account for at least 75% of the atmospheric flux as suggested by *EPA* [1997]. Another possibility is that emissions from municipal and medical waste combustion have not been reduced to the level targeted by EPA in 1997 and still contribute significantly to the regional Hg emission rate, or that other sources outside the power sector, such as area or manufacturing sources, make a previously underestimated contribution to regional emissions. In any case, this study underscores the incomplete state of knowledge of Hg emission sources, and suggests that policy strategies for abatement of regional Hg pollution should not focus solely on the electric power sector. However, it must be emphasized that Figure 2.7 clearly demonstrates the importance of the electric power sector in regional Hg emissions in the northeast. Figure 2.7 both emphasizes the criticality of power plants to regional-scale Hg emissions in the northeast, and demonstrates that the relative contributions of other sources are poorly understood.

A major uncertainty in this analysis is the Hg emission factor for coal combustion. The Hg emission factor used for coal (10 lb/trillion Btu) was based on the median value reported by *Chu and Porcella* [1995]) and *EPA* [1989] for coal-burning power plants that deployed minimal air pollution control, usually for particulate removal and typically an electrostatic precipitator. This emission factor is uncertain, as the few data that exist are highly variable. For example, the measurements of *Chu and Porcella* [1995] ranged from 4 to 22 lb/trillion Btu.

EPA [1997] used an Hg emission factor of 16 lb/trillion Btu for uncontrolled, uncleaned coal. This is unrealistically high, as all coal-burning power plants are at least outfitted with particulate control technology and usually burn cleaned coal, and typical control technology is thought to remove approximately 40% of Hg released from coal combustion in the U.S. [*EPA*, 1997; *EPRI*, personal communication]. Combining the total Hg emission from utilities reported by *EPA* [1997] with a heat content and total coal consumption for 1994 yields an emission factor of approximately 12 lb/trillion Btu, which would bring the inventory flux slightly closer to the atmospheric estimate but would not alter the conclusion that total Hg emissions from the electric power sector was much lower than anticipated. In fact, even if an uncontrolled emissions factor is assumed, the inventory flux for the power sector can only account for less than 60% of the atmospheric (primarily elemental) Hg flux. It should also be noted that some plants include flue gas desulfurization systems that are much more effective for Hg removal than the minimum control technology assumed in this study (*Chu and Porcella* [1995]). In addition, the emission factor used for oil combustion (6.8 lb/trillion Btu) is the same one used by *EPA* [1997]. More recent evidence suggests that this emission factor may be an order of magnitude too high [*Chu and Porcella*, 1995; *EPA*, 1995]. Substituting a lower emission factor for oil combustion (e.g., 0.46 lb/trillion Btu as reported by *Chu and Porcella* [1995]) would actually lower the electric power sector emission estimate even further (by, on average, 15%).

2.4. Conclusions

The combination of trajectory modeling and long-term tracking of the regional TGM emission rate by tracer analysis presented in this study provides a generally applicable framework for timely assessment of trends in regional-scale emission of Hg and other pollutants. This framework may enhance our ability to detect annual or seasonal changes in emission, determine source region of pollutants and evaluate the effectiveness of legislative strategies for reducing pollutant emissions.

This study reveals that the regional Hg emission rate in the northeast U.S. can change significantly on an annual basis. After a 40% decrease from 1999/2000 to 2001/2002, the Hg emission rate increased steadily between the winters of 2001/2002 and 2003/2004. Trajectory analysis revealed little interannual variation in source region, suggesting that the significant variation in emissions cannot be explained by climatological impacts. The strong correlation between the trend in Hg fluxes calculated from inventory consumption data from the electric power sector and the atmospheric tracer analysis indicates that regional-scale emissions of Hg are highly sensitive to interannual variation in coal and petroleum consumption by the electric power sector in the source region.

Despite uncertainty in the Hg emission factor from coal combustion, the inventory Hg flux for the electric power sector was lower than anticipated when compared to the regional, atmospheric flux estimate. Coal-burning power plants are a focal point of pollution abatement strategies because they are thought to be by far the dominant anthropogenic source of Hg in the northeast, especially given the perceived reduction in emissions from municipal and medical waste combustion during the past 10 years. Results presented here underscore their importance to regional Hg emissions but suggest that other sources may be of more importance than previously thought. While the ultimate explanation for the discrepancy between the atmospheric measurement and the power sector Hg flux is not clear, possible explanations are that power plants emit a larger percentage of elemental Hg than believed, Hg emissions from municipal and medical waste combustion have not been curtailed to the targeted level in the northeast, or that there is another anthropogenic source that has been grossly underestimated.

The significant interannual variation in the observed Hg emission highlights the importance of long-term observations and the tracer analysis. Given the complexity among Hg source categories, changing nature of control technologies, large uncertainty in emission factor estimates, and logistical limitations, the inventory approach is an unsatisfactory means of understanding Hg emission. The “top-down” approach of the atmospheric tracer correlation method provides near real-time estimates of emission of toxic pollutants with less uncertainty. This approach may therefore be a valuable means of evaluating the progress of policy strategies for pollution abatement.

Acknowledgements

Thanks to Dr. J. William Munger of Harvard University for access to Harvard Forest CO_2 data as well as the use of the Harvard Forest tower to measure TGM during the summer of 2002. Dr. N.J. Themilis of Columbia University provided helpful information regarding combustion sources of Hg in the northeast. Funding for CO_2 measurements was supported by the Biological Environmental Research Program (BER), U.S. Dept. of Energy, through the northeast regional center of the National Institute for Global Environmental Change (NIGEC) under Cooperative Agreement No. DE-FC03-90ER61010, and by in-kind contribution from the Great Mountain Forest Corporation, Connecticut.

2.5. References

Andres, R.J., Marland, G., Fung, I., and Matthews, E.A. (1996), 1° x 1° distribution of carbon dioxide emissions from fossil fuel and cement manufacture, 1950-1990, *Global Biogeochem. Cycles*, 10, 419-429.

Bakwin, P.S., Tans, P.P., and Novelli, P.C. (1994), Carbon monoxide budget in the Northern Hemisphere, *Geophys. Res. Lett.*, 21, 433-436.

Bakwin, P.S., Hurst, D.F., Tans, P.P, and Elkins, J.W. (1997), Anthropogenic sources of halocarbons, sulfur hexaflouride, carbon monoxide and methane in the southeastern United States, *J. Geophys. Res.*, 102, 15915-15925.

Blasing, T.J., C.T. Broniak, and G. Marland (2004), Estimates of Annual Fossil-Fuel CO_2 Emitted for Each State in the U.S.A. and the District of Columbia for Each Year from 1960 through 2001. In Trends: A Compendium of Data on Global Change, Carbon Dioxide Information Analysis Center, Oak Ridge National Laboratory, U.S. Department of Energy, Oak Ridge, TN, U.S.A.

Blasing, T.J., C.T. Broniak, and G. Marland (2005), The annual cycle of fossil-fuel carbon dioxide emissions in the United States, *Tellus B*, 57, 107-115.

Brunke, E.-G., Labuschagne, C., and Slemr, F. (2001), Gaseous mercury emissions from a fire in the Cape Peninsula, South Africa, during January 2000, *Geophys. Res. Lett.*, 28, 1483-1486.

Bullock, O.R., Brehme, K.A., and Mapp, G.R. (1998), Lagrangian modeling of mercury air emission, transport, and deposition: an analysis of model sensitivity to emissions uncertainty, *Sci. Tot. Env.*, 213, 1-12.

Carpi, A. (1997), Mercury from combustion sources: A review of the chemical species emitted and their transport in the atmosphere, *Water Air Soil Poll.*, 56, 745-767.

Chen, H., Yang, X., and Perkins, C. (2004), Trend and variability of total gaseous mercury (TGM) in the state of Connecticut during 1997-1999, *Water Air Soil Poll.*, 151, 103-116.

Cheng, M.-D., Hopke, P.K., Barrie, L., Rippe, A., Olson, M., and Landsberger, S. (1993), Qualitative determination of source regions of aerosol in Canadian high Arctic, *Env. Sci. Tech.*, 27, 2063-2071.

Cheng, M.-D. and Schroeder, W.H. (2000), Potential atmospheric transport pathways for mercury measured in the Canadian high Arctic, *J. Atmos. Chem.*, 35, 101-107.

Chu, P. and Porcella, D.B. (1995), Mercury stack emissions from U.S. electric utility power Plants, *Water Air Soil Poll.*, 80, 135-144.

Cooper, O.R., Moody, J.L., Thornberry, T.D., Town, M.S., and Carroll, M.A. (2001), PROPHET 1998 meteorological overview and air-mass classification*, J. Geophys. Res.*, 106, 24289-24299.

Draper, N.R. (1992), Straight line regression when both variables are subject to error, Tech Rep. No. 890, Dept. of Statistics, Univ. of Wisconsin, Madison, 18pp.

Draxler, R.R., and Hess, G.D. (1997), Description of the HYSPLIT_4 Modeling System, NOAA Technical Memorandum ERL ARL-224, 24 pp.

EIA (United States Energy Information Administration) (2004a), Electric Power Annual 2003, www.eia.doe.gov/cneaf/electricity/epa/epa_sum.html.

EIA (2004b), Annual Energy Review 2003, www.eia.doe.gov/aer/.

EIA (2004c), Emissions of Greenhouse Gases in the United States, www.eia.doe.gov/oiaf/1605/ggrpt/index.html.

EIA (2005), Monthly Energy Review (Archives), www.tonto.eia.doe.gov/ FTPROOT/ monthlyhistory.htm.

EPA (United States Environmental Protection Agency) (1997), Mercury Study Report to Congress, www.epa.gov/mercury.html.

EPA (2005), AP-42, Compilation of air pollutant emission factors, www.epa.gov/ttn/chief/ap42/index.html.

EPRI (Electric Power Research Institute) (1996), Mercury in the Environment – A Research Update, Final Report. Palo Alto, CA, USA.

Friedli, H.R., Radke, L.F., Lu, J.Y., Banic, C.M., Leaitch, W.R., and MacPherson, J.I. (2003), Mercury emissions from burning of biomass from temperate North American forests: laboratory and airborne measurements, *Atmos. Env.*, 37, 253-267.

Galbreath, K.C., and Zygarlicke, C.J. (1996), Mercury speciation in coal combustion and gasification flue gases*, Env. Sci. Tech.*, 30, 2421-2426.

Kim, K.-H., Lindberg, S.E., and Meyers, T.P. (1995), Micrometeorological measurements of mercury vapor fluxes over background forest soils in eastern Tennessee, *Atmos. Env.,* 29, 267-282.

Kim, K., and Kim, M. (2001), The temporal distribution characteristics of total gaseous mercury at an urban monitoring site in Seoul during 1999-2000, *Atmos. Env.*, 35, 4253-4263.

Landis, M.S., Vette, A.F., and Keeler, G.J. (2002), Atmospheric mercury in the Lake Michigan Basin: Influence of the Chicago/Gary urban area, *Env. Sci. Tech.*, 36, 4508-4517.

Lee, X., Bullock, O.R., and Andres, R.J. (2001), Anthropogenic emission of mercury to the atmosphere in the northeast United States, *Geophys. Res. Lett.*, 28, 1231-1234.

Lin, C.-J., Cheng, M.-D., and Schroeder, W.H. (2001), Transport patterns and potential sources of total gaseous mercury measured in Canadian high Arctic in 1995, *Atmos. Env.*, 35, 1141-1154.

Lindberg, S.E., and Stratton, W.J. (1998), Atmospheric mercury speciation: Concentrations and behavior of reactive gaseous mercury in ambient air, *Env. Sci. Tech.*, 32, 49-57.

Massachusetts Department of Environmental Protection (MA DEP) (2002), Municipal Waste Combustor Facility and Trend Reports, www.mass.gov/dep/mwc/mwcfr.htm.

Moody, J.L., Munger, J.W., Goldstein, A.H., Jacob, D.J., and Wofsy, S.C. (1998), Harvard Forest regional-scale air mass composition by Patterns in Atmospheric Transport History (PATH), *J. Geophys. Res.,* 103, 13181-13194.

Nadim, F., Perkins, C., Liu, S., Carley, R.J., and Hoag, G.E. (2001), Long-term investigation of atmospheric mercury contamination in Connecticut, *Chemosphere*, 45, 1033-1043.

Poissant, L. (1999), Potential sources of atmospheric total gaseous mercury in the St. Lawrence River valley, *Atmos. Env.*, 33, 2537-2547.

Potosnak, M.J., Wofsy, S.C., Denning, A.S., Conway, T.J., Munger, J.W., and Barnes, D.H. (1999), Influence of biotic exchange and combustion sources on atmospheric CO_2 concentrations in New England from observations on a forest flux tower, *J. Geophys. Res.,* 103, 9561-9569.

Prestbo, E.M., and Bloom, N.S. (1995), Mercury speciation adsorption (MESA) method for combustion flue gas methodology, artifacts, intercomparison and atmospheric implications, *Water Air Soil Poll*., 80, 145-158.

Richardson, A.D. (2000), Coarse root elongation rate estimates for interior Douglas-fir, *Tree Physiology*, 20, 825-829.

Sigler, J.M., Lee, X., and Munger, W. (2003), Emission and long-range transport of gaseous mercury from a large-scale Canadian boreal forest fire, *Env. Sci. Tech.*, 37, 4343-4347.

Slemr, F., Schuster, G., and Seiler, W. (1985), Distribution, speciation and budget of atmospheric mercury, *J. Atmos. Chem.*, 3, 407-434.

Stehr, J.W., Dickerson, R.R., Hallock-Waters, K.A., Doddridge, B.G., and Kirk, D. (2000), Observations of NO_y, CO and SO_2 and the origin of reactive nitrogen in the eastern United States, *J. Geophys. Res.*, 105, 3553-3563.

Suntharalingam, P., Jacob, D.J., Palmer, P.I., Logan, J.A., Yantosca, R.M., Xiao, Y., and Evans, M.J. (2004), Improved quantification of Chinese carbon fluxes using CO_2/CO correlations in Asian outflow, *J. Geophys. Res.*, 105, Art. No. D18S18.

Themelis, N.J., and Gregory, A.F. (2002), Mercury emissions from high-temperature sources in the NY/NJ Hudson-Raritan basin, *Amer. Soc. Mech. Eng. Proc. NAWTEC* 10, pp. 205-215.

Wang, T., Cheung, T.F., Li, Y.S., Yu, X.M., and Blake, D.R. (2002), Emission characteristics of CO NO_x, SO_2 and indications of biomass burning observed at a rural site in eastern China, *J. Geophys. Res.*, 107 Art. No. 4157.

Wofsy, S.C., Fan, S.-M., Blake, D.R., Bradshaw, J.D., Sandholm, S.T., Singh, H.B., Sachse, G.W., and Harris, R.C. (1994), Factors influencing atmospheric composition over subarctic North America during summer, *J. Geophys. Res.*, 99, 1887-1897.

Xiao, Z.F., Munthe, J., Schroeder, W.H., and Lindqvist, O. (1991), Vertical fluxes of volatile mercury over forest soil and lake surface in Sweden, *Tellus*, 43, 276-279.

Chapter 3:

[2]Gaseous mercury in background forest soil in the northeastern United States

---

[2] Manuscript accepted by *Journal of Geophysical Research – Biogeosciences,* February, 2006.

Abstract

Although the soil gaseous mercury (Hg) reservoir is an important component of the soil Hg emission process, little is known of the behavior of gaseous Hg in soil pores and the processes governing the ultimate evasion of Hg from soil surfaces. In this study, gaseous Hg in background forest soil in the northeastern United States was examined during 2003 and 2004 using a novel flask sampling technique. This represents the first detailed study of gaseous Hg concentration within the soil profile. Soil gaseous Hg varied seasonally with soil temperature, and highest concentrations consistently occurred in the O- and upper A-horizons. The study revealed clear gradients in gaseous Hg concentrations, similar to those in bound Hg. In addition, measurements of soil Hg flux were correlated with soil gaseous Hg concentrations at 2-cm depth. These results indicate that the upper soil layers, rich in bound Hg, act as a source of gaseous Hg that may ultimately be emitted to the atmosphere. Large changes in soil gaseous Hg over shallow layers underscore the importance of fine vertical resolution of measurements, and therefore the utility of flask sampling.

3.1. Introduction

The total atmospheric load of mercury (Hg) consists of both anthropogenic and natural sources. Natural source contributions are not known with great certainty. Although anthropogenic sources have been thought to contribute the most to the global Hg cycle [e.g. *Fitzgerald*, 1989; *Schroeder and Munthe*, 1998], natural sources may be more important than previously believed, and possibly of equal importance to anthropogenic sources [*Fitzgerald*, 1995; *Gustin et al.*, 1999]. Research during the past decade has established the importance of soils in environmental Hg cycling, showing that emission from soils, especially naturally enriched substrates, may contribute substantially to the global atmospheric load of Hg [*Gustin et al.*, 1996*; Zhang and Lindberg*, 1999; *Gustin and Lindberg*, 2000; *Engle et al.*, 2001; *Engle and Gustin*, 2002; *Coolbaugh et al.*, 2002].

Understanding and quantifying the mechanisms controlling the exchange of Hg between terrestrial surfaces and the atmosphere is therefore critical toward overall comprehension of the global Hg cycle. However, achievement of this goal is hindered by lack of direct experimental data. Fluxes of Hg from soil and vegetation are influenced by soil temperature, radiation and other meteorological variables [*Lindberg et al.*, 1992; *Kim et al.*, 1995; *Lindberg et al.*, 1998; *Poissant and Casimir*, 1998], and therefore long-term, interseasonal studies may be required to accurately quantify these emissions.

Forest soils receive Hg inputs from throughfall, litter and dry deposition. However, recent studies suggest that Hg emission from forest soil is comparable to or greater than depositional inputs [*Kim et al.*, 1995]. Although net emission from soil is a small percentage of total canopy emission, [*Lindberg et al.*, 1998], the development of global and regional Hg budgets and models is incomplete without a better understanding of Hg exchange over terrestrial surfaces. Knowledge of Hg cycling in and emission from background forest soils (i.e., soils subject to minimal influence from pollution), particularly in the United States, is limited, as few direct experiments have been performed. *Zhang et al.* [2001] measured Hg fluxes over background forest soil in the Michigan Upper Peninsula that were comparable to those measured over forest soils in Canada [*Poissant and Casimir*, 1998] and Sweden [*Schroeder et al.*, 1989; *Xiao et al.*, 1991]. Slightly higher fluxes observed over temperate forest soils in the United States [*Lindberg et al.*, 1995] may reflect the influence of Hg deposition from local emission sources. These studies represent our limited body of knowledge of the magnitude of Hg emission from forest soils.

A more detailed knowledge of not only the magnitude of background forest soil emissions and the environmental variables that influence them, but of the physical and chemical behavior of Hg within soils in general is essential to a full understanding of regional and global Hg budgets. Relatively little experimental evidence exists to confirm modes of Hg transport within and evasion from soil, or the exact desorption sites of oxidized Hg. It is known that oxidized forms of Hg are more prevalent and persistent in soils with high organic matter content [*Yin et al.*, 1997]. Although data are limited, field studies have shown that bound Hg is concentrated in the upper, organic matter-rich soil layers (O and A-horizons) where it is deposited after long-range atmospheric transport and forms stable complexes with humic compounds [*Schlüter*, 2000; *Ambirbahman*, 2004; *Tyler*, 2004].

Mercury vapor exists in the gases that occupy soil pore space, primarily as elemental Hg (Hg0), and has been observed in background soils in concentrations ranging from 1-53 ng m-3 [*Johnson and Lindberg*, 1995]. This gaseous Hg exists in kinetic steady state with Hg in soil solution and its partitioning into the gas phase has been described as a function of the temperature-dependent Henry's Law coefficient [*Scholtz et al.*, 2003].

Although recent experimental evidence suggests that the ultimate release of Hg from soil may not be diffusion-controlled and therefore not purely a function of gaseous Hg concentrations within the soil [*Johnson et al.*, 2003], gaseous Hg is transported over small distances within soil matrices by diffusion, and may be sorbed by the organic matter in the upper soil layers [*Schlüter*, 2000]. Most of the Hg that is ultimately emitted from soil is likely from those layers where the highest concentrations of bound Hg are found, under conditions favoring the formation of volatile, gaseous Hg0 and where little binding to overlying soil layers will occur – i.e., the O and A-horizons [*Schlüter*, 2000]. In those layers, Hg may be desorbed by surface processes such as increases in soil temperature, exchange of Hg sorbed onto soil particles with water molecules, or sunlight-enhanced reactions by which Hg(II) is reduced by humic substances [*Pehkonen and Lin*, 1998; *Lindberg et al.*, 1999; *Scholtz et al.*, 2003], thereby increasing the pool of gaseous Hg0 available for emission. In addition, it has been hypothesized that Hg0 transpired from forest canopies may originate from gaseous Hg0 in soil pores, which provides another impetus for quantifying this parameter.

The soil gaseous Hg reservoir is therefore undoubtedly an important component in the soil Hg emission process. Direct measurements of soil gaseous Hg profiles may be useful toward identifying sites of Hg desorption, or soil layers that act as active sources or sinks of Hg and therefore influence if not govern the ultimate evasion of Hg from soil. However, few field measurements of this kind have been made, owing primarily to the lack of a widely accepted measurement method.

The primary objective of this study was to determine typical gaseous Hg concentrations within background forest soil in the northeast United States. This is intended to be the first detailed study of gaseous Hg in soil. Field data were collected using a novel flask sampling technique (see Appendix) and examined for seasonal variation in soil gaseous Hg concentration and the relationships between soil gaseous Hg and environmental variables. Also, the existence of vertical gradients of gaseous Hg within the soil profile, the sites or layers of active sorption of gaseous Hg within the soil, and the possible relationship of those sites to the ultimate flux of gaseous Hg from the soil surface were investigated.

3.2. Methods

3.2.1. Flask Sampling System

Johnson et al. [2003] measured gaseous soil Hg by inserting Teflon wells to two depths in soil (20 and 40 cm) and withdrawing small air samples with a syringe and found differences in Hg concentration according to well size. These differences were possibly attributable to absorption to the walls of the well or to restriction of diffusion of air to the interior of the well by the presence of the materials. *Wallschläger et al.* [2002] measured gaseous soil Hg at 10-cm depth by pulling air through a steel tube with a Teflon interior at a rate of 1.5 L min-1. Concentrations were diluted by the intrusion of ambient air due to the high flow rate and sample volume. A robust system for measuring gaseous Hg in soil should therefore have the ability to sample known volumes of air with minimal disturbance to the surrounding soil, and promote mass flow into the system without drawing in ambient air from above the surface.

Flask sampling, which has been successfully used to determine carbon dioxide (CO_2) concentrations in both air [*Ehleringer and Cook*, 1998] and at depth in soil [*de Jong and Schappert*, 1972; *Cerling et al.*, 1991; *Hersterberg and Seigenthaler*, 1991; *Wood et al.*, 1993; *Fang and Moncrieff*, 1998], has been largely unexplored as a means of determining soil gaseous Hg concentrations. In this study, a flask sampling system for determining gaseous Hg concentrations at depth in soils was developed and tested in the laboratory, and then used to determine gaseous soil Hg profiles at a background forest site in the northeast United States in field campaigns during consecutive years (2003-2004). This system is low-cost, easy to deploy in the field and is intended to have general applicability to the study of soil Hg and other trace gases.

The flask sampling system developed here entails collection of a soil air sample in a 1-L Teflon flask equipped with three ports and fitted with a steel pressure fixture. Air is drawn into one outer tube port through Teflon tubing (60 cm length, 0.64 cm OD) connected to a Teflon funnel (6.4 cm diameter), which can be placed at varying depths in soil. The funnel is placed aperture-downward in the soil. During field application, soil disturbance during funnel installation could potentially affect vertical variation in soil gaseous Hg. Therefore, soil should be carefully removed by layer and then replaced over the funnel in the same sequence, preserving the existing profile as much as possible.

Also, displaced soil should be allowed to settle around the funnel for several days before sampling. A diagram of the field set-up is shown in the Appendix (Figure A1).

Since more than one week would be required to reach an equilibrium Hg concentration in the flask by diffusion, the collection period is shortened by attaching a low flow (450 mL min-1) pump (model NMP05 minipump, KNF Inc.) to the second outer port. The pump flow is split by flowmeters so that the actual flow out of the soil is normally 20 mL min-1. A small flow rate combined with a large funnel aperture should minimize the intrusion of ambient air. A flow rate of 30 mL min-1 is sufficient to minimize the dilution effect on soil CO_2 measurements [*Fang and Moncreif*, 1998]. Also, vertical air speed caused by natural wind pumping in the top 10 cm of the soil is in the range of 10-4 to 10-2 m s-1 [*Farrell et al.*, 1966; *Colbeck*, 1989]. Air speed produced by the flask sampling should be smaller than this to minimize ambient air intrusion. In the system described here, the vertical air speed across the funnel aperture is 9×10-5 m s-1**.** This flow is lower than that used for soil CO_2 in *Fang and Moncrieff* [1998] and should hasten the flushing without creating suction and drawing in ambient air.

Air is collected over a 4-hour period, and is therefore cycled through the flask volume approximately five times to ensure thorough flushing. The flask is then detached from the funnel tubing and connected via a valve assembly (Figure 3.1) to a mercury vapor analyzer (model 2537A, Tekran, Inc., Toronto, Canada), which produces 5-minute averages of total gaseous mercury (TGM). The valve assembly consists of three solenoid valves (Tekran, Inc.), each with three ports. The common ports on each valve, labeled as ‘c’ in Figure 3.1, connect the analyzer sample stream to a “zero” (or clean) air canister by Teflon tubing. In the default mode (valves not energized), the zero air bypasses the flask and enters the analyzer. When valve III is energized, the analyzer samples ambient air near the soil surface. In order to analyze the TGM concentration inside the flask, the flask is first attached to ports 2 on valves I and II, and valve III is deactivated so that ambient air is no longer drawn into the analyzer. Valves I and II are then energized, the flask ports are opened and the flask air is drawn into the analyzer using the zero air as carrier.

While sampling zero air, the analyzer may detect small blank, or baseline, levels of TGM (typically ≤0.1 ng m-3). Accordingly, the flask should be flushed for three to four additional 5-minute cycles after the soil air sample is released into the analyzer, so that the blank concentration is determined. By recovering the blank, the sample concentration can be more accurately determined by subtracting the average blank from that of the detected sample concentration.

Preliminary field testing of the system indicated that a dry flask and zero air stream is desirable. Moist air within the flask or the valve assembly may result in high blanks and an inability to determine a flask TGM concentration above baseline. This problem is minimized by operating in dry conditions and by allowing the incoming air stream to pass through a container of silica gel desiccant before the zero air canister (Figure 3.1).

3.2.2. Site description and Hg profile measurements

Measurements of soil gaseous Hg were taken at a forested site in Coventry, Connecticut (CT), United States (41 ° 47" N, 72 ° 21" W) during separate field campaigns in 2003 (July-November) and 2004 (May-October). The site, managed by the University of Connecticut (UCONN) Department of Natural Resources Management and Engineering, is a mixed-species forest (primarily red maple, white pine and oak) near an agricultural field. The site is less than 1 km from a heavily traveled road and within 40 km of Hartford, CT and could therefore be subject to local pollution sources. However, mean soil Hg content in the upper 5 cm is 0.24±0.21 μg g-1 [soil samples were collected and analyzed for Hg content (cold vapor atomic absorption spectroscopy) by the UCONN Environmental Research Institute]. Though somewhat higher than background forest soils in Michigan [*Zhang et al.*, 2001], this is comparable to other background sites [*Lindqvist et al.*, 1991; *Kim et al.*, 1995; *Alriksson*, 2001; *Johansson et al.*, 2001; *Grigal*, 2003] and lower than U.S. forest soils impacted by local pollution sources [*Lindberg et al.*, 1998]. The site can therefore be considered a background site with total soil Hg < 0.5 μg g-1 [*Lindberg et al.*, 1999].

Soil gaseous Hg was measured using a mercury vapor analyzer (model 2537A, Tekran, Inc., Toronto, Canada), which produces 5-minute averages of total gaseous mercury (TGM). TGM includes elemental Hg (Hg0), reactive gaseous mercury (RGM) and particulate Hg. However, soils emit predominantly Hg0 [*Kim et al.*, 1995]. The analyzer was housed in a small shed located on-site. Soil air samples were collected and ultimately analyzed using a flask sampling technique, which has been successfully used to determine carbon dioxide (CO_2) concentrations in both air [*Ehleringer and Cook*, 1998] and at depth in soil [*de Jong and Schappert*, 1972; *Cerling et al.*, 1991; *Hersterberg and Seigenthaler*, 1991; *Wood et al.*, 1993; *Fang and Moncrieff*, 1998], but is unexplored as a means of determining soil gaseous Hg concentrations. A detailed description of the development, testing and field application of this system is provided in the Appendix.

Soil TGM measurements were taken in three separate plots with slightly different elevations and soil characteristics. The plots were laid out along a slope (~25%) with a westerly aspect, and are referred to simply as “west,” “central” and “east.” The west plot was situated on flat ground (~145 meters in elevation) and the east plot furthest upslope (~160 m). All plots lay below thick canopy cover and were therefore primarily shaded and subject to constantly changing light regimes and sun fleck activity.

The plots were characterized by a thin O-horizon (~5 cm for the west plot, 3 cm for the east and central plots). Each O-horizon contained moderately to highly decomposed, amorphous organic matter topped by a thin (~1 cm) layer of slightly decomposed leaf litter. This litter layer was of similar composition for all plots (white pine, red maple, yellow birch and oak). Both the central and west plots contained some small patches of exposed organic matter, while the east plot was completely covered with litter. Each plot contained similar hardwood understory growth, primarily red maple and yellow birch. The east and west plots contained 3-5 seedlings each (≤50 cm in height) and few vascular plants. The central plot was richer in both understory growth (~10 small seedlings) and vascular plants (e.g., oak fern).

In the central and west plots, the O-horizon was underlain by an A-horizon (8-cm) of partially decomposed organic matter and sandy material. The west plot A-horizon was darker and richer in organic matter which was also somewhat more fibrous and less decomposed than the material in the central plot. The west plot also tended to be wettest, as the water table was close (at times within 70 cm) to the surface. Each of these plots was underlain by B-horizons of approximately 8 cm, and a deep C-horizon composed of sand and some organic matter.

In the east plot, the O-horizon was thinner (3 cm) and underlain by a shallow (1 cm) A-horizon and a sandy B-horizon of greater than 20 cm. Both of these horizons were of lighter color than the central and west plots. Although organic matter content was not measured, visual inspection and measurements of percentage of solid matter suggest that organic matter content throughout the profile depth was lowest at the east plot, and highest at the west (UCONN ERI, personal communication, 2004).

During the 2003 field campaign, soil TGM was measured at 5-cm depth at each plot, approximately once per week from early July through September, and sporadically during October and November. A deeper profile was measured at the central plot, with funnels installed at 20 and 50 cm. In this case, funnels were placed 10-15 cm apart laterally in order to avoid disturbance during installation. Typically, samples from different depths were measured in sequence from 5 cm to 50 cm. Profile measurements were performed once per week from mid-July through mid-September.

Surface and profile measurements of soil TGM were repeated in 2004, although the experiment was expanded in several important ways. To better assess TGM gradients within the soil, sampling funnels were installed at 2-cm depth, which is essentially the interface between the litter layer and the upper organic soil layer, at each plot. To better understand vertical and horizontal variability in soil TGM, full profile measurements were taken at all plots, so that each of the three plots had sampling funnels installed at 2, 5, 20 and 50 cm depth. A full profile at one plot was measured per site visit, and two visits per week were made from late May through September of 2004, with several additional visits in October (the full profiles were not installed at each plot until early June).

3.2.3. Flux chamber measurement

To better understand relationships between soil TGM concentrations and evasion of mercury from forest soil, a dynamic flux chamber was used during the 2004 campaign to measure TGM flux from each soil plot during flask collection periods. This is the same chamber used in *Gillis and Miller* [2000a/b], and a full description of its operation can be found in those papers. Briefly, the chamber is a 30 × 60 × 30-cm Teflon box with nine 2.5-cm diameter holes cut into the front. Air was drawn through the chamber by a Teflon tube (OD 0.64 cm) attached to the exhaust side of the chamber. This tube was connected via T-junction to a pump and a 3-way solenoid valve controlled by a CR10X data logger (Campbell Scientific Inc., Logan, UT). A flow meter was used to restrict the flow rate through the chamber to 11.5 L min-1. Uncertainties caused by pressurization effects within flux chambers due to changes in flow rate are well documented [e.g., *Lund et al.*, 1999; *Wallschläger et al.*, 1999; *Lindberg et al.*, 2002]. This flow rate was chosen to be consistent with *Gillis and Miller* [2000a/b] and other studies [*Carpi and Lindberg*, 1998; *Poissant and Casimir*, 1998].

The solenoid valve was also attached to the analyzer sampling line, and another Teflon tube led from the valve to the chamber inlet. The TGM concentration was measured at the chamber inlet and outlet using the same 25-m Teflon line. A 45-second time lag between the data logger and the Hg analyzer was introduced to ensure that the sampling line would be clear of inlet air before the valve switched to outlet sampling (or vice versa). To account for variation in ambient TGM concentration and cartridge bias, fluxes were typically calculated as the average of four inlet samples and two outlet samples (therefore, over a span of 30 minutes). The difference in concentration between inlet and outlet samples (*ΔC*, ng m-3) was used to determine soil TGM flux (*F*) as

$$F = R\left[\Delta C\right]A^{-1}$$

where *R* is air volume flow rate through the chamber (L min-1) and *A* is the area of the exposed soil within the chamber (0.18 m2). Laboratory blanks indicated slight absorption but were not significantly different from zero (-0.1 ± 0.13 ng m-2 hr-1, n=8). Fluxes measured in the field were therefore not corrected for blank values. During each site visit, fluxes were measured concurrently with and in the same plot as soil TGM profile sampling. Typically, 8-10 hourly flux observations were made per site visit.

3.2.4. Supporting measurements

During the flask collection period, the analyzer continuously measured ambient TGM at 40 cm above the soil. Additionally, soil temperature was measured every hour using a hand-held digital thermometer at funnel depth for the 2 and 5-cm measurements, and at 5-cm during the 20 and 50-cm measurements. Soil moisture was measured at 10, 20, 30 and 40 cm using a portable soil moisture probe (PR1, Dynamax, Inc., Houston, TX). Soil moisture data were lacking for most of August 2003 due to a malfunction of this instrument. Incident solar radiation was measured using a homemade solarimeter placed on top of the chamber.

3.3. Results and Discussion

3.3.1. Laboratory test results[3]

Four laboratory experiments were conducted to test the reliability and accuracy of the flask sampling system. The first involved collection and recovery of zero air. The flask was connected to the valve assembly, flushed with zero air for 10-15 minutes, sealed with zero air trapped inside and sampled after periods of 2-12 hours. The second experiment involved collection and recovery of room air. The flask lid was opened for a period of 18-24 hours, allowing room air to enter by diffusion, then sealed and sampled. The third experiment involved direct injection of Hg vapor into the flask. A 50 μL syringe was used to draw known volumes (5 to 30 μL) of saturated Hg vapor from a bottle of pure liquid Hg placed in a water bath at a known temperature. The Hg vapor was injected through a septum into the flask. The mass of injected Hg was determined by multiplying the known concentration of the saturated Hg vapor by the syringe volume. For three of the injections, the flask was left sealed and undisturbed for 14, 19 and 24 hours before sampling, in order to test for slow leakage.

In the fourth experiment, the entire system (flask collection setup and valve assembly) was tested in the laboratory. Room air was pumped through the Teflon funnel and into the flask over a 4-hour period. Simultaneously, valve III was energized (Figure 3.1) and room air was sampled by the analyzer. At the end of the collection period, the analyzer was switched to zero air as the flask was attached. Several 5-minute cycles of zero air were obtained both before and after the flask air was sampled. Unless sorption of

---

[3] This section provides a truncated account of laboratory methodology and test results included in a manuscript submitted for publication. A more detailed version is provided in appendix I.

Hg is occurring within the system, the converted flask concentration should be approximately equal to the average room concentration during the collection period.

Average TGM concentrations recovered from the flask sample in the zero air tests were 0.05 ± 0.02 ng m-3, similar to those in standard, zero air samples, which tend to be <0.1 ng m-3 (during the test, standard zero air concentrations were 0.02 ± 0.04 ng m-3). The same was true when the flask was left undisturbed for a 12-hour period. When the same test was performed with ambient air substituted for zero, TGM concentrations in flask air (2.09 ± 0.38 ng m-3) typically agreed with those of ambient air within approximately 3% (2.15 ± 0.37 ng m-3).

The direct injection experiment yielded a significant linear correlation ($y = 0.14+1.02x$, $r = 0.98$, $n = 27$, where x is injected Hg, y is measured Hg, and r is the linear correlation coefficient) between measured and injected TGM concentrations. No significant differences were observed when the flask was allowed to sit for 14-19 hours between injection and sampling. A somewhat diluted concentration measured after a 24-hour wait between injection and sampling may indicate some slow leakage from the container over periods longer than 19 hours.

Results from the full-system tests are shown in Figure 3.2. In general, good agreement between flask and ambient air was achieved. Two outliers are represented as open circles in Figure 3.2, one indicating under-recovery of flask TGM and the other indicating over-recovery. The latter case, which represents our first room air collection with the funnel setup, is explained by the use of a LDPE funnel, as a Teflon funnel was unavailable at that time (for all other collections, a Teflon funnel was used). The former case may be explained by the fact that the ambient concentration represents a 4-hour average and was biased high by unusually large room air concentrations early during the collection period. Use of the average concentration over the second half of the collection period (2.5 ng m-3) would result in much better agreement.

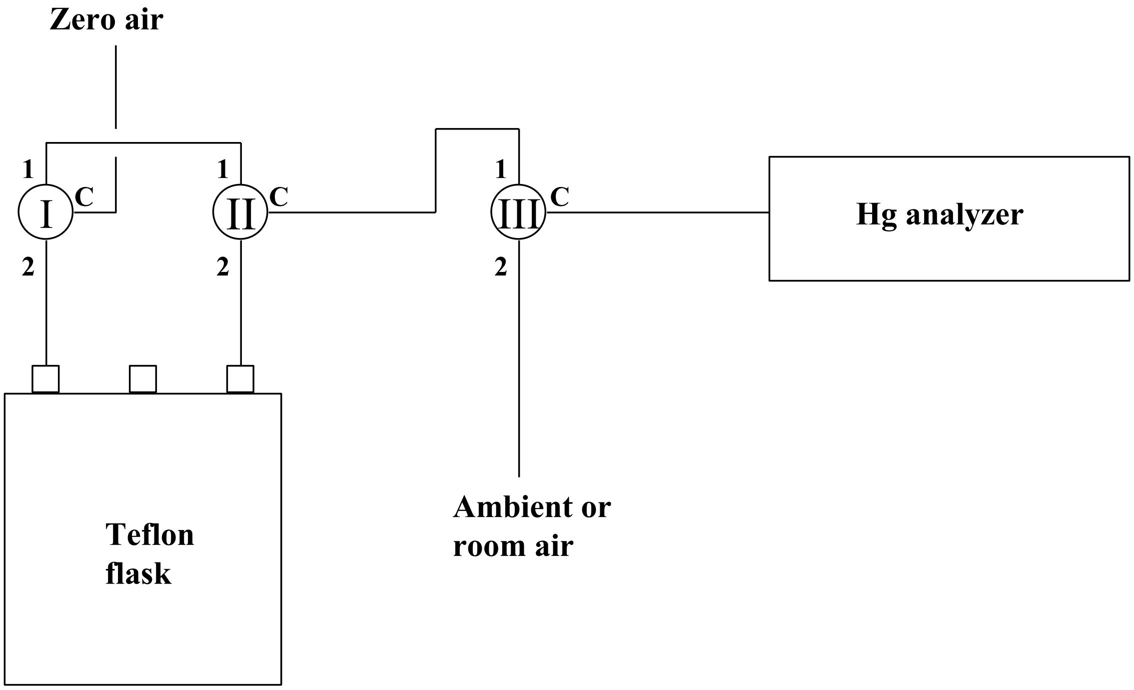

Figure 3.1: Schematic diagram of valve assembly. Each valve has three ports. In the unenergized mode, port 1 is connected to the common port (labeled as ‘c’). During the collection period, valve III is energized to allow direct measurement of ambient air near the soil-air interface. The central flask port covers a septum used for direct injection of Hg vapor.

The combined results of these four experiments support two important conclusions. First, neither the flask collection nor valve assembly experiences significant leakage over periods as long as 12 hours. Leakage in the system would draw in ambient air, resulting in recovered concentrations above baseline in the zero air tests and below the large concentrations considered in the injection experiment (mean ambient TGM concentrations in the laboratory were 1.5-2.0 ng m^{-3}). Second, the system is able to accurately recover known TGM concentrations at very low levels. Results indicate no contamination within the flask collection setup or valve assembly, or inability of the system to accurately analyze the air trapped within the flask. The system is therefore robust for collecting and analyzing soil or ambient air samples in the field, and can be used to collect and transport field samples to a laboratory within a 19-hour time frame for analysis.

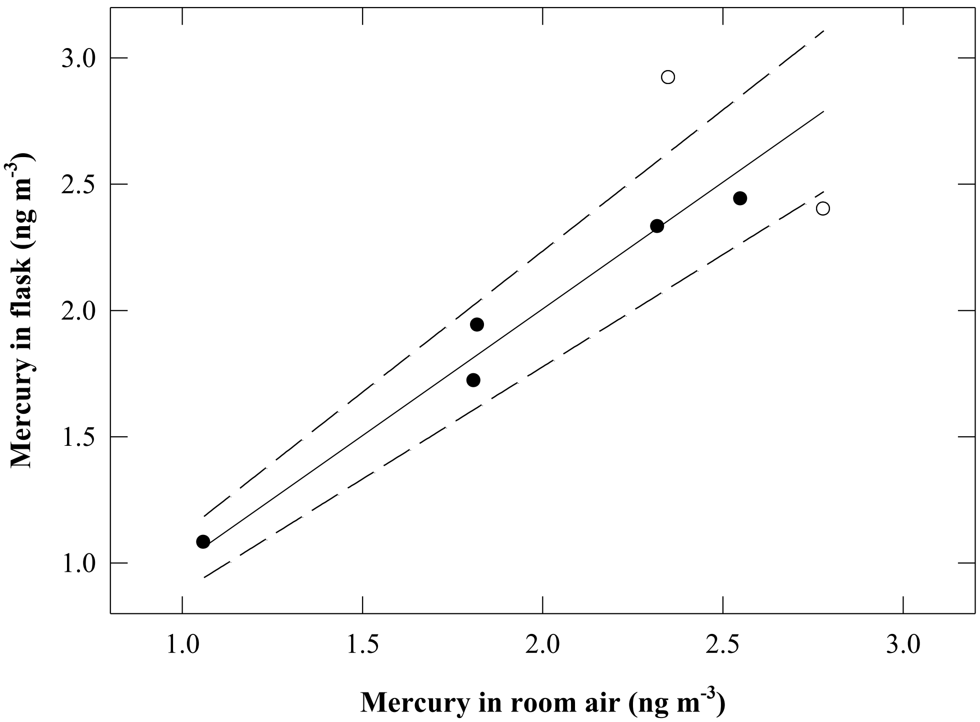

Figure 3.2: Comparison of 4-hour average room air and flask Hg concentrations. The solid line is the linear regression line ($y = 0.22 + 0.91x$; $r = 0.88$, $p<0.05$, $n = 7$). Dashed lines represent 95% confidence intervals.

3.3.2. Field Measurements

3.3.2.1. Soil gaseous mercury and environmental variables

Soil TGM concentrations measured at Coventry during both field campaigns varied from below the detection limit of the system (0.75 ng m-3, assuming an analyzer sampling volume of 7.5 L and analyzer detection limit of 0.1 ng m-3) to 22 ng m-3, but typically ranged from 1-4 ng m-3. Two important objectives of the field experiment were to examine the data for seasonal variation in soil gaseous Hg concentration and relationships between soil gaseous Hg and environmental variables. Observations during both field campaigns confirmed seasonal variation in soil TGM, especially in the upper soil layers (Figures 3.3 and 3.4). Concentrations at 2 and 5 cm were generally higher in mid to late summer and decreased during autumn. Soil TGM was strongly dependent on temperature in the upper soil layer (Figure 3.5, Table 3.1). This relationship is best explained by an exponential function, much like that for Hg vapor pressure and temperature, and also similar to observed relationships between soil TGM flux and soil temperature [e.g., *Carpi and Lindberg*, 1998; *Zhang et al.*, 2001]. This temperature dependence is the primary reason for the observed seasonal variation, as soil temperature is highly dependent on ambient air temperature (note correlation between soil TGM and air temperature, Table 1, which may be a result of covariation of soil and air temperature). Soil TGM at 20 and 50 cm was also correlated with soil temperature, though more weakly than in the upper layers, as the variation in TGM was much smaller.

During the 2003 experiment, soil TGM measurements were most often negatively correlated with soil moisture, though the relationship was not as strong as with soil temperature (Table 3.1). The correlation is possibly explained by increased sorption of

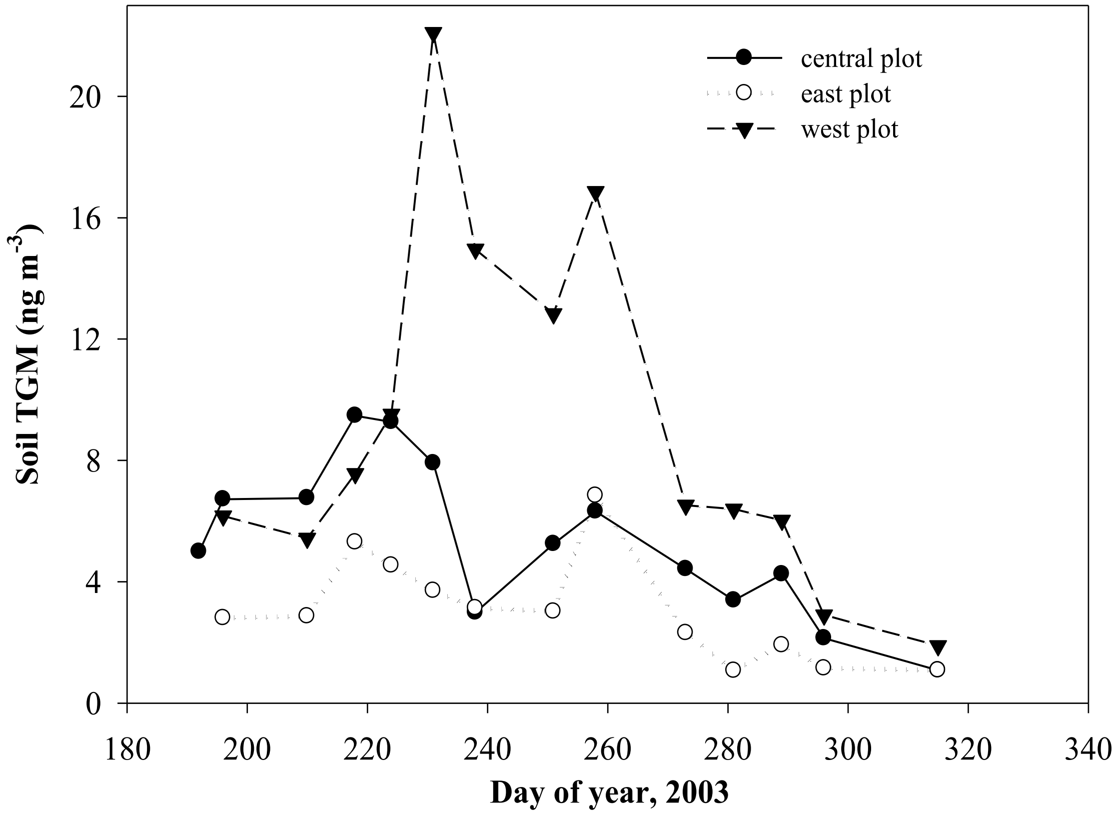

Figure 3.3: Variation in soil TGM at 5-cm depth at Coventry forest site, July-November 2003.

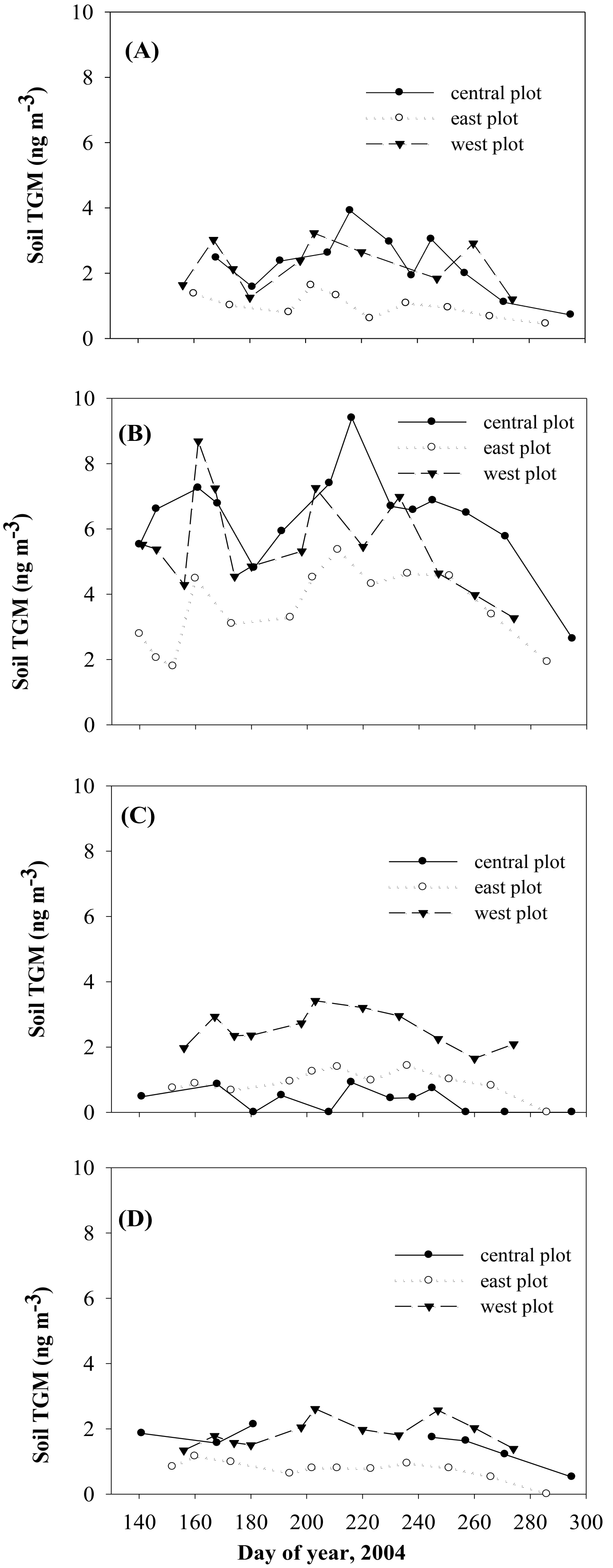

Figure 3.4: Variation in soil TGM at (A) 2 cm, (B) 5 cm, (C) 20 cm and (D) 50 cm depth at Coventry site, May-October 2004.

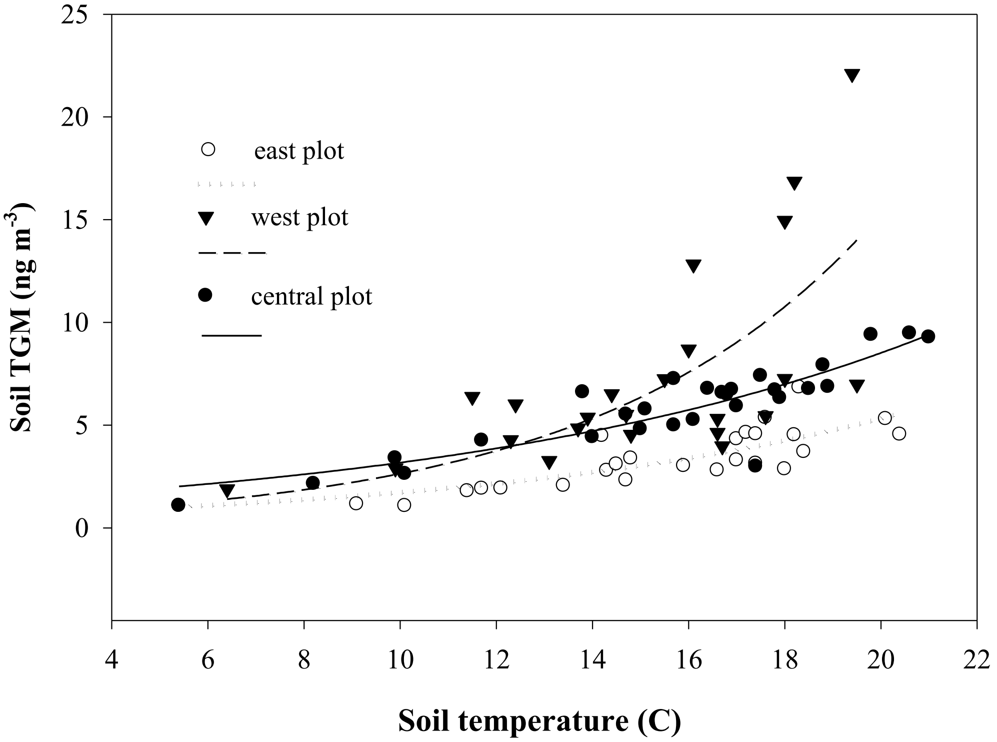

Figure 3.5: Exponential regressions of soil temperature and soil TGM at 5 cm depth, east ($y = 0.56e^{0.113x}$, r = 0.81, p<0.01, *n* = 26), central ($y = 1.19e^{0.01x}$, r = 0.88, p<0.01, *n* = 28), and west ($y = 0.46e^{0.176x}$, r = 0.66, p<0.01, *n* = 23) plots, Coventry forest site, during 2003-2004 field campaigns.

Table 3.1: Linear correlation coefficients (r) for soil TGM and environmental variables, Coventry forest site. Data are for 2003-2004 campaigns combined, except radiation and 2-cm TGM data, which were only collected during 2004. Soil moisture at 10-cm depth was used for 2- and 5-cm TGM correlation, and at 20 and 40 cm, respectively, for 20- and 50-cm TGM correlation.

	Soil temperature	**Air temperature**	**Radiation**	**Soil moisture**	**Ambient TGM**
TGM, 2 cm					
East plot	0.66 (10)*	0.74 (10)*	0.35 (7)	-0.32 (10)	0.71 (10)*
West plot	0.82 (10)**	0.82 (10)**	0.37 (5)	-0.17 (10)	0.67 (10)*
Central plot	0.89 (11)**	0.81 (11)**	0.37 (9)	0.10 (11)	0.32 (11)
TGM, 5 cm					
East plot	0.81 (26)**	0.83 (24)**	0.09 (8)	-0.09 (21)	0.32 (26)
West plot	0.60 (27)**	0.84 (25)**	0.56 (7)	-0.63 (23)**	-0.08 (26)
Central plot	0.88 (28)**	0.71 (25)**	0.08 (9)	-0.32 (23)	0.16 (28)
TGM, 20 cm					
East plot	0.71 (9)*	0.67 (9)*	0.32 (8)	-0.02 (9)	0.15 (8)
West plot	0.55 (11)	0.53 (11)	0.40 (5)	-0.20 (11)	0.30 (7)
Central plot	0.45 (20)	0.28 (20)	0.47 (8)	0.20 (17)	0.04 (18)
TGM, 50 cm					
East plot	0.32 (11)	0.63 (11)*	0.47 (6)	0.14 (11)	0.30 (9)
West plot	0.71 (11)*	0.77 (11)**	0.10 (5)	-0.35 (9)	-0.24 (9)
Central plot	0.45 (15)	0.55 (12)	0.48 (4)	0.13 (7)	0.31 (14)

*significant at $p<0.05$

**significant at $p<0.01$

Hg to water molecules [*Fang*, 1981; *Schlüter*, 2000]. However, this relationship was less often observed during the 2004 experiment (Table 3.1 combines data from both field campaigns). This result and the somewhat weak correlation between moisture and soil TGM observed in 2003 may owe to the lack of significant variation in soil moisture (typically less than 10% at any depth) during both field campaigns. More research is therefore needed to confidently understand the relationship of soil TGM with moisture.

A conspicuous spike in TGM (22 ng m-3) at 5 cm was observed at the west plot during August 2003 (Figure 3.3). Although short-term contamination of the sampling system cannot be ruled out as a possible reason for this spike, environmental conditions during this event present a plausible explanation. The spike is at least partially explained by enhanced soil temperature (Figure 3.5). However, Figure 3.5 also shows that 5-cm measurements taken at similar soil temperatures in 2004 did not result in the same high concentrations. Accordingly, the west plot linear correlation coefficient for 2003-2004 combined is much lower than that for the east and central plots (the west plot linear correlation coefficient for 2003 data alone is 0.99). Although the concentrations are not as high, the east and central plots showed enhanced 5-cm TGM concentrations at or near the same day of year as the west plot (Figure 3.3), and all three plots also showed increases in TGM during mid-September (day of year 260 in Figure 3.3). It is possible that these enhancements are related to both high soil temperature and unusually dry conditions at the site, given that some measurements indicated a negative correlation between soil moisture and TGM, especially during 2003 (Table 3.1). Although accurate soil moisture measurements were not available during August 2003 due to equipment malfunction, the Coventry area experienced only a trace of precipitation during the middle two weeks of the month, more than 95% below normal. This period was the driest of both field experiments. Similarly, precipitation was 60% below normal during the first half of September, 2003.

Although solar radiation does not penetrate the soil, some correlation between soil TGM and radiation in the uppermost soil layers (e.g., 2-cm depth) might be possible since Hg(II) may be desorbed from organic matter exposed to sunlight and thereby enhance Hg volatilization from soil [*Senesi and Schnitzer*, 1977], and the 2 and 5-cm measurements were taken near the interface between the soil and litter layers. Soil TGM in the upper soil layers was positively though weakly correlated with solar radiation in 2004 (Table 3.1). However, any possible relationship between soil TGM near the surface and irradiance on exposed leaf litter or organic matter is difficult to gauge in this experiment because air samples were collected over 4-hour periods, while radiation at the forest floor fluctuates constantly. Also, the solarimeter was placed on or near the flux chamber, which was positioned up to 1 m from the funnel inlets to minimize disturbance, and the correlation shown in Table 1 is based on relatively few observations, especially at 50-cm. Due to gaps in the canopy, sunflecks were common and resulted in spatial variability in forest floor light levels. Also, the correlation may merely be a result of covariance between solar radiation and soil temperature. It is therefore difficult to assess the relationship between solar radiation and TGM within the upper soil layers without further experimentation.

3.3.2.2. Soil TGM profiles

Mean soil TGM profiles during 2003 (central plot only) and 2004 are shown in Figure 3.6. The profiles were similar at each plot (Figure 3.6a). The remarkable

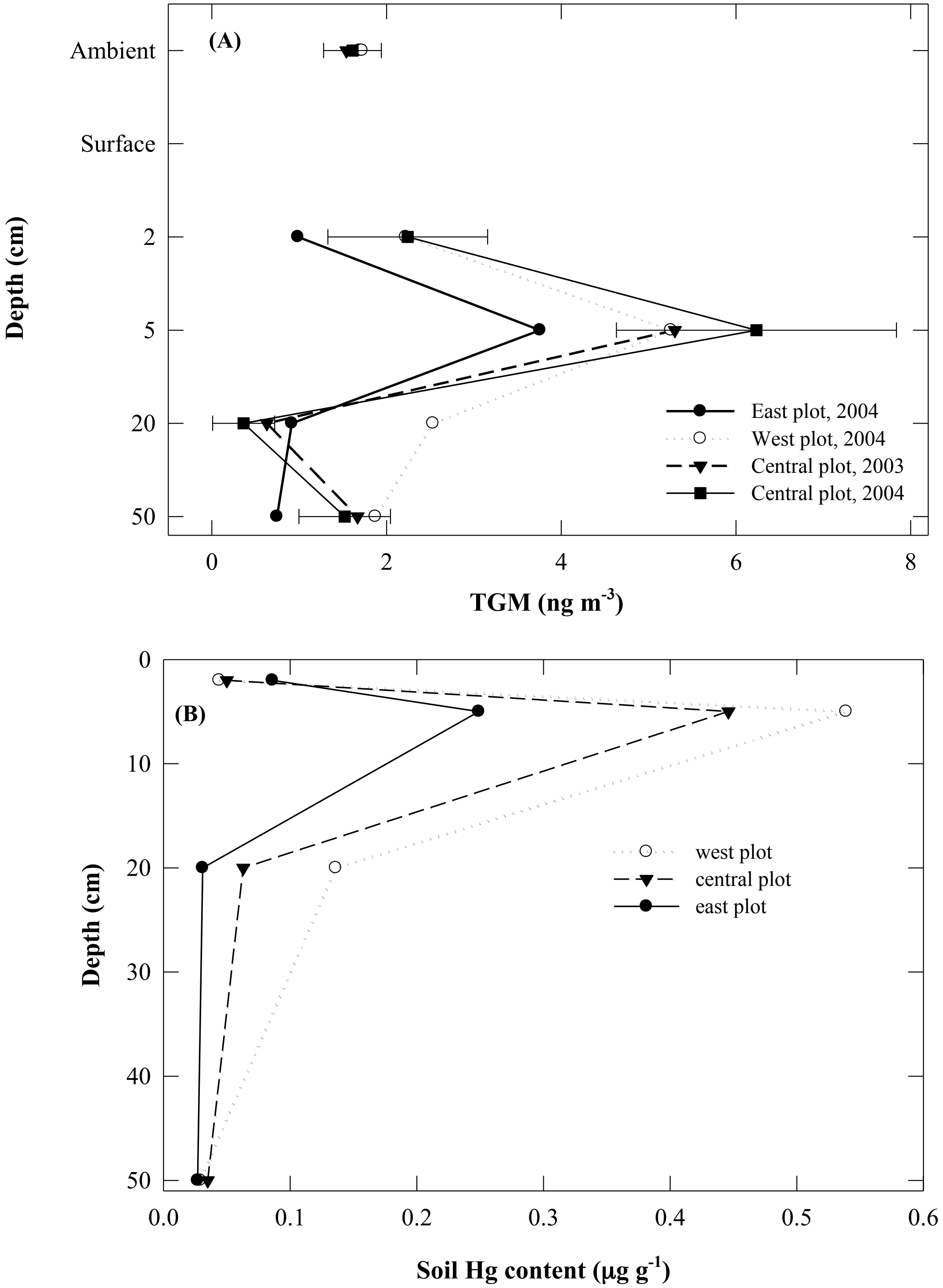

Figure 3.6: (A) Mean soil TGM profiles at Coventry forest, 2003 and 2004. Standard deviations for central plot (2004) measurements are shown. Ambient measurements (40 cm above surface) represent averages during flask collection periods. (B) Profile of soil Hg content at each plot, September 2004 (0 cm represents surface of litter layer).

consistency of the profile shapes from week to week in addition to the relationship of measured soil TGM with soil temperature (Figure3.5) suggests a robust methodology.

The data reveal the existence of gradients in gaseous Hg in background soils. As shown in Figure 3.6, clear gradients in TGM were consistently observed, especially above 20-cm depth. With the exception of the east plot, TGM concentrations at 2 cm were slightly higher than ambient. In all cases, TGM was highest at 5 cm and showed marked decreases above and below that depth.

Both slight increases (central plot, both years) and decreases (east and west plots, 2004) in TGM between 20 and 50 cm were observed. However, concentrations at these depths were typically small, and often below the detection limit of the flask sampling system at 20 and 50 cm depths at the east plot, and at 20 cm at the central plot in both field campaigns.

A significant increase ($p<0.001$) in TGM was observed between 20 and 50 cm at the central plot in both field campaigns. Possible funnel contamination was ruled out when samples collected using fresh Teflon tubing inserted to the same depths without flasks yielded concentrations within the standard deviation of the other measurements (0.4 ng m-3 at 20 cm, 1.3 ng m-3 at 50 cm). This observation as well as the larger 20-cm concentration observed at the west plot in 2004 (Figure 3.6) indicates small spatial variability in soil TGM profiles, possibly dependent on local differences in porosity, organic matter and Hg content.

The consistent observations of soil TGM gradients in both field campaigns are notable as they are in contrast to other studies [e.g., *Johnson et al.*, 2003] which, as in this study, found no vertical TGM gradients in soil between 20 and 40 cm, but did not examine TGM concentrations above 20-cm depth. These observations may indicate the presence of active zones of desorption of Hg in the upper soil layers that could contribute to the pool of Hg that is ultimately released by soil.

For further exploration, bound Hg content was measured at each sampling depth in each plot. The mean soil TGM profiles measured during the 2004 campaign are compared to the soil Hg content (µg g-1) at each depth in Figure 3.6b. Both total Hg content and vertical variation were similar to other background soils in the sense that bound Hg content was high in the organic layer (O- and upper A-horizon) and much lower with increasing depth [*Alriksson*, 2001; *Johansson et al.*, 2001; *Grigal*, 2003]. The profile in soil Hg content is strikingly similar to the mean TGM profiles at each site. In particular, maximum TGM concentrations were observed at 5-cm depth, where Hg content is uniformly highest. Below 5 cm, the soil is depleted in Hg.

Inter-site comparison of profiles in both TGM and Hg content (Figure 3.6) reveals a pattern of correlation between these two variables (Figure 3.7). For example, just as TGM at 20 and 50 cm at the east plot was typically close to or below the detection limit of the flask sampling system, soil Hg content at those locations was close to the instrument detection limit. TGM concentration at 5 cm was high and not significantly different at the central and west plots, but was significantly lower ($p<0.01$) at the east plot, corresponding to the marked depletion in soil Hg content in the east plot at this depth (Figure 3.6b). Also, both Hg content and TGM at 20 cm at the west plot are more than twice as high as measurements at the same depths at the other plots. Therefore, there appears to be a relationship between the presence of bound Hg and gaseous Hg within the soil profile. If Hg content data in the regression shown in Figure 3.7 are converted to volumetric units (not shown), the slope of the regression line possibly indicates the fraction of bound Hg contributing to gaseous Hg [$y = 0.0057x + 0.66$ ($r = 0.91$), where y is soil TGM (ng m-3) and x is bound Hg (ng m-3, mass of Hg per unit bulk soil volume)]. However, it should be noted that the regression shown in Figure 3.7 is largely driven by four out of 16 data points. Although there is a general pattern of correlation, more data is needed to firmly establish a specific, fractional relationship between bound and gaseous Hg.

There are exceptions to this pattern. For instance, mean TGM at 5 cm was higher at the central plot in 2004 while bound Hg was higher at the west plot. However, mean TGM concentrations at these plots were not significantly different ($p>0.9$), and the bound Hg concentrations are similar (also, mean TGM concentration at 5 cm was higher at the west plot during the 2003 campaign). The near absence of detectable TGM at 20 cm at the central plot is also notable given that Hg content at that depth was twice that of the east plot. A possible explanation for this discrepancy is that soil samples were not taken from the exact location of the funnel and organic matter content may not be uniform within the plot.

Figure 3.6 indicates that the organic layers (O- and upper A-horizons) are the richest zones in both Hg content and gaseous Hg in the soil pore spaces. The soil is depleted in both bound and gaseous Hg below these layers. It is possible that gaseous Hg diffuses upward through the soil and is sorbed, likely by organic matter. These data also suggest that the Hg-rich organic layer is actively desorbing Hg, thereby acting as a source of gaseous Hg in soil pore spaces that may ultimately be emitted to the atmosphere, as Hg released in the organic layer may be transported by diffusion toward the litter layer. The strong, positive correlation (r = 0.7-0.9, p<0.1) between TGM observed at 2 and 5 cm at all plots is possible evidence of this process.

Soil organic matter is known to play a central role in the storage and release of Hg in soils [e.g., *Grigal*, 2003]. Organic matter content was not measured in this study. However, even without direct measurements, circumstantial evidence suggests a possible link between bound (and therefore, gaseous) Hg and spatial variation in organic matter. For example, measurements of percent solid matter, which are typically inversely related to organic matter content [*Brady and Weil*, 2002], were strongly and negatively correlated with bound Hg (r = -0.7, p<0.01)). Also, visual inspection of the soil indicated that the east plot was lighter in color, sandier and therefore lower in organic matter below 3 cm depth than the other plots. At the west and central plots, the 5-cm measurements were made at or near the interface between the O- and A-horizons (see section 3.2.2), which should be enriched in organic matter. Measurements at this depth also showed high concentrations of TGM and bound Hg. The 5-cm TGM measurements in the east plot, which were always significantly lower than the other plots, were made below the A-horizon and therefore likely in a zone with lower organic content. Conversely, the west plot, richest in bound Hg, was darker than the other plots down to 50 cm which could reflect higher organic matter content. Additionally, a study conducted in Connecticut forests showed vertical enhancement of organic carbon content between the surface and the upper 7.5 cm of soil, and decreased levels below [*Finzi et al.*, 1998]. Other soil studies in forests in Connecticut and Massachusetts have shown declines in organic matter from 0-5 cm to 20-cm depth [*Gulledge et al.*, 2004], or exponential declines in carbon content between 3-6 cm and 50-cm depths [*Kulmatistki et al.*, 2003]. These trends

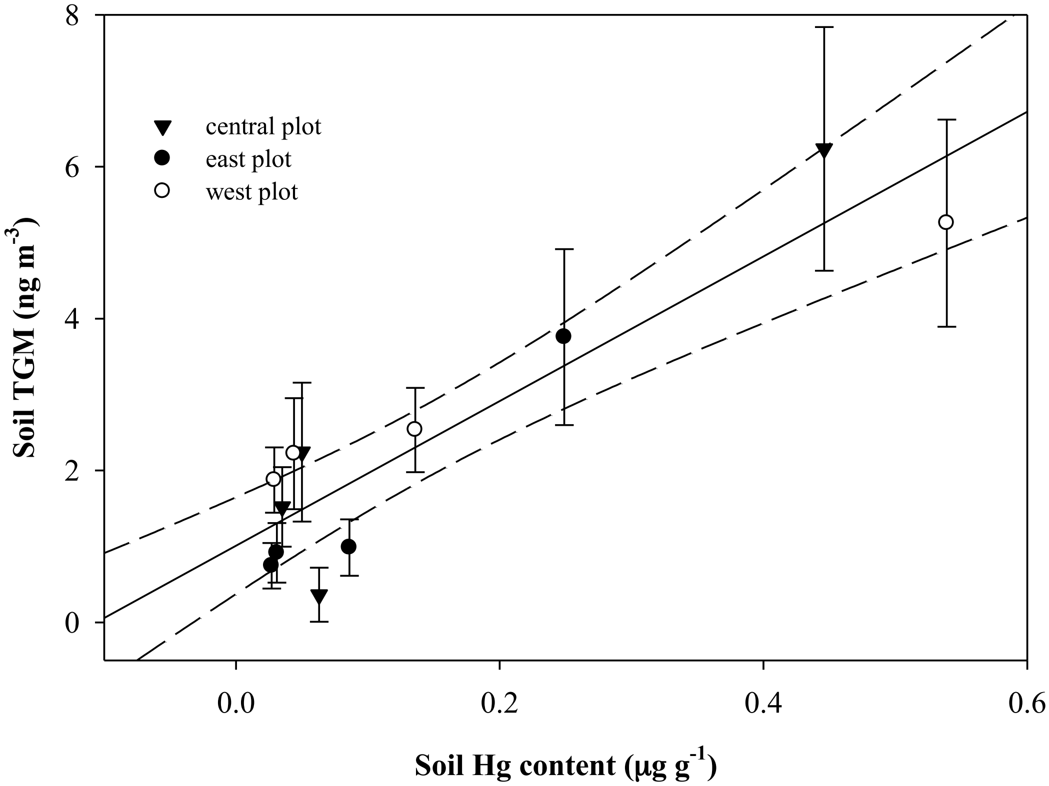

Figure 3.7: Linear regression of soil TGM observations (May-October 2004) and soil Hg content (September 2004) at Coventry forest ($y = 9.52x + 1.01$; $r = 0.97$, $p<0.01$, $n = 12$). Error bars represent standard deviations of plot- and depth-specific soil TGM measurements, May-October 2004. Dashed lines represent 95% confidence interval.

are somewhat similar to the profile in bound and gaseous Hg shown in Figure 3.6. Although actual measurements of organic matter content are necessary in order to firmly conclude a link between organic matter content and gaseous Hg within the soil profile, spatial variation of organic matter is a possible explanation for the observed horizontal and vertical variability in soil gaseous Hg.

A drawback of the flask sampling system is the inability to analyze soil air samples with high time resolution. To avoid contamination and disturbance, it is essential to draw in soil air at a low flow rate and over a long sampling period. It is therefore difficult to investigate potential diurnal changes in soil TGM, which may be expected given observed diurnal variation in soil Hg emission, and presents difficulty in examining the impacts of highly variable meteorological parameters such as solar radiation. This drawback could be improved by placing multiple funnels at a common depth within a soil plot and initiating air sampling at staggered starting times using multiple flasks.

3.3.2.3. Soil TGM flux measurements

Mean daytime soil TGM fluxes observed at all three plots at the forest during May-October 2004 were 2.2 ± 5.2 ng m-2 hr-1. Deposition events (slightly negative flux, -0.5 ng m-2 hr-1) were observed on three occasions during the early morning (6-8:00 LST); otherwise, all observations indicated emission (0.1-43 ng m-2 hr-1) with maximum fluxes in the afternoon (14:00 LST). Mean fluxes were comparable to those observed at other background forest sites [*Schroeder et al.*, 1989; *Poissant and Casimir*, 1998; *Zhang et al.*, 2001]. These relatively low fluxes combined with few deposition events and low bound Hg content in the soil may indicate low Hg loading at the site from deposition or throughfall [*Zhang et al.*, 2001].

On average, fluxes were slightly higher at the central plot, although not significantly different from the west plot ($p>0.9$). Fluxes at the east plot were significantly lower than west and central ($p\leq0.06$). As in other studies [e.g., *Zhang et al.*, 2001], this variation is likely explained by lower Hg content and soil TGM in the east plot (Figure 3.6). When fluxes at each plot were normalized to soil Hg content (5 cm), no significant differences were observed among the plots ($p>0.2$; not shown).

Similar to soil TGM (Figures 3.3 and 3.4), some seasonal variation in soil TGM flux was observed (Table 3.2). However, it should be emphasized that monthly observations presented in Table 3.2 are typically based on only 2-3 days of observation per plot. Unlike soil TGM, seasonal variation appears to be more strongly related to changes in solar radiation levels than temperature, as fluxes were actually highest in May and early June before maximum foliage levels, and increased during October when canopy foliage had thinned considerably.

On a diurnal basis, hourly fluxes were correlated with both air temperature (mean daily r-value of 0.62) and, more weakly, soil temperature (mean daily r-value of 0.52) at each plot. This is consistent with other measurements of soil Hg flux at a variety of sites, although many studies have shown fluxes to be more strongly correlated with these variables, especially soil temperature [*Carpi and Lindberg*, 1998; *Poissant and Casimir*, 1998; *Lindberg et al.*, 1999; *Zhang et al.*, 2001]. The weaker correlation observed in this study was possibly related to the lack of high-resolution measurements of soil temperature, which was measured on average once per hour. Also, soil temperature typically varied by no more than 1.5°C for the duration of each site visit.

Table 3.2: Monthly means and standard deviations of soil TGM flux (ng m-2 hr-1) at Coventry forest site, 2004.

	Mean flux, central	**Mean flux, east**	**Mean flux, west**
May	9.5 (±11.6)	1.9 (±1.2)	2.8 (±1.9)
June	2.7 (±2.7)	2.5 (±2.0)	3.2 (±3.1)
July	1.8 (±2.5)	1.8 (±0.9)	2.0 (±0.8)
August	1.5 (±1.9)	1.0 (±0.4)	1.5 (±0.7)
September	0.9 (±0.8)	1.0 (±0.6)	1.3 (±0.7)
October	3.0 (±2.9)	1.2 (±1.1)	N/A
All data	2.8 (±5.5)	1.6 (±1.2)	2.1 (±1.9)

No correlation between soil TGM flux and soil moisture was observed. This is not surprising as moisture did not change diurnally in the absence of rain, and varied little throughout the experiments. Also, fluxes were not measured during rain events, which are known to lead to increases in soil Hg emissions. The lack of correlation between soil TGM flux and moisture may be indicative of the short-term (12-24 hours) response of soil Hg emissions to rainfall [*Lindberg et al.*, 1999].

Correlation between soil TGM flux and solar radiation was observed at all plots (mean daily r-value of 0.73, eight hourly observations per visit) throughout the 2004 campaign. This correlation, illustrated in Figure 3.8 and similar to other studies which showed correlation between flux and radiation [e.g., *Carpi and Lindberg*, 1998; *Zhang et al.*, 2001], was typically stronger than that observed between flux and soil or air temperature. The linear correlation coefficient (r) between hourly fluxes and solar radiation was less than 0.6 on only three site visits, and above 0.7 on more than half of the visits.

This correlation was recorded despite the seeming paradox that the chamber was not transparent. Six observations of fluxes >10 ng m-2 hr-1 were recorded, all during late May to mid-June. Although radiation data were not collected when these observations were made, they occurred during periods when the plot was illuminated by direct sunlight. Synchronous with these episodes, the time series of TGM concentration outside of the chamber showed sudden 3-6 ng m-3 enhancements to levels much higher than normal ambient concentration (~1.6 ng m-3). These high fluxes were therefore probably not a chamber artifact. These observations are similar to those from other field

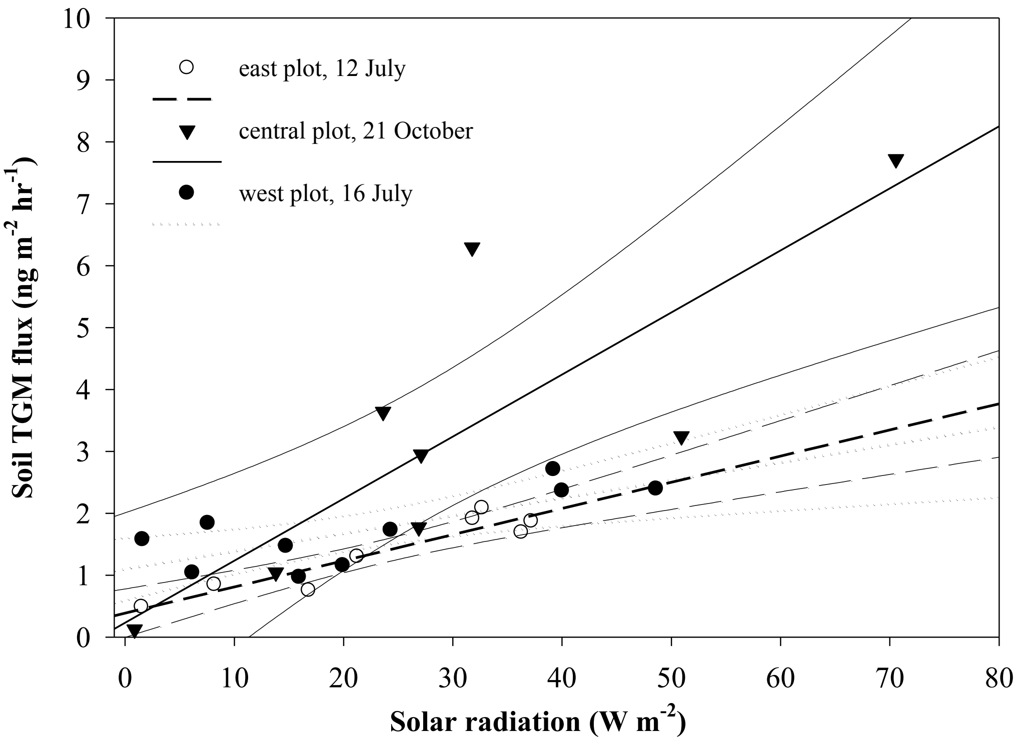

Figure 3.8: Linear regression of soil TGM flux and solar radiation at central plot, 21 October 2004 (*r* = 0.85, *p*<0.05), east plot, 12 July 2004 (*r* = 0.93, *p*<0.01), and west plot, 16 July 2004 (*r* = 0.76, *p*<0.1), Coventry (CT) forest site. Data represent hourly averages. Curved lines flanking regressions are 95% confidence intervals.

experiments using opaque chambers and may show that TGM freely circulates within soil pores independent of chamber placement [*Poissant and Casimir*, 1998].

Results of other field studies suggest that radiation, not increase in temperature, is the dominant mechanism for enhanced soil Hg fluxes [*Carpi and Lindberg*, 1998; *Engle et al.*, 2001; *Zhang et al.*, 2001], as strong correlation between solar radiation and soil Hg flux has been observed even when soil temperature is held constant [e.g., *Zhang et al.*, 2001]. The strength of the observed correlation between soil TGM flux and radiation exemplified in Figure 3.8 supports this notion. Although partially explained by differences in soil Hg content among plots (see section 3.3.2.4), the observation of significantly higher fluxes at the central and west plots compared to the east could also support the hypothesis of Hg desorption from small patches of organic matter exposed to radiation, which were present only in the central and west plots (see section 3.2.1). However, no controlled experiments were performed during the field study. Therefore, the possibility that the correlations illustrated in Figure 3.8 are the result of covariance between solar radiation and soil temperature (and ultimately heating rather than photochemistry) cannot be ruled out, especially since the solarimeter was placed on top of the opaque chamber. The interrelations between these environmental parameters makes quantitative determination of the underlying mechanisms controlling soil Hg flux difficult in this particular study.

The highest mean (Table 3.2) and instantaneous soil Hg fluxes (>40 ng m-2 hr-1) were measured at the central plot. This plot also consistently showed the steepest response curve to solar radiation (Figure 3.8) and although radiation levels at each plot were not significantly different throughout the 2004 experiment ($p>0.2$), experienced the highest instantaneous radiation levels (70-80 W m-2, 12:00-14:00 LST). The presence of small pockets of organic matter exposed to higher instantaneous radiation levels than what was observed in the west plot is a possible explanation in support of the notion that photochemistry is the dominant mechanism. However, it is notable that the central plot possessed somewhat different understory characteristics than the east and west plots. Although leaf litter composition and exposed organic matter were similar to the west plot, more seedlings and vascular plant species were present (see section 2.1). It is possible that the difference in emission recorded at the central plot is in part explained by biotic factors (e.g., soil-root interaction or enhanced transpiration) related to the somewhat denser surface vegetation.

3.3.2.4. Relationship of soil Hg flux and soil TGM concentrations

A major purpose of this study was to investigate the relationship of the soil gaseous Hg profile, and therefore the role of different soil layers, with the ultimate effusion of gaseous Hg from the soil surface. Therefore, flux measurements were compared with soil TGM measurements. When averaged over the duration of each soil gas collection period, no correlation was found between soil TGM flux and soil TGM at 5, 20 or 50 cm. However, flux was strongly correlated with gaseous Hg concentrations at 2 cm (Figure 3.9). This suggests that the points of desorption of Hg and ultimate release from the soil are within the upper 5 cm and is consistent with studies showing correlation between soil CO_2 flux and CO_2 concentrations at shallow (1-cm) depths in background forest soils [*Risk et al.*, 2002; *Oishi and Lee*, 2002]. If this pattern holds in other forests, any measurements of TGM concentrations or gradients deeper in the soil will show little relation to flux.

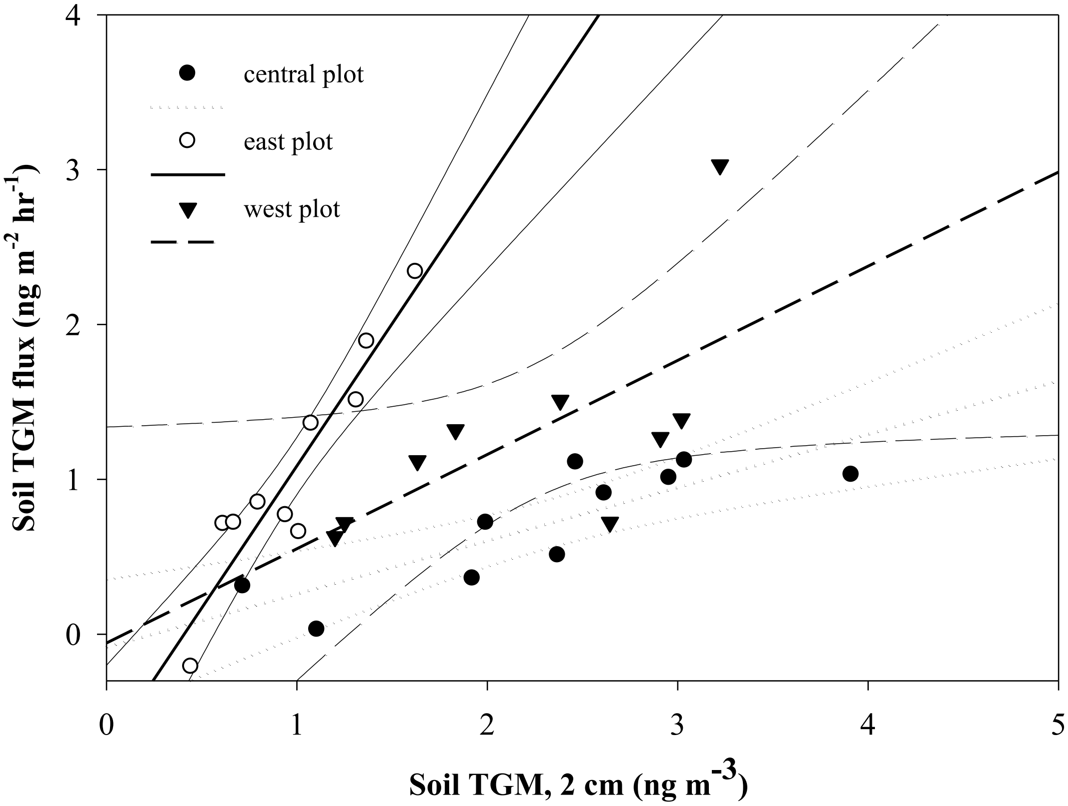

Figure 3.9: Regression of soil TGM at 2 cm and soil TGM flux at central (*r* = 0.84, *p*<0.01), east (*r* = 0.94, *p*<0.01) and west (*r* = 0.65, *p*<0.1) plots, Coventry (CT) forest site, May-October 2004. 95% confidence intervals are shown.

The relationships depicted in Figures 3.5, 3.8 and 3.9 show slight to considerable variation among plots. To explore a possible reason for this variation, soil TGM measurements were normalized to soil Hg content at 5 cm. This depth was chosen because Hg content was highest and varied more significantly among plots than the 2-cm measurement. Normalizing by Hg content reduces the spread of the data shown in Figure 3.9, and increases the overall correlation, shown by the dashed line in Figure 3.9, by one-third. Similar results occur when soil TGM concentrations or fluxes in Figures 3.5 and 3.8 are normalized to Hg content (not shown). Therefore, variations in the individual regression lines shown in Figures 3.5, 3.8 and 3.9 are at least in part due to differences in soil Hg content among the plots (Figure 3.6b).

3.4. Conclusions

The observed correlation between soil flux and TGM at 2-cm depth (Figure 3.8) and the large gradients in soil TGM observed over relatively small depths (e.g., 2-5 cm, 5-20 cm; Figure 3.6) are notable. Previous studies of this kind revealed no gradients in soil TGM over larger depths (20-40 cm) and found no correlation between flux and gaseous Hg within the soil. This may be due to a lack of soil TGM measurements above 20 cm depth [*Johnson et al.*, 2003].

Soil TGM measurements at 5-cm depth suggest that the organic layer, is rich in bound Hg, may also be an active source, or desorption site, of gaseous Hg which may ultimately be emitted to the atmosphere. The correlation between flux and TGM at 2 cm may suggest that the litter layer is the approximate point of release of soil TGM into the air. Lack of correlation between flux and TGM concentration at 5 cm suggests that soil material, possibly organic matter, between the litter layer and the funnel placement at 5 cm is actively sorbing or desorbing Hg. Therefore, TGM concentrations are likely not uniform throughout the organic layer. Changes in soil temperature strongly influences soil TGM concentration at any depth, but temperature profile and possible changes in organic and bound Hg content should result in vertical variation in TGM concentration, even within the organic layer. The surface processes that result in the emission of Hg into the atmosphere (e.g., photochemical reactions) likely occur within the litter layer or over a small, finite layer at the interface between the A-horizon and the litter layer.

In any case, these results underscore the importance of soil TGM measurements with high spatial resolution within the vertical soil profile and the importance of the upper 5 cm of soil in the soil gaseous Hg pool. Measurements taken below the organic layer will show no relationship between flux and soil TGM concentration, even though such a relationship exists close to the surface. Measurement systems which are subject to contamination from ambient air are limited in their ability to observe fine soil TGM gradients or capture processes within the organic layer. The flask sampling system developed in this study is therefore valuable as it allows analysis of soil gas samples, even at depths close to the surface, with minimal contamination from ambient air.

Acknowledgements

Thanks to Prof. David R. Miller of the University of Connecticut (UCONN) for making the forest research site available to me, allowing for and providing instructions on the use of his flux chamber and also for occasional sleeping accommodations. Jesse Bash of UCONN collected soil samples for laboratory analysis, and we thank the UCONN Environmental Research Institute for performing those analyses. Ellen Denny enabled use of liquid Hg for laboratory experimentation. The work was supported in part by a Yale Institute for Biospheric Studies fellowship, and a John F. Enders fellowship from the Yale graduate school. Also, thanks to one reviewer and an associate editor at *Journal of Geophysical Research-Biogeosciences* for helpful comments on a submitted manuscript related to this chapter.

3.5. References

Alriksson, A. (2001), Regional variability of Cd, Hg, Pb and C concentrations in different horizons of Swedish forest soils, *Water Air Soil Poll. Focus*, 1, 325-341.

Amirbahman, A., Ruck, P.L., Fernandez, I.J., Haines, T.A., and Kahl, J.S. (2004), The effect of fire on mercury cycling in the soils of forested watersheds: Acadia National Park, Maine, U.S.A, *Water Air Soil Poll.*, 152, 313-331.

Brady, N.C., and Weil, R.R. (2002), *The Nature and Properties of Soils* (13th Ed), 960 pp., Prentice Hall, New Jersey.

Carpi, A., Lindberg, S.E. (1998), Application of a Teflon dynamic flux chamber for quantifying soil mercury flux: tests and results over background soil, *Atmos. Env.*, 32, 873-882.

Cerling, T.E., Solomon, D.K., Quade, J., and Bowman, J.R. (1991), On the isotopic composition of carbon in soil carbon dioxide, *Geochim. Cosmochim. Acta*, 55, 3402-3405.

Colbeck, S.C. (1989), Air movement in snow due to windpumping, *Journal of Glaciology*, 35, 209-213.

Coolbaugh, M.F., Gustin, M.S., and Rytuba, J.J. (2002), Annual emissions of mercury to the atmosphere from natural sources in Nevada and California, *Env. Geol.*, 42, 338-349.

de Jong, E., and Schappert, H.J.V. (1972), Calculation of soil respiration and activity from CO_2 profiles in the soil, *Soil Science*, 113, 328-333.

Engle, M.A., Gustin, M.S., and Zhang, H. (2001), Quantifying natural source mercury emissions from the Ivanhoe Mining District, north-central Nevada, USA, *Atmos. Env.*, 35, 3987-3997.

Engle, M.A., and Gustin, M.S. (2002), Scaling atmospheric mercury emissions from three naturally enriched areas: Flowery Peak, Nevada; Peavine Peak, Nevada; and Long Valley Caldera, California, *Sci. Tot. Env.*, 290, 91-104.

Ehleringer, J.S., and Cook, C.S. (1998), Carbon and oxygen isotope ratios of ecosystem respiration along an Oregon conifer transect: preliminary observations based on small-flask sampling, *Tree Phys.*, 18, 513-519.

Fang, S.C. (1981), Studies on the sorption of elemental Hg vapor by soils, *Arch. Environ. Contam. Toxicol.*, 10, 193-201.

Fang, C., and Moncrieff, J.B. (1998), Simple and fast technique to measure CO_2 profiles in soil, *Soil Biology and Biochemistry*, 30, 2107-2112.

Farrell, D.A., Graecen, E.L., and Gurr, C.G. (1966), Vapor transfer in soil due to air Turbulence, *Soil Science*, 102, 305-313.

Finzi, A., Van Breemen, N., and Canham, C.D. (1998), Canopy tree-soil interactions within temperate forests: Species effects on soil carbon and nitrogen. *Ecol. App.*, 8, 440-446.

Fitzgerald, W.F. (1989), Atmospheric and oceanic cycling of mercury, In *Chemical Oceanography Series*, Ch. 57, Volume 10, Riley, J.P., Chester, R. (Eds.), Academic Press, New York.

Fitzgerald, W.F. (1995). Is mercury increasing in the atmosphere? The need for an Atmospheric Mercury Network (AMNET), In Porcella, D.B., Huckabee, J.W., and Wheatley, B. (Eds.), *Mercury as a global pollutant*, pp. 245-254, Kluwer Academic Publishing, Dordrucht.

Gillis, A., and Miller, D. (2000a), Some potential errors in the measurement of mercury gas exchange at the soil surface using a dynamic flux chamber, *Sci. Tot. Env.*, 260, 81-189.

Gillis, A., and Miller, D. (2000b), Some local environmental effects on mercury emission and absorption at a soil surface, *Sci. Tot. Env.*, 260, 191-200.

Grigal, D.F. (2003), Mercury sequestration in forests and peatlands: A review, *J. Environ. Qual.,* 32, 393-405.

Gustin, M.S., Tayler, G.E., Leonard, T., and Keislar, R. (1996), Atmospheric mercury concentrations associated with geologically active and anthropogenically enriched sites in central western Nevada, *Env. Sci. Tech.*, 30, 2572-2579.

Gustin, M.S., Lindberg, S.E., Marsik, F., Casimir, A., Ebinghaus, R., Edwards, G., Hubble-Fitzgerald, C., Kemp, R., Kock, H., Leonard, T., London, J., Majewski, M., Montecinos, C., Owens, J., Pilote, M., Poissant, L., Rasmussen, P., Schaedlich, F., Schneeberger, D., Schroeder, W., Sommar, J., Turner, R., Vette, A., Wallschlaeger, D., Xiao,, Z., and Zhang, H. (1999), Nevada STORMS project: Measurement of mercury emissions from naturally enriched surfaces, *J. Geophys. Res.*, 104, 21831-21844.

Gustin, M.S., and Lindberg, S.E. (2000), Assessing the contribution of natural sources to the global mercury cycle: the importance of intercomparing dynamic flux measurements, *Fresen. J. Analytical Chem.*, 366, 417-422.

Gulledge, J., Hrywna, Y., Cavanaugh, C., and Steudler, P.A., Effects of long-term nitrogen fertilization on the uptake kinetics of atmospheric methane in temperate forest soils. *FEMS Microbiol. Ecol.* 49, 389-400

Hersterberg, R., and Seigenthaler, U. (1991), Production and stable isotopic composition of CO_2 in a soil near Bern, Switzerland, *Tellus*, 43B, 197-205.

Johansson, K., Bergbäck, B., and Tyler, G. (2001), Impact of atmospheric long range transport of lead, mercury and cadmium on the Swedish forest environment, *Water Air Soil Poll. Focus*, 1, 279-297.

Johnson, D.W. and Lindberg, S.E. (1995), The biogeochemical cycling of Hg in forests: Alternative methods for quantifying total deposition and soil emission, *Water Air Soil Poll.*, 80, 1069-1077.

Johnson, D.W., Benesh, J.A., Gustin, M.S., Schorran, D.S., Lindberg, S.E., and Coleman, J.S. (2003), Experimental evidence against diffusion control of Hg evasion from soils, *Sci. Tot. Env.*, 304, 175-184.

Kim, K-H., Lindberg, S.E., and Meyers, T.P. (1995), Micrometeorological measurements of mercury vapor fluxes over background forest soils in eastern Tennessee. *Atmos. Env.*, 29, 267-282.

Kulmatiski, A., Vogt, D.J., Siccama, T.G., and Beard, K.H. (2003), Detecting nutrient pool changes in rocky forest soils, *Soil Sci. Soc. Am. J.*, 67, 1282-1286.

Lindberg, S.E., Meyers, T.P., Taylor, G.E., Turner, R.R., and Schroeder, W.H. (1992), Atmosphere-surface exchange of mercury in a forest: results of modeling and gradient approaches, *J. Geophys. Res.*, 97, 2519-2528.

Lindberg, S.E., Kim, K.-H., Meyers, T.P., and Owens, J.G. (1995), Micrometeorological gradient approach for quantifying air/surface exchange of mercury vapor: tests over contaminated soils, *Env. Sci. Tech.*, 29, 126-135.

Lindberg, S.E., Hanson, P.J., Meyers, T.P., and Kim, K.-H. (1998), Air/surface exchange of mercury vapor over forests – The need for a reassessment of continental biogenic emissions. *Atmos. Env.*, 32, 895-908.

Lindberg, S.E., Zhang, H., Gustin, M., Vette, A., Marsik, F., Owens, J., Casimir, A., Ebinghaus, R., Edwards, G., Fitzgerald, C., Kemp, J., Kock, H.H., London, J., Majewski, M., Poissant, L., Pilote, M., Rasmussen, P., Schaedlich, F., Schneeberger, D., Sommar, J., Turner, R., Wallschläger, D., and Xiao, Z. (1999), Increases in mercury emission from desert soils in response to rainfall and Irrigation, *J. Geophys. Res.*, 104, 21879-21888.

Lindberg, S.E., Zhang, H., Vette, A.F., Gustin, M.S., Barnett, M.O., and Kuiken, T. (2002), Dynamic flux chamber measurement of gaseous mercury emission fluxes over soils: part 2 – effect of flushing flow rate and verification of a two-resistance exchange interface simulation model, *Atmos. Env.*, 36, 847-859.

Lindquist, O., Johansson, K., Aastrup, M., Andersson, A., Bringmark, L., Hovsenius, G., Hakanson, L., Iverfeldt, A., Meili, M., and Timm, B. (1991), Mercury in the Swedish environment – Recent research on causes, consequences and corrective methods, *Water Air Soil Poll.*, 55,73-100.

Lund, C.P., Riley, W.J., Pierce, L.L., and Field, C.B. (1999), The effects of chamber pressurization on soil-surface CO_2 flux and the implications for NEE measurements under elevated CO_2, *Global Change Biology*, 5, 269-281.

Oishi, A.C., and Lee, X. (2002), Temporal and spatial variation of soil CO_2 in a temperate forest with shallow soil, American Meteorological Society 25th Conference on Agricultural and Forest Meteorology, Preprint Volume, pp 65-66.

Pehkonen, S.O., and Lin, C.-J. (1998), Aqueous photochemistry of mercury with organic Acids, *J. Air Waste Manage. Assoc.*, 48, 144-150.

Poissant, L., and Casimir, A. (1998), Water-air and soil-air exchange rate of total gaseous mercury measured at background sites. *Atmos. Env.*, 32, 883-893.

Risk, D., Kellman, L., and Beltrami, H. (2002), Carbon dioxide in soil profiles: Production and temperature dependence, *Geophys. Res. Lett.*, 29, Art. No. 1087.

Schlüter, K. (2000), Review: Evaporation of mercury from soils. An intergration and synthesis of current knowledge, *Env. Geol.*, 39, 249-271.

Scholtz, M.T., Van Heyst, B.J., and Schroeder, W.H. (2003), Modelling of mercury emissions from background soils, *Sci. Tot. Env.*, 304, 185-207

Schroeder, W.H., Munthe, J., and Lindquist, O. (1989), Cycling of mercury between water, air and soil compartments of the environment, *Water Air Soil Poll.*, 48, 337-347.

Schroeder, W.H., and Munthe, J. (1998), Atmospheric Mercury – An Overview. *Atmos. Env.*, 32, 809-822.

Senesi, N., and Schnitzer, M. (1977), Effects of pH, reaction time, chemical reduction and irradiation on ESR spectra of fulvic acid. *Soil Sci.*, 123, 224-234.

Tyler, G. (2004), Vertical distribution of major, minor and rare elements in a Haplic Podzol, *Geoderma*, 119, 277-290.

Wallschläger, D., Turner, R.R., London, J., Ebinghaus, R., Kock. H.H., Sommar, J., and Xiao, Z. (1999), Factors affecting the measurement of mercury emissions from soils with flux chambers, *Jour. Geophy. Res.*, 104, 21859-21871.

Wallschläger, D., Kock, H.H., Schroeder, W.H., Lindberg, S.E., Ebinghaus, and R., Wilkin, R.-D. (2002), Estimating gaseous mercury emission from contaminated floodplain soils to the atmosphere with simple field measurement techniques, *Water Air Soil Poll.*, 135, 39-54.

Wood, B.D., Keller, C.K., and Johnstone, D.L. (1993), In situ measurement of microbial activity and controls on microbial CO_2 production in the unsaturated zone, *Water Resources Research*, 29, 647-659.

Xiao, Z.F., Munthe, J., Schroeder, W., and Lindquist, O. (1991), Vertical fluxes of volatile mercury over forest soil and lake surfaces in Sweden, *Tellus-B*, 43, 267-279.

Yin, Y, Allen, H.E., Huang. C.P., Sparks, D.L., and Sanders, P.F. (1997), Kinetics of mercury (II) adsorption and desorption on soil, *Env. Sci Tech.*, 31, 496-503.

Zhang, H. and Lindberg, S.E. (1999), Processes influencing the emission of mercury from soils: A conceptual model, *J. Geophys Res.*, 104, 21889-21896.

Zhang, H., Lindberg, S.E., Marsik, F.J., and Keeler, G.J. (2001), Mercury air/surface exchange kinetics of background soils if the Tahquamenon river watershed in the Michigan upper peninsula, *Water Air Soil Poll.*, 126, 151-169.

Chapter 4:

[4]Emission and long-range transport of mercury from a Canadian boreal forest fire during July 2002: Implications for regional and global mercury budgets

---

[4] Published as Sigler, J.M., Lee, X., and Munger, W. (2003), Emission and long-range transport of gaseous mercury from a large-scale Canadian boreal forest fire, *Env. Sci. Tech.*, 37, 4343-4347.

Abstract

Field observations made at Harvard Forest [Petersham, Ma., U.S.A. (42º54´N, 72º18´W)] during early July 2002 show clear evidence of long-range transport of gaseous mercury (Hg) in a smoke plume from a series of boreal forest fires in northern Quebec. These measurements indicated significant and highly correlated increases in Hg and CO during the plume event. The Hg:CO emissions ratio determined from the data (8.61×10^{-8} mol mol^{-1}) was combined with previously published information on CO emissions and biomass burned to determine a mean area-based Hg emission flux density for boreal forest fires (1.5 g Hg ha^{-1}), annual Hg emissions from Canadian forest fires (3.5 tonnes) and annual global Hg emissions from boreal forest fires (22.5 tonnes). Annual Hg emissions from boreal fires in Canada may equal 30% of annual Canadian anthropogenic emissions in an average fire year, and could be as high as 100% during years of intense burning. The Hg:CO emissions ratio of this study was much lower than those reported for a temperate forest in Ontario and a pine/shrub vegetation in South Africa, suggesting that fire emission is dependent on biome/species and that any extrapolation from a single fire event to determine the global fire emission is speculative.

4.1. Introduction

Mercury (Hg) is an important trace element because of its potentially harmful impact on human health. Gaseous elemental mercury (Hg^0), which makes up >95% of the background global atmospheric concentration of Hg, is not readily absorbed by bare terrain, water or vegetation, has a residence time in the atmosphere of 0.5 – 2 years [*Munthe and McElroy*, 1992] and can therefore be transported over long distances [*Lindqvist and Rodhe*, 1985; *Bullock*, 2000]. Transported Hg^0 can be deposited to remote aquatic environments [*Fitzgerald et al.*, 1998; *Allan*, 1999] where it undergoes methylation and subsequently bioaccumulate to dangerous levels in fish [*Kehrig and Malm*, 1999; *Mason et al.*, 2000]. Therefore, atmospheric emissions and transport are of particular importance to our interest in the global biogeochemical cycle of Hg.

Roughly half of the global atmospheric load of Hg is believed to be anthropogenic [*Nriagu,* 1989; *Mason et al.*, 1994]. Recent studies have suggested that large uncertainties are associated with present estimates of emission from natural sources and re-emission of previously deposited atmospheric Hg, and that better data are required in order to assess the magnitude, spatial distribution and importance of these emissions relative to the direct anthropogenic emission [*Schroeder and Munthe*, 1998; *Bergen et al.*, 1999].

Forest fires are an important pathway of material exchange between the biosphere and atmosphere. They result in the re-emission of previously deposited anthropogenic Hg along with some fraction of natural Hg present in both soil and biomass[*Lindberg et al.*, 1998]. A recent study of a mixed-vegetation fire in the southern Cape Peninsula in Africa [*Brunke et al.*, 2001] suggests that Hg emissions from biomass burning in general may be a more significant pathway of Hg exchange between the biosphere and atmosphere than was previously believed, potentially accounting for 12-28% of annual global total gaseous mercury (TGM) emission. Laboratory experiments suggest that burning of litter and green vegetation results in nearly complete release, in mostly gaseous form, of Hg contained in the fuel, and that release of Hg from fires may be 104-526 Mg y^{-1} or 3.5-17.5% of natural Hg emissions and 1.6-8.0% of all emissions [*Friedli et al.*, 2001].

The magnitude of Hg emission from boreal forest fires is not well quantified. Direct measurements of Hg release from actual boreal fires would add confidence to our understanding of the contribution of this source to the global Hg budget. To this point, there is no published record of Hg emission from a large-scale natural fire in the Canadian boreal forests, much less subsequent long-range transport to the United States. However, large fires in this region have been linked to enhancements in carbon monoxide (CO) and volatile organic compounds (VOCs) in the mid-latitudes [*Wofsy et al.*, 1994]. These species as well as ozone (O_3) and aerosols may be transported in Canadian forest fire plumes as far as the southeastern United States, causing local enhancements in their concentrations [*Wotowa and Trainer*, 2000]. This raises questions regarding the role of fire in the annual Hg budget in North America, especially in Canada where anthropogenic emissions of Hg are significantly lower than in the United States [*EPA*, 1997; *Environment Canada*, 2000].

In this study, evidence of long-range transport of Hg from a Canadian boreal fire was revealed by a clear relationship between enhancements in CO and Hg concentrations observed at a rural site in the northeastern United States and a large natural fire in northern Quebec. The relationship between Hg and CO emission from biomass combustion was used to estimate area-based and annual Hg emissions for Canadian fires and assess the potential contribution of natural boreal forest fire emissions to the regional and global atmospheric Hg budget.

4.2. Fire Event and Experimental Methods

This study focuses on a series of natural fires that occurred in the James Bay region of Quebec, approximately 500 km north of Montreal, during early July 2002. Approximately 250 fires burned more than 1,000,000 ha during July over an area of 20,000,000 ha bounded roughly by the James Bay coast on the west, the Manicouagan Reservoir in the east, Lake Mistassini in the south and the Grande River in the north [*Fortin*, personal communication]. The dominant species in this region are black spruce and jack pine, occurring primarily in monospecific stands [*Lavoie and Sirois*, 1998].

NASA MODIS images clearly showed that northwesterly winds carried the fire plume as far south as southern New England and northern Pennsylvania/New Jersey on 6 July 2002, and as far south as northern Virginia, a distance of over 1300 km, on 7 July (Figure 4.1). By 8 July, much of the plume had moved off of the East Coast of the United States, no longer impacting southern New England. Backward air mass trajectories were computed from Harvard Forest using NOAA HYSPLIT-4 [*Draxler and Hess*, 1997]. Thirty-six hour trajectories computed before, during and after the event verify that the air masses impacting the site at the time of plume influence originated over the burn area (Figure 4.2). HYSPLIT trajectories show an increasingly westerly trend by 23:00 UTC (18:00 local time) on 7 July as the plume moved off of the East Coast.

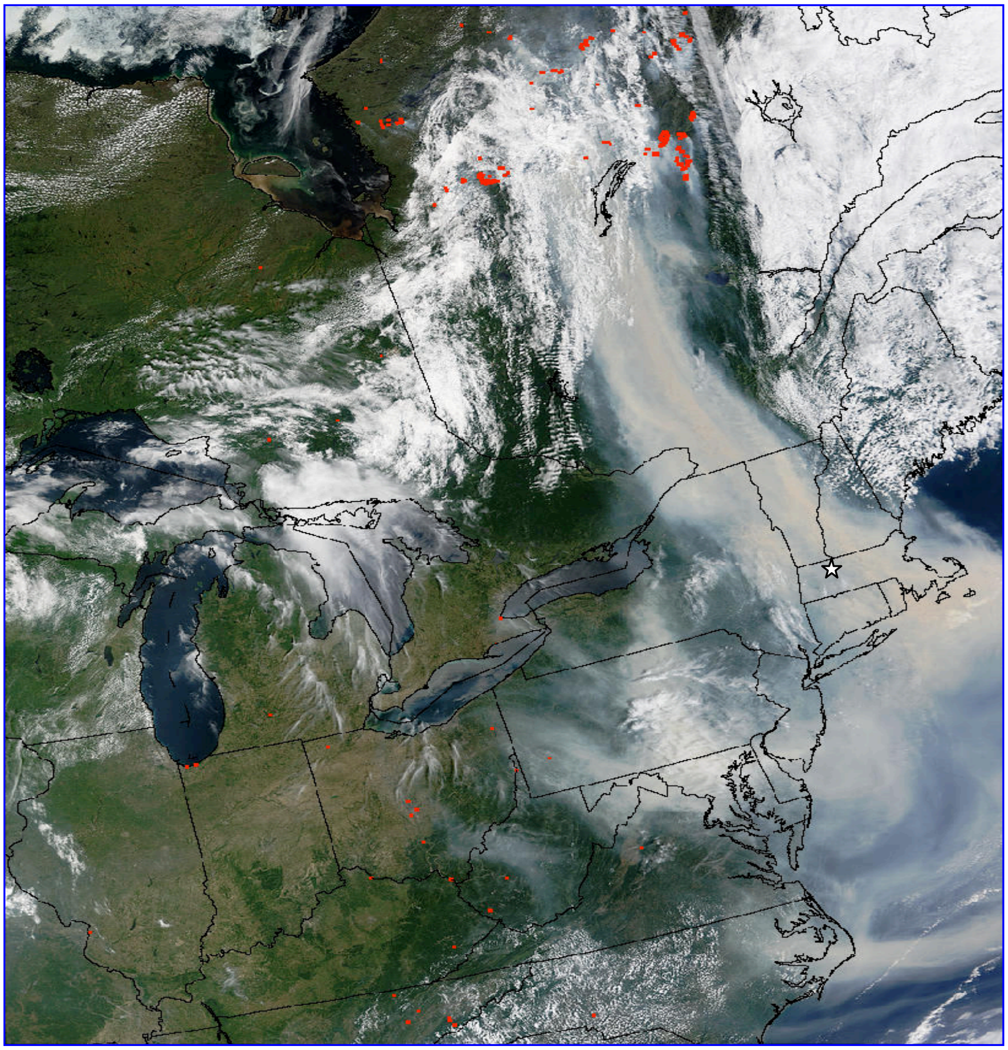

Figure 4.1: NASA Terra satellite image of Quebec fire plume extending along the East Coast of the United States (7 July 2002, 16:35 UTC). The general burn area is enclosed in the white circle. The white star indicates measurement location (Harvard Forest). Photo courtesy NASA MODIS Image Gallery.

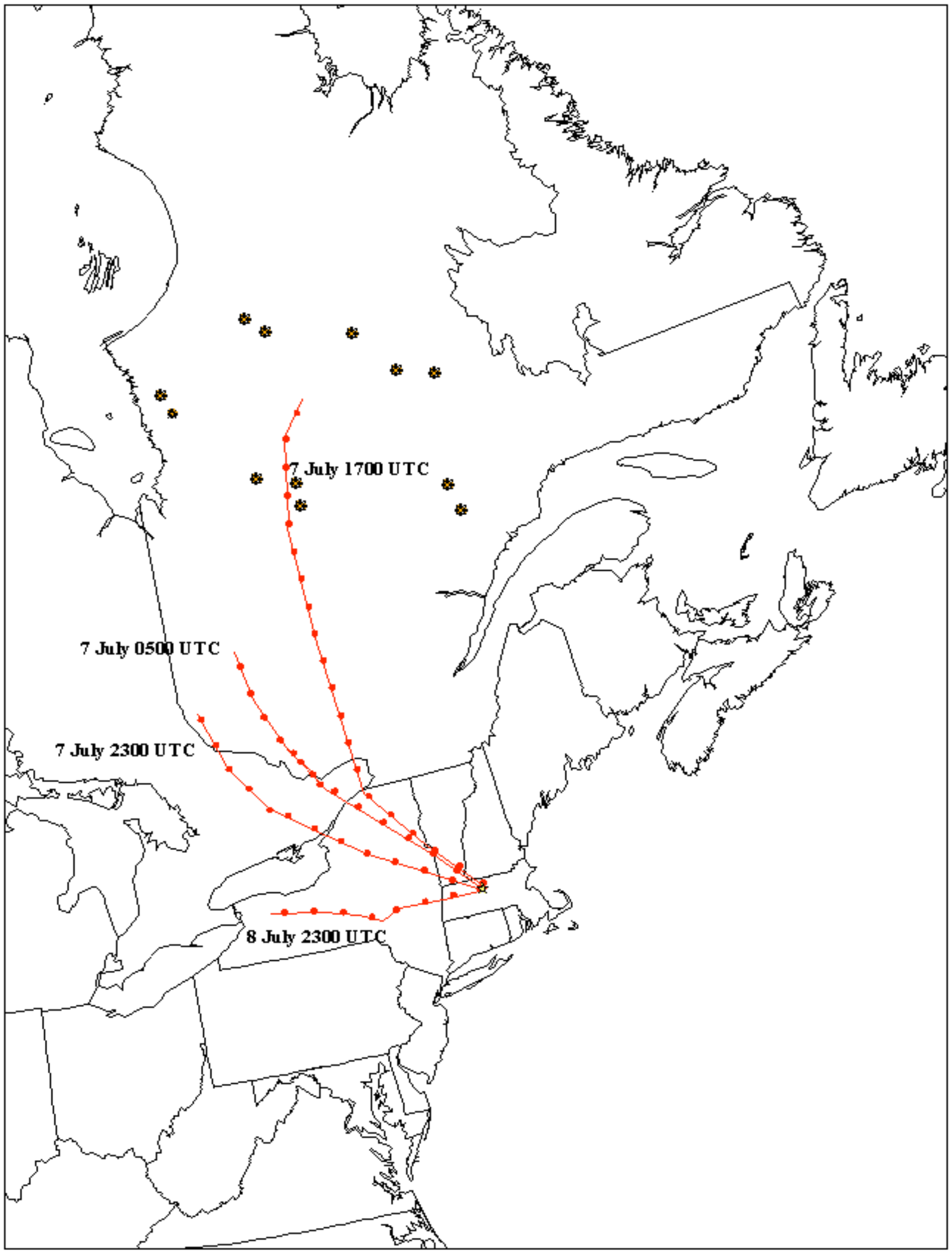

Figure 4.2: Ensemble of 36-hour backward trajectories from Harvard Forest before, during and after plume event. Asterisks represent major burn areas.

The plume signal was monitored at Harvard Forest, a Long-Term Ecological Research (LTER) site located near Petersham, Ma. (42º54´N, 72º18´W). This is a rural site located > 100 km from Boston, MA. and Hartford, CT. A Teflon filter was mounted at the canopy height (24 m) on a 30-m walk-up tower. Air was drawn through the filter and into a mercury vapor analyzer (Model 2537A, Tekran, Inc.) that measured TGM at 5-minute intervals. The analyzer was calibrated daily against an internal permeation source and housed in a temperature-controlled trailer near the tower. The internal permeation source was verified to within 6% by laboratory manual injection tests. Continuous measurements of CO were made with a Dasibi absorbance analyzer on a 10-m tower located approximately 50 m from the walk-up tower [*Potosnak et al.*, 1999].

Trajectory analysis was used to determine which TGM and CO data collected at Harvard Forest were from the Quebec smoke plume. The Hg:CO emission ratio was calculated using orthogonal, or geometric mean regression slope as outlined in *Richardson* [2000]. Only gaseous Hg was measured in this study, the vast majority of which was Hg^0 [*Friedli et al.*, 2001; *Friedli et al.*, 2003].

4.3. Results

The Quebec plume signal was clearly detected at Harvard Forest on 7 July. CO concentrations reached a maximum of 950 ppb at 14:30 LST on 7 July (Figure 4.3), exceeding background levels by a factor of 4.5. CO concentration then steadily declined, returning to background levels by 06:00 LST on 8 July as wind direction and air mass trajectory shifted from northerly to northwesterly (Figure 4.2). Maximum TGM concentrations during the event approached 2.0 ng m^{-3}, an enhancement of approximately

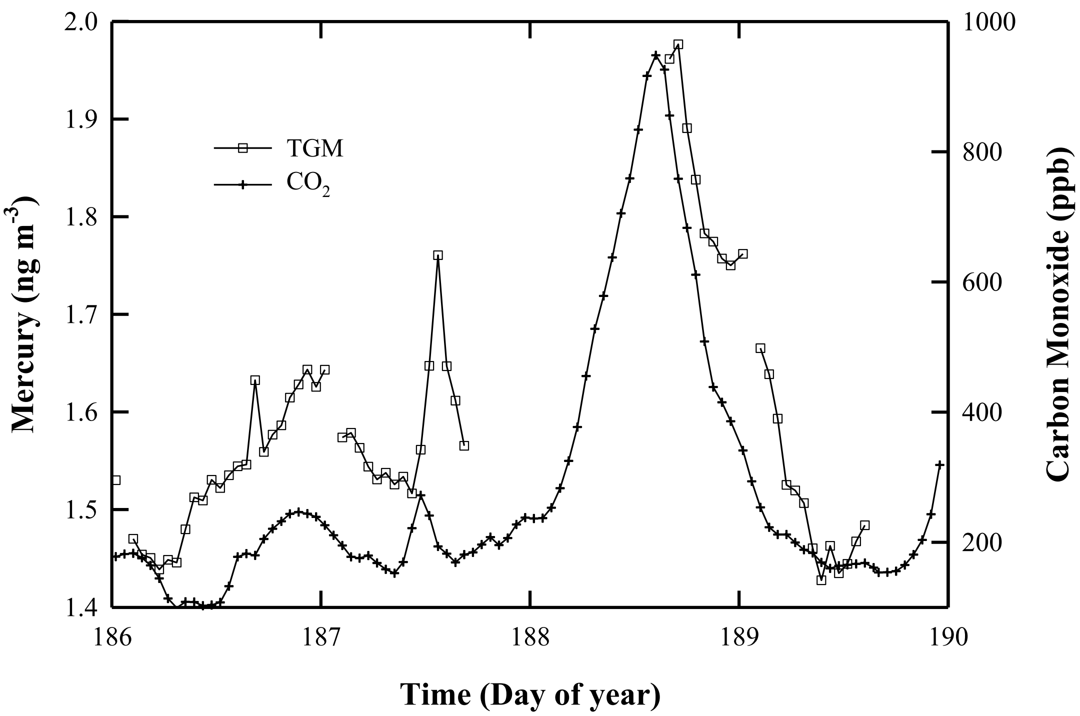

Figure 4.3: Temporal variation of mercury and carbon monoxide at Harvard Forest, MA, during local pollution and the fire plume event, 5-8 July (day of year 186-189), 2002. Data are hourly averages. The gaps in TGM data result from analyzer malfunction.

.

40% above background (~1.4 ng m^{-3}). Degradation or enhancement of TGM or CO within the plume during transport was unlikely because of the lack of pollution sources along the flow path, the long lifetime of Hg^0 and the sufficiently long lifetime of CO (approximately two months in the summer), which makes it an excellent, regional-scale tracer of biomass burning [*Kato et al.*, 2002].

Both CO [*Brunke et al.*, 2001] and CO_2 [*Lee et al.*, 2001] have been used as tracer variables for determining Hg emission rates. In this case, a strong correlation between ambient Hg and CO was observed at Harvard Forest during the plume event. Orthogonal linear regression yields a Hg:CO emissions ratio of 8.61×10^{-8} mol mol^{-1} [6.15×10^{-7} g Hg $(g\ CO)^{-1}$, $R^2=0.89$, $p<0.01$, $n=15$, Figure 4.4] during the event. When combined with the trajectory analysis (Figure 4.2), the highly significant correlation between CO and Hg provides credible evidence of long-range transport of Hg from a boreal forest fire. The data points for the plume event were isolated using the trajectory analysis, which is an effective means of determining plume influence at Harvard Forest based on changes in trajectory endpoint and direction (Figure 4.2). Also, a series of data points representing local and regional flow patterns preceding the plume event were selected and are displayed in Figure 4.4. The emissions ratio calculated for the plume event is considerably less than that for local and regional influences at Harvard Forest (2.80×10^{-7} mol mol^{-1}, $R^2=0.59$, $p<0.01$, $n=92$), reflecting strong influences from local and regional pollution sources.

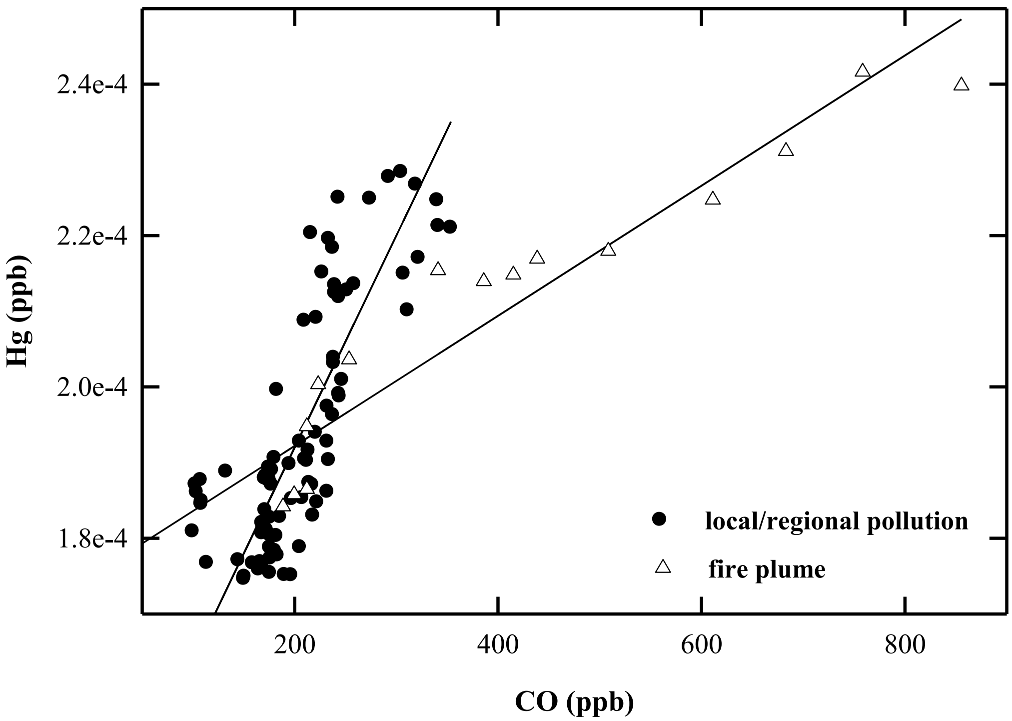

Figure 4.4: Regression of Hg vs. CO for local/regional pollution sources [$Y = (1.36\times10^{-4}) + (2.80\times10^{-7})x$; $R^2=0.6$, $p<0.01$, $n=92$]* and during Quebec fire plume [$Y = (1.75\times10^{-4}) + (8.61\times10^{-8})x$; $R^2 = 0.9$, $p<0.01$, $n=15$]* at Harvard Forest, July 2002. Data are hourly averages. *Slope and intercept of these equations were calculated manually from geometric mean regression as outlined in *Richardson* [2000].

4.4. Discussion

In comparison with other similar studies, the data presented here have both unique advantages and weaknesses. Though remotely obtained, this is a direct measurement of Hg emission from a large-scale, naturally-occurring boreal fire, which has advantages over previous studies of fire emissions which focused on small-scale prescribed fires [e.g. *Hobbs et al.*, 1996] or laboratory experiments [e.g., *Friedli et al.*, 2001]. Prescribed fires are by nature small, spot measurements, burn fuels which are often slashed, trampled or bulldozed and employ set moisture, weather and fuel parameters intended to ensure a controlled and complete burn and therefore represent ideal and possibly unrealistic conditions. Though difficult to undertake, the importance of measuring emissions from large-scale wildfires is further underscored by the observation that they represent 90% of the total, global boreal forest area burned [*Cofer et al.*, 1996]. In this particular case, since the observed smoke plume represented a conglomeration of emissions from many fires spread over a large area, these measurements are less subject to the potential bias due to site variability that may characterize spot measurements of emissions from individual, prescribed fires. However, a drawback of measurements of large fire events is that combustion stage and fuel types are not known precisely, making cross-validation against controlled experiments difficult.

Application of the Hg:CO emission ratio reported here to approximate Hg release per unit area as well as extrapolation to large scales requires data on CO emission factor, species composition and fuel consumption of the burn area. It is known that both CO and Hg emission factors depend on fire stage [*Cofer et al.*, 1998; *Friedli et al.*, 2001]. Since the ambient concentration measurement at Harvard Forest represents a mixture of fires in various stages of burn, it is appropriate to use a fire-averaged CO emission factor. The emission factors found in the literature for black spruce and jack pine for prescribed burns [*Cofer et al.*, 1991; *Susott et al.*, 1991; *Ward et al.*, 1992] and wildfires [*Friedli et al.*, 2003] are quite consistent, giving a mean value of 99.1 g CO (kg biomass)$^{-1}$ and a small standard deviation of 11.7 g CO (kg biomass) $^{-1}$ (number of observations = 7).

Based on data from an experimentally validated model, a mean fuel consumption of 2.40 (standard deviation 0.81) kg m^{-2} has been reported for Canadian boreal forests [*Amiro et al.*, 2001]. Combining this mean fuel consumption, the fire-averaged CO emission factor and the Hg:CO emissions ratio given above, yields estimated CO and Hg emission flux densities from Canadian boreal forest fires of 2400 kg CO ha^{-1} and 1.5 g Hg ha^{-1}. Combining the mean Hg flux density with an approximate area burned in the Quebec fires during July 2002 [1.1 million ha (*Fortin*, personal communication)] results in a total release of 1.6 Mg Hg. This should be viewed as an order of magnitude estimate only because the exact fuel consumption is not known.

Since spruce/jack pine-dominated fuel type represents a significant fraction of nearly every Canadian ecozone [*Amiro et al.*, 2001], it is appropriate to apply the above Hg emission flux density estimate to Canadian fires. Assuming a mean burn area of 2.3 million ha y^{-1} in the boreal zone [*CCFM*, 2002] yields an annual release of 3.5 Mg Hg from Canadian boreal forest fires. This is equal to roughly one third of inventory estimates of annual anthropogenic Hg emission in Canada [~11 Mg in 1995; *Environment Canada*, 2000]. Boreal fires therefore play a highly significant role in the overall Canadian Hg budget. This role may be amplified during years of intense activity. Total forest area burned in Canada may be as high as 7.5 million hectares in a particular year

[*Amiro et al.*, 2001]. Based on the measurements presented here, such an intense fire year may result in a release of approximately 11 Mg of Hg. A single large fire such as the one studied by *Wotawa and Trainer* [2000], which burned more than 3 million ha over a two-week period, could release 4.5 Mg of Hg.

Boreal forest fires are highly stochastic phenomena, determined largely by meteorological conditions and, to some extent, fuel availability and consumption. Total area burned throughout the biome often varies interannually by more than an order of magnitude [*Cahoon et al.*, 1994]. Such variability in area burned contrasts with African savannah fires, which typically account for the vast majority of global biomass burning emissions but tend to be relatively constant in interannual range and distribution [*Cahoon et al.*, 1992]. The total area burned by boreal fires worldwide is not known to any great degree of certainty. Estimates vary from 5 – 10 million ha y^{-1} [*Stocks et al.*, 1996] to more than 15 million ha y^{-1} [*Conard and Ivanova*, 1997]. Satellite data suggest that the total area burned in a given year could vary between 3 million and at least 22 million ha [*Cofer et al.*, 1996]. If 15 million ha y^{-1} is assumed to be the mean area burned globally, the measurements presented here imply a mean annual global Hg emission from boreal fires of approximately 22.5 Mg. In a particularly intense year during which 22 million ha are burned, 33 Mg of Hg could be emitted globally from boreal fires.

Calculations based on the area-based Hg emission factor used here can only be considered order of magnitude estimates since they assume a uniform canopy composition, biomass consumption pattern and Hg loading which may be disparate among Canadian and Russian boreal forests. For this same reason, extrapolation of these data to the entire globe is difficult. The Hg:CO emissions ratio reported here is approximately 40% and 55% of those reported for a wildfire in a pine/shrub landscape in South Africa [*Brunke et al.*, 2001] and a small-scale temperate/boreal wildfire in Ontario [*Friedli et al.*, 2003], respectively, reflecting the relatively low Hg concentration in live coniferous fuel [*Friedli et al.*, 2001] and relative absence of local pollution sources in northern Quebec. The variation in the emissions ratio suggests that fire emission is dependent on biome/species. Biomass burning is estimated to release 400 – 700×10^{6} Mg CO y^{-1} to the atmosphere globally [*Andreae*, 1993; *Graedel and Crutzen*, 1993]. If this is combined with the Hg:CO emissions ratio found in [*Brunke et al.*, 2001], the global fire emission of Hg would be 510 – 1140 Mg y^{-1}. This estimate would be lowered to only 250 – 430 Mg y^{-1} if the emissions ratio of this study is applied. Therefore, accurate determination of global Hg emissions from biomass burning using observations from one or a very few fire events, as existing studies have [*Brunke et al.*, 2001; *Friedli et al.*, 2001; *Friedli et al.*, 2003], is difficult. That the vast majority of global C emission from biomass burning occurs in tropical grasslands with a much different species composition for which no emissions data exist further implies that the total contribution of global biomass burning cannot be accurately determined without a better understanding of variation in Hg:CO emissions ratios across biomes.

Acknowledgements

Brian Amiro, Yves Bergeron, Julie Fortin, Rob Fraser, Sylvie Gauthier, Nick Payne, Brian Stocks and Steve Wofsy deserve thanks for helpful personal communications. The Harvard Forest Environmental Measurement Site was established with support from the Long-Term Ecological Research Program of the National Science Foundation. Additional support was provided by the Biological and Environmental Research Program (BER), U.S. Department of Energy, through the Northeast Regional Center of the National Institute for Global Environmental Change (NIGEC) under Cooperative Agreement No. DE-FC03-90ER61010. Also, thanks to three very helpful reviewers for *Environmental Science & Technology* who provided helpful criticisms of a submitted manuscript on this chapter's results.

4.5. References

Allan, R.J. (1999), Atmospheric mercury contamination of remote aquatic ecosystems in Canada. *Wat. Sci. Tech.*, 12, 173-177.

Amiro, B.D., Todd, J.B., Wotton, B.M., Logan, K.A., Flannigan, M.D., Stocks, B.J., Mason, J.A., Martell, D.L., and Hirsch, K.G. (2001), Direct carbon emissions from Canadian forest fires, 1959-1999. *Can. Jour. Forest Res.*, 31, 512-525.

Andreae, M.O. (1993), The influence of tropical biomass burning on climate and atmospheric chemistry. In R.S. Oreland (Ed.), Biogeochemistry of Global Change: Radiatively Active Trace Gases. Chapman and Hall, N.Y., pp. 113-150.

Bergen, T., Gallardo, L., and Rodhe, H. (1999), Mercury in the global troposphere: A three-dimensional model study. *Atmos. Env.*, 33, 1575-1585.

Brunke, E-G., Labuschagne, C., and Slemr, F. (2001), Gaseous mercury emissions from a fire in the Cape Peninsula, South Africa, during January 2000. *Geophys. Res. Lett.*, 28, 1483-1486.

Bullock, O.R. (2000), Current methods and research strategies for modeling atmospheric mercury. *Fuel Proc. Tech.*, 65-66, 459-471.

Cahoon, D.R., Stocks, B.J., Levine, J.S., Cofer, W.R., and Chung, C.C. (1992), Evaluation of a technique for satellite-derived estimation of biomass burning. *J. Geophys. Res.*, 99, 18627-18638.

Cahoon, D.R., Stocks, B.J., Levine, J.S., Cofer, W.R., and Pierson, J.M. (1994), Satellite Analysis of the severe 1987 forest fires in northern China and southeastern Siberia. *J. Geophys. Res.,* 99, 18627-18638.

Canadian Council of Forest Ministers (2002), National Forestry Database Program, http://nfdp.ccfm.org.

Cofer, W.R., Levine, J.S., Winstead, E.L., and Stocks, B.J. (1991), In *Global Biomass Burning: Atmospheric, Climatic and Biospheric Implications*; Levine, J.S., Ed.; MIT Press, Cambridge, Ma., pp. 203-208.

Cofer, W.R., Winstead, E.L., Stocks, B.J., Cahoon, D.R., Goldammer, J.G., and Levine, J.S. (1996), In *Fires in Ecosystems of Boreal Eurasia*; Goldhammer; J.G.; Furyaev, V.V., Eds.; Kluwer, Dordrecht-Boston-London, pp. 465-475.

Cofer, W.R., Winstead, E.L., Stocks, B.J., Overbay, L.W., Goldammer, J.G., Cahoon, D.R., and Levine, J.S. (1996), Emissions from Boreal Forest Fires: Are the Atmospheric Impacts Underestimated? In Levine, J.S. (ed.), Biomass Burning and Global Change (Vol. 2). MIT Press, Cambridge, Ma., 834-839.

Cofer, W.R., Winsted, E.L., Stocks, B.J., Goldammer, J.G., and Cahoon, D.R. (1998), Crown fire emissions of CO_2, CO, H_2, CH_4, and TNMHC from a dense jack pine boreal forest fire. *Geophys. Res. Lett.*, 25, 3919-3922.

Conard, S.G., and Ivanova, G.L. (1997), Wildfire in Russian boreal forests – potential impacts of fire regime characteristics on emissions and global carbon balance estimates. *Env. Poll.*, 98, 305-313.

Draxler, Roland R., and Hess, G.D. (1997), Description of the HYSPLIT_4 Modeling System. NOAA Technical Memorandum ERL ARL-224, 24 pp.

Environment Canada (2000), The Status of Mercury in Canada. http://www.cec.org/Programs_projects/pollutants_health/smoc/pdfs/hgcan-e.pdf.

EPA (1997), Mercury Study Report to Congress. http://www.epa.gov/mercury.html.

Fitzgerald, W.F., Engstrom, D.R., Mason, R.P., and Nater, E.A. (1998), The case for atmospheric mercury deposition in remote areas. *Env. Sci. Tech.*, 32, 1-7.

Fortin, J. (2002), Quebec Ministry of Natural Resources, personal communication.

Friedli, H.F., Radke, L.F., and Lu, J.Y. (2001), Mercury in smoke from biomass fires. *Geophys. Res. Lett.*, 28, 3223-3226.

Friedli, H.F., Radke, L.F., Lu, J.Y., Banic, C.M., Leaitch, W.R., and McPherson, J.I. (2003), Mercury emissions from burning of biomass from temperate North American forests: laboratory and airborne measurements. *Atmos. Env.*, 37, 253-267.

Graedel, T.E., and Crutzen, P.J. (1993), Atmospheric change: an Earth system perspective. W.H. Freeman and Co., N.Y., 446 pp.

Hobbs, P.V., Reid, J.S., Herring, J.A., Nance, J.D., Weiss, R.E., Ross, J.L., Hegg, D.A., Ottmar, R.D., and Liousse, C. (1996). Particle and trace-gas measurements in the smoke from prescribed burns of forest products in the Pacific Northwest. In Levine, J.S. (ed.), Biomass Burning and Global Change (Vol. 2). MIT Press, Cambridge, Ma. 697-715.

Kato, S., Pochanart, P., Hirokawa, J., Yoshizumi, K., Akimoto, H., Ozaki, Y., Obi, K., Katsuno, T., Streets, D.G., Minko, N.P. (2002), The influence of Siberian forest fires on carbon monoxide concentrations at Happo, Japan. *Atmos. Env.*, 36, 385-390.

Kehrig, H.D., and Malm, O. (1999), Methylmercury in fish as a tool for understanding the Amazon mercury contamination. *App. Organomet. Chem.*, 13, 689-696.

Lavoie, L. and Sirois, L. (1998), Vegetation changes caused by recent fires in the northern boreal forest of eastern Canada. *J. Veg. Sci.,* 9, 483-492.

Lee, X., Bullock, O.R., and Andres, R.J. (2001), Anthropogenic emission of mercury to the atmosphere in the northeast United States. *Geophys. Res. Lett.*, 28, 1231-1234.

Lindberg, S.E., Hanson, P.J., Meyers, T.P., and Kim, K.-H. (1998), Air/surface exchange of mercury vapor over forests – The need for a reassessment of continental biogenic emissions. *Atmos. Env.*, 32, 895-908.

Lindquist, O., and Rodhe, H. (1985), Atmospheric mercury – a review. *Tellus* 37B, 136-159.

Mason, R.P., Fitzgerald, W.F., and Morel, F.M.M. (1994), The biogeochemical cycling of elemental mercury: anthropogenic influences. *Geochem. et Cosmochem. Acta,* 58, 3191-3198.

Munthe, J., and McElroy, W.J. (1992), Some aqueous reactions of potential importance in the atmospheric chemistry of mercury. *Atmos. Env.*, 26A, 553-557.

Nriagu, J.O. (1989), A global assessment of natural sources of atmospheric trace metals. *Nature*, 338, 47-49.

Potosnak, M.J., Wofsy, S.C., Denning, A.S., Conway, T.J., Munger, J.W., and Barnes, D.H. (1999), Influence of biotic exchange and combustion sources on atmospheric CO_2 concentrations in New England from observations on a forest flux tower, *J. Geophys. Res.,* 103, 9561-9569.

Richardson, A.D. (2000), Coarse root elongation rate estimates for interior Douglas-fir, *Tree Physiology*, 20, 825-829.

Schroeder, W.H., and Munthe, J. (1998), Atmospheric Mercury – An Overview. *Atmos. Env.*, 32, 809-822.

Susott, R.A., Ward, D.E., Babbitt, R.E., and Latham, D.J. (1991), In *Global Biomass Burning: Atmospheric, Climatic and Biospheric Implications*; Levine, J.S., Ed., MIT Press, Cambridge, Ma., pp. 245-257.

Ward, D.E., Susott, R.A., Waggoner, A.P., Hobbs, P.V., and Nance, J.D. (1992), In Proc 29th Annual Meeting of the PNW International Section of the Air and Waste Management Assoc., pp 6.2:1-12.

Wofsy, S.C., Fan, S-M., Blake, D.R., Bradshaw, J.D., Sandholm, S.T., Singh, H.B., Sachse, G.W., and Harriss, R.C. (1994), Factors influencing atmospheric composition over subarctic North America during summer. *J. Geophys. Res.*, 99, 1887-1897.

Wotawa, G., and Trainer, M. (2000), The influence of Canadian forest fires on pollutant concentrations in the United States, *Science*, 288, 324-328.

Chapter 5:

Summary and Implications

5.1. Summary

This study dealt broadly with natural and anthropogenic emissions of mercury (Hg) to the atmosphere. Emphasis was placed on Hg emissions in the northeastern United States, because this region is known to possess the highest anthropogenic Hg emission rate in the nation [*EPA*, 1997], and may therefore experience significant loading of Hg to the environment. Additionally, both natural and anthropogenic emissions in the northeast have been either understudied or are not known with a high degree of accuracy or time resolution. However, some components of the research were intended to address global uncertainties or to make broad improvements in our ability to measure and analyze both natural and anthropogenic emission or cycling of Hg and other trace gases. The methodologies were therefore designed with the more general goal of improving the state of the science whether by developing, testing and implementing a new measurement system or providing a novel framework for analyzing field data.

A primary goal of the study was to determine recent trends in the regional Hg emission rate in the northeast and to investigate factors that influence these trends, whether climatological or anthropogenic. Regional Hg emission rates were determined using the technique of tracer analysis, combining wintertime measurements of Hg with a combustion tracer (carbon dioxide) at a background site located at Great Mountain Forest, Connecticut (CT). Tracer analysis was applied over a multi-year time period for the first time. Results showed that regional anthropogenic Hg emission is dynamic and varies significantly from year to year, decreasing by 40% between the winters of 1999/2000 and 2001/2002, and increasing by approximately 20% between 2001/2002 and 2003/2004.

The observation of significant interannual variability in the Hg emission rate underscores the importance of this method, which allows for more recent and higher resolution flux estimates than inventory estimates [e.g., *EPA*, 1997]. As a toxic environmental pollutant, Hg has become of increasing concern from the public health and environmental policy sector. The progress of policies designed to curb emissions cannot be assessed using emissions inventory methodology, which is more likely to be updated on a decadal rather than annual or seasonal basis and therefore cannot reveal short-term response to legislation, changes in anthropogenic sources, control technology improvements etc. The “top-down,” long-term atmospheric approach used in this study provides a more accurate, timely and altogether suitable framework for emissions monitoring.

This study did not merely seek to quantify trends in regional Hg emission in the northeast, but also to address the reasons that such trends may occur. This problem was initially approached by investigating climatological impacts on TGM measurements at Great Mountain. Wintertime air trajectory modeling combined with a potential source contribution function revealed a source region of Hg influencing the site that typically encompasses most of the mid-Atlantic and New England states, Maryland and Delaware. The source region showed small interannual variation. This observation suggests that although climatology may be a mitigating factor in determining the regional Hg emission rate, it cannot fully or even primarily explain the significant interannual variation in the emission rate.

If climatology is not the primary control, the interannual variation in regional Hg emissions may be related to changes in the anthropogenic point sources of Hg within the source region. Therefore, emissions from the electric power sector were investigated, as this is the most important Hg emissions category in the northeast. Calculations of Hg flux from the regional electric power sector showed strong correlation with the trend in Hg emission derived from the atmospheric measurements, suggesting that the power sector strongly influences the regional Hg flux to the atmosphere.

The framework used in this study for estimating and interpreting trends in regional Hg emissions is novel and intended to have broad application in the study of regional-scale emissions of pollutants which are not accurately characterized by inventory data. The combination of tracer analysis and trajectory modeling over a multi-year time period allows for a more accurate and timely assessment of emissions trends and a means of judging whether climatology or some other factor (e.g., changes in anthropogenic sources) is primarily responsible for emissions trends.

Perhaps the most significant finding in this phase of the study is the observation that, when averaged over the five winters, the estimated Hg emission rate from the power sector was 75% of the flux derived from the atmospheric measurements and tracer analysis. This is striking, because the vast majority (>95%) of the atmospherically-derived flux is elemental Hg. If 50% or more of Hg emitted by power sources is speciated (Hg^{2+} or particulate Hg) and deposits locally, as is generally believed [e.g., *Chu and Porcella*, 1995; *EPA*, 1997], the power sector can account for 40% of the observed Hg flux to the atmosphere. While underscoring the importance of the electric power sector in the regional Hg emission rate, this suggests that emissions from sources outside the power sector are underestimated, or that Hg emissions resulting from combustion of municipal and medical waste have not been curbed to the EPA targeted level.

Another goal of this study was to contribute to the understanding of natural sources of Hg; most importantly, emission from soil. Not only is soil Hg emission thought to be much more significant globally than previously believed, there is a limited understanding of how or where bound Hg is desorbed and released from soil. Detailed study of gaseous Hg within soil pore spaces would shed light on this process, but no such studies exist due primarily to a lack of a widely accepted measurement method. In this light, the flask sampling system for sampling and analyzing soil gaseous Hg developed here represents an important contribution to the study of Hg and other trace gases in soils. The system can accurately recover low concentrations of gaseous Hg without leakage or contamination, is relatively inexpensive (minus the cost of the Hg vapor analyzer), rugged, easy to deploy and allows for either on-site sampling or transport of samples to the laboratory for analysis within a 19-hour time frame. This represents a significant improvement over other methodologies which are more cumbersome or expensive, are subject to contamination or create a suction which draws in ambient air from above the soil [e.g., *Wallschläger et al.*, 2002; *Johnson et al.*, 2003].

The flask sampling system was used to measure gaseous Hg in background forest soil at Coventry, CT in 2003 and 2004. This represents the first detailed study of gaseous Hg concentrations within the soil profile. Soil gaseous Hg varied seasonally with soil temperature, and highest concentrations consistently occurred in the O- and upper A-horizons. Most significantly, the study revealed clear gradients in gaseous Hg concentrations. Such gradients had not previously been observed in soil, and their repeated observation over two field experiments seems to provide further indication that the measurement system is robust.

During the second field experiment in 2004, soil Hg flux was measured. Flux was similar in magnitude to other studies which measured soil Hg flux in background forest sites. While soil gaseous Hg was more strongly related to soil temperature, soil Hg flux was better correlated with solar radiation. Further study with improved design, particularly in terms of radiation measurements, is required to understand whether photochemical reactions or changes in soil temperature are primarily responsible for the ultimate release of Hg from soil.

Flux measurements were also analyzed in the context of their relationship to gaseous Hg within the soil profile. The observed gradients in soil gaseous Hg bore striking resemblance to gradients in bound Hg. Although organic matter content was not measured, there appeared to be some circumstantial evidence that bound and gaseous Hg were related to spatial variation in organic matter content. In addition, measurements of soil Hg flux were correlated with soil gaseous Hg concentrations at 2-cm depth. Taken together, these results indicate that the upper organic layers act as a source of gaseous Hg that may ultimately be emitted to the atmosphere. Large changes in soil gaseous Hg over shallow layers (2 to 5 cm depth) underscore the importance of fine vertical resolution of measurements, and therefore the utility of the flask sampling system.

During the summer of 2002, TGM measurements within the smoke plume of a large-scale Canadian boreal forest fire were captured at Harvard Forest, Massachusetts. Though not anticipated, this was an opportunity to document long-range transport of Hg from boreal fires to the northeast United States and the consequent short-term impact on ambient TGM levels, and also to use carbon monoxide measurements and tracer analysis to make an order-of-magnitude estimate of typical Hg release from a large-scale, natural fire event in the boreal region. This is a valuable contribution, as only a few studies exist [e.g., *Brunke et al.*, 2001; *Friedli et al.*, 2003] that report Hg emissions from biomass burning in any ecosystem, and none on the scale of this particular event, which was comprised of hundreds of fires scattered over a large geographic area (~20,000,000 ha). Results indicated that Hg release from biomass burning may contribute significantly to regional and national Hg budgets, typically equal in magnitude to approximately one-third of Canadian anthropogenic emissions. However, natural forest fire activity is a highly stochastic process, and during years with intense burning, results of this study suggest that annual Hg emissions from boreal fires may be equivalent to annual anthropogenic emissions. A single large fire event such as the one studied by *Wotowa and Trainer* [2000], roughly three times as large as the event studied here, could release as much or more Hg into the atmosphere as is typically released by power plants in the northeastern U.S. during the entire wintertime (see Chapter 2).

The Hg:CO emissions ratio determined for boreal forest fires in this study is roughly half of that determined in other studies which examined Hg release in temperate/boreal fires in Ontario, Canada [*Friedli et al.*, 2003] and pine/shrub landscapes in South Africa [*Brunke et al.*, 2001]. However, both of these studies extrapolated their results to global biomass burning. If the Hg:CO emission ratio determined for boreal forest fires in this study is extrapolated to all global biomass burning, the estimated global emission is less than half of the estimate given in the aforementioned studies. This indicates that Hg release from forest fires likely has a strong relationship to proximity to anthropogenic sources or species composition and biome.

5.2. Implications

There are several important messages, implications, or areas ripe for future research in each phase of this study. They are summarized here:

1). Regional anthropogenic Hg emissions may change significantly on an interannual basis, primarily in response to changes in fuel type, activity levels, control technology etc among major combustion sources. Therefore, inventory estimates of emission levels are an inadequate means of understanding Hg loading to the atmosphere in polluted regions. Not only is the inventory approach cumbersome and by nature inaccurate, but it only provides a one-year "snapshot" of emission rates and has poor capacity for tracking changes in emission which may be related to legislative efforts meant to curb pollution. Long-term atmospheric measurements are a more appropriate means of assessing the response of emissions to changes in control technology, legislation, fuel types etc. Atmospheric monitoring may be particularly important for areas rich in combustion sources. Further monitoring in the northeast U.S. during the next decade may be a useful means of monitoring progress of future legislation addressing Hg emission from coal-burning power plants.

2). The tracer analysis presented in Chapter 2 unequivocally demonstrates the importance of electric power plants to regional Hg emissions in the northeast U.S. Interannual variation in the regional Hg flux derived from atmospheric measurements is highly sensitive to interannual changes in combined emissions from the region's electric power sector. More specifically, the overall regional Hg emission flux is responsive to changes in the power sector fuel mix. In particular, small percent decreases (e.g., 10-15%) in the total, annual consumption of coal or oil by the power sector results in similar decreases in power sector Hg flux, and appears to have an impact on total, regional Hg emissions from all sources. Furthermore, comparison of regional Hg emissions based on the tracer analysis with the inventory power sector flux suggests that the power sector may account for on the order of 40% of the observed flux. It therefore stands to argue that a policy-required reduction in the combustion of oil and, especially, coal by the electric power sector, or broad implementation of Hg control technology, will result in significant reduction of the overall regional anthropogenic Hg emission rate.

While highlighting the importance of the electric power sector to regional Hg emissions in the northeast, the tracer analysis revealed an unexpected disparity between the regional Hg emission rates in the northeast U.S. determined from atmospheric measurements and electric power inventory data over a five-year period. EPA inventory estimates suggest that the electric power sector should account for a higher percentage of regional anthropogenic Hg emissions in the northeast than what was observed here, and the high percentage of reactive Hg believed to be emitted by power plants (more than 50%) therefore result in an electric power inventory flux that is much higher than the atmospheric measurement, which consists almost entirely of elemental Hg. Although the reasons for the disparity are highly speculative, it raises the possibility of a “missing source” of Hg. Perhaps the most plausible explanation is that emissions from municipal and medical waste combustion, which once accounted for over 40% percent of Hg emissions in the northeast [*EPA*, 1997], have not been curbed by >90% throughout the region since 1997, as intended by the EPA New Source Performance Standards. While evidence of substantial emissions reductions from these sources in both the northeast and the entire nation was reported as early as the late 1990s [*Themelis and Gregory*, 2002, *MA DEP*, 2002; *Themilis*, personal communication], the EPA standards did not apply to smaller combustors. Though significantly reduced since the early 1990s, municipal waste combustion may still account for a large percentage of the emission rate derived from atmospheric observations.

Another possible explanation for the disparity between the atmospheric and electric power inventory fluxes is that some anthropogenic source was underestimated in *EPA* [1997], or now accounts for a larger percentage of overall emissions than it did a decade ago. Still another possibility, supported by some preliminary field measurements, is that reactive Hg emitted by power plant combustion stacks is rapidly converted to elemental Hg shortly after release from the stack [*Edgerton et al.*, 2004]. To explore the issue, a future research endeavor should measure reactive Hg in addition to TGM. However, *Edgerton et al.* [2004] report speciation percentages of 20% at 10-25 km away from a combustion stack. If it is assumed that this measurement is representative of power plants in general, the reduction of speciation percentage (20%, rather than the 50% assumed in the discussion in Chapter 2), is still insufficient to explain the larger than expected difference in atmospheric and power sector inventory Hg emissions. This may lend further credence to the “missing source” argument, and certainly suggests that Hg emission from anthropogenic point sources are far more poorly characterized than previously thought.

3). As reported in Chapter 3, data from two field experiments showed that significant gradients in gaseous Hg concentrations exist in the upper soil profile (<20 cm) in background forest soils. Furthermore, gaseous Hg concentrations are strongly related to bound Hg content, and are highest within the upper organic soil layer, suggesting that bound Hg, which is possibly bound in turn to soil organic matter, is being actively desorbed and released into the soil pores. Soil Hg flux measurements were correlated with gaseous Hg concentrations at shallow depths (2 cm).

These findings may have significant implications for our understanding of the processes governing Hg emission from soils. It was once speculated that Hg emission from soil was a diffusive process that could be described using Fick's Law [e.g., *Zhang and Lindberg*, 1999]. However, recent studies have claimed that soil Hg flux is controlled purely by surface processes (e.g., changes in temperature, photochemical reactions, wind pumping) and not diffusion [*Johnson et al.*, 2003]. Among the main reasons for this claim are a lack of observed gradients in gaseous Hg within soil, or correlation between flux and gaseous Hg concentrations at depth in the soil profile, as is the case for other gases which whose flux from soil can be described by diffusion models (CO_2). The data presented here show that significant gradients in gaseous Hg do exist in the uppermost layers of background forest soil, and that soil Hg flux is correlated with gaseous Hg concentrations near the interface between the O-horizon and the litter layer (2 cm depth). The reason that other studies did not reveal these relationships may be that no sampling of gaseous Hg took place above 20-cm depth, and the most active layer in terms of gaseous Hg desorption was neglected.

Surface processes undoubtedly play a major role in the release of Hg from soil surfaces. This is underscored in this study by the correlation between soil Hg flux and soil and air temperature and solar radiation, and perhaps by the strong relationship between gaseous Hg concentrations and soil temperature observed at the Coventry forest site. However, results presented here indicate that the conclusion that the process is in no way diffusive is premature. The fine vertical resolution provided by the flask sampling system developed in this study reveals gradients in gaseous Hg over shallow soil layers along which gaseous Hg may move diffusively, and reveals relationships between flux and gaseous Hg concentrations at 2-cm. Future research may test the hypothesis that measurements at slightly more shallow depths, if they can be made without contamination from air above the soil, would yield stronger correlation with flux. This may improve modeling studies of soil Hg emission, which typically do not incorporate soil TGM gradients.

4). Hg emission from boreal forest fires plays a significant role in the Canadian Hg budget, typically amounting to nearly one-third of annual anthropogenic Hg emissions in Canada, and during years of intense fire activity, may equal or exceed anthropogenic emissions. This underscores the sporadic nature of biomass burning events in the boreal zone.

Most importantly, comparison of the Hg emission estimates from boreal forest fires in this study with the few published studies which measured Hg emission from biomass burning in situ [*Brunke et al.*, 2001; *Friedli et al.*, 2003] reveals significant differences in Hg emission factors from biomass burning across biomes or geographic regions. These differences in emission factor could be related to proximity to anthropogenic sources (much of the Hg volatilized from forest soil and biomass may have been deposited from anthropogenic sources) or differences in species composition. Therefore, using data from one particular burning event or biome to estimate global Hg emissions from biomass burning, which the aforementioned studies have done, is highly suspect. The large spatial variability in emission factors combined with the lack of measurements of Hg release from tropical grassland where most biomass burning takes place, reveals that previously published estimates of global Hg emission from biomass burning are likely inaccurate. Little understanding of the global contribution of this particular natural source of Hg can be known until extensive measurements yield a better understanding of changes in emission factors across biomes.

5). Understanding Hg emissions and deposition, as well as the global Hg budget in air, soil, water or vegetation is made considerably difficult by the volatility of Hg. A significant fraction of deposited Hg may be re-emitted to the atmosphere before it can be incorporated into soil, water etc. Also, Hg emitted from anthropogenic sources may be deposited to surfaces and then directly re-emitted. Therefore, the identification of certain sources as “natural” is misleading because, though physically or biologically controlled, the emitted Hg may ultimately be of anthropogenic origin [*Lindqvist and Rodhe*, 1985]. For instance, 50% or more of Hg emitted by natural forest fires (Chapter 4) is probably from forest soil [*Friedli et al.*, 2003], and an unknown percentage of that Hg, as well as the Hg on leaf surfaces, is doubtlessly of anthropogenic origin, even in remote ecosystems. In fact, “once mercury has been released into the atmosphere and has become incorporated into the biogeochemical cycle, its original source (whether natural or anthropogenic) can no longer be discerned" [*Schroeder and Munthe*, 1998]. This study may, at least on a regional scale, improve our understanding of the relative importance of anthropogenic and natural cycling to atmospheric and soil Hg budgets and lends further insight into the important role of power plant emissions in regional Hg cycling.

In Chapter 3, soil emission was presented as a "natural" source of Hg. However, it has been suggested that up to 80% of Hg that is deposited to soil is re-emitted to the atmosphere [*Grigal*, 2002]. Most or all of the Hg deposited to soils in an industrialized area such as the northeastern U.S. is likely from regional anthropogenic sources [e.g., *EPA*, 1997; *Landis et al.*, 2004]. According to modeling studies undertaken by *EPA* [1997], total Hg deposition throughout the northeast is approximately 10-20 $\mu g\ m^{-2}\ yr^{-1}$, or 27-54 $ng\ m^{-2}\ day^{-1}$. Soil Hg emissions at Coventry were, on average, 2.2 $ng\ m^{-2}\ hr^{-1}$; or, assuming 12 hours of emission per day (perhaps a conservative assumption during the summer[5], since slightly positive emissions were often measured before sunrise at Coventry, and deposition events were rare), approximately 27 $ng\ m^{-2}\ day^{-1}$. The possibility is therefore raised that, at least during the summertime when soil Hg fluxes are likely highest, the atmospheric sink of Hg from deposition in the northeast is roughly balanced by background soil emission. In addition, forest soil emission is likely on the order of 10-25% of total forest Hg emissions in the northeast during the summertime [*Lindberg et al.*, 1998; *Bash et al.*, 2004]. This raises the possibility that Hg emission from forested ecosystems may be greater than the depositional sink, so that these ecosystems may be net sources of Hg to the atmosphere in the northeast during most of

---

[5] Although soil Hg fluxes are likely decreased during wintertime due to cold temperatures and radiation intensity, significant Hg fluxes have been measured over background soils in the U.S during the winter [*Gabriel et al.*, 2005].

the year. Also, a soil emission rate that is roughly equal to the deposition rate raises questions of the degree to which Hg is sequestered in terrestrial surfaces in the northeast, especially since soil Hg content at Coventry suggests little long-term Hg loading from deposition (see Chapter 3). Future field studies in the northeast should seek to measure depositional inputs of Hg to background surfaces, as well as provide additional measurements of forest and background soil emissions which would help resolve such questions.

The electric power sector in the northeast contributes, on average, ~2 g Hg km^{-2} month^{-1} during the wintertime (see Chapter 2). Assuming constant emissions throughout the year (emissions may be somewhat higher during the summer based on coal consumption [*Blasing et al.*, 2005]), this is equivalent to ~24 μg Hg m^{-2} yr^{-1}. If it is assumed that at least 50% of power plant emissions are reactive Hg [e.g., *EPA*, 1997], then Hg emitted by power plants in the northeast deposits regionally at an approximate rate of 12 μg Hg m^{-2} yr^{-1}. This estimate falls within the range of total Hg deposition estimated by *EPA* [1997] and may suggest that the vast majority of deposited Hg in the northeast originates from power plant emissions. Therefore, power plants are not only of critical importance to regional, bulk emissions of Hg to the atmosphere (Chapter 2), but may be the by far the most important contributor towards actual loading of Hg to terrestrial and aquatic ecosystems in the northeast.

5.3. References

Bash, J.O., Miller, D.R., Meyer, T.H., and Bresnahan, P.A. (2004), Northeast United States and Southeast Canada natural mercury emissions estimated with a surface emission model, *Atmos. Env.*, 38, 5683-5692.

Blasing, T.J., C.T. Broniak, and G. Marland (2005), The annual cycle of fossil-fuel carbon dioxide emissions in the United States, *Tellus B*, 57, 107-115.

Brunke, E-G., Labuschagne, C., and Slemr, F. (2001), Gaseous mercury emissions from a fire in the Cape Peninsula, South Africa, during January 2000. *Geophys. Res. Lett.*, 28, 1483-1486.

Chu, P. and Porcella, D.B. (1995), Mercury stack emissions from U.S. electric utility power Plants, *Water Air Soil Poll*., 80, 135-144.

Edgerton, E.S., Hartsell, B.E., Jansen, J.J. (2004), Field observations of mercury partitioning in power plant plumes, Atmospheric Research & Analysis Inc., www.atmospheric-research.com.

EPA (United States Environmental Protection Agency) (1997), Mercury Study Report to Congress, www.epa.gov/mercury.html.

Friedli, H.F., Radke, L.F., Lu, J.Y., Banic, C.M., Leaitch, W.R., and McPherson, J.I. (2003), Mercury emissions from burning of biomass from temperate North American forests: laboratory and airborne measurements. *Atmos. Env.*, 37, 253-267.

Gabriel, M.C., Williamson, D.G., Brooks, S., Zhang, H., and Lindberg, S.E. (2005), Spatial variability of mercury emissions from soils in a southestern US urban environment, *Environ.Geol.*, 48, 955-964.

Grigal, D.F. (2002), Inputs and outputs of mercury from terrestrial watersheds: A review. *Environ. Rev.,* 10, 1-39.

Johnson, D.W., Benesh, J.A., Gustin, M.S., Schorran, D.S., Lindberg, S.E., and Coleman, J.S. (2003), Experimental evidence against diffusion control of Hg evasion from soils, *Sci. Tot. Env.*, 304, 175-184.

Landis, M., Keeler, G.J., Al-Wali, K.I., and Stevens, R.K. (2004), Divalent inorganic reactive gaseous mercury emissions from a mercury cell chlor-alkali plant and its impact on near-field atmospheric dry deposition, *Atmos. Env.*, 38, 613-622.

Lindberg, S.E., Hanson, P.J., Meyers, T.P., and Kim, K.-H. (1998), Air/surface exchange of mercury vapor over forests – The need for a reassessment of continental biogenic emissions. *Atmos. Env.*, 32, 895-908.

Lindqvist, O., and Rodhe, H. (1985), Atmospheric mercury – A review. *Tellus*, 37B, 136-159.

Massachusetts Department of Environmental Protection (MA DEP) (2002), Municipal Waste Combustor Facility and Trend Reports, www.mass.gov/dep/mwc/mwcfr.htm.

Schroeder, W.H., and Munthe, J. (1998), Atmospheric mercury – An overview, *Atmos. Env.*, 32, 809-822.

Themelis, N.J., and Gregory, A.F. (2002), Mercury emissions from high-temperature sources in the NY/NJ Hudson-Raritan basin, *Amer. Soc. Mech. Eng. Proc. NAWTEC* 10, pp. 205-215.

Wallschläger, D., Kock, H.H., Schroeder, W.H., Lindberg, S.E., Ebinghaus, and R., Wilkin, R.-D. (2002), Estimating gaseous mercury emission from contaminated floodplain soils to the atmosphere with simple field measurement techniques, *Water Air Soil Poll.*, 135, 39-54.

Wotawa, G., and Trainer, M. (2000), The influence of Canadian forest fires on pollutant concentrations in the United States, *Science*, 288, 324-328.

Zhang, H., and Lindberg, S.E. (1999), Processes influencing the emission of mercury from soils: A concep

Appendix I:

Description of design and laboratory testing of flask sampling system

The potential of direct flask sampling of soil gas for determination of soil Hg concentration was heretofore largely unexplored. A recent study suggested that direct sampling of soil air has potential for at least semiquantitative description of flux [*Wallschläger et al.*, 2002], and direct flask sampling has been successfully used to determine carbon dioxide (CO_2) concentrations in both air [e.g., *Ehleringer and Cook*, 1998] and at depth in soil [*de Jong and Schappert*, 1972; *Cerling et al.*, 1991; *Hersterberg and Seigenthaler*, 1991; *Wood et al.*, 1993; *Fang and Moncrieff*, 1998]. Such a technique may have important implications for quantification of soil gaseous Hg concentrations and our general understanding of soil Hg emissions by enabling detection of large Hg gradients within the soil without significant microenvironmental disturbance.

Chapter 3 was devoted to analysis of field application of a flask sampling apparatus for determining gaseous Hg at depth in soil. Here, the development and laboratory testing of the apparatus is described in more detail.

A1. Flask sampling system design

Several different soil gas sampling methods have been employed for CO_2. *Fang and Moncrieff* [1998] buried aluminum traps in soil with holes drilled into the cross-section. These holes were attached via nylon tubes to a pump at the surface. The pump was attached by a silicon plastic tube to a 3-way valve, providing a closed loop. Air was pumped through the tubes at a very low flow rate (30 cc min^{-1}) and sampled by inserting a syringe into the silicon tube after a 10-minute circulation period. Other methods employ a PVC pipe with holes drilled for gas exchange. This air-tight pipe is placed in the soil and can be accessed by plastic tubing capped at the surface with a septum, stopcock or other gastight fitting and gas samples are collected either by syringe extraction [*de Jong and Schappert*, 1972] or by pumping or diffusion after connecting glass or stainless steel containers (0.1-1 L) to the fitting [*Cerling et al.*, 1991; *Wood et al.*, 1993].

The flask collection setup developed in this study is shown in Figure A1. The air sample is collected in a 1 L Teflon flask equipped with three ports as well as a stainless steel pressure fixture to ensure air-tightness. The two outer ports are connected to PFA/PTFE stopcocks while a septum is placed in the central port. Air is drawn into one outer tube port through Teflon tubing (60 cm length, 0.32 cm inner diameter) connected to a Teflon funnel (6.4 cm diameter). Since a period of more than one week would be required for the TGM concentration in the flask to reach equilibrium by molecular diffusion alone, we shorten the collection period by promoting mass flow through the flask. We achieve this by attaching a low flow (450 cc min^{-1}) pump (model NMP05 minipump, KNF Inc.) to the second outer port via Teflon tubing. The pump flow is split by a T-junction connected to two flowmeters so that the actual flow out of the soil and through the flask is 20 cc min^{-1}. This flow is lower than that used for soil CO_2 in *Fang and Moncrieff* [1998] and should hasten the flushing without creating suction and drawing in ambient air from above the surface. To ensure that the flask is thoroughly flushed, air is collected over a 4-hour period, and is therefore cycled through the entire flask volume approximately five times.

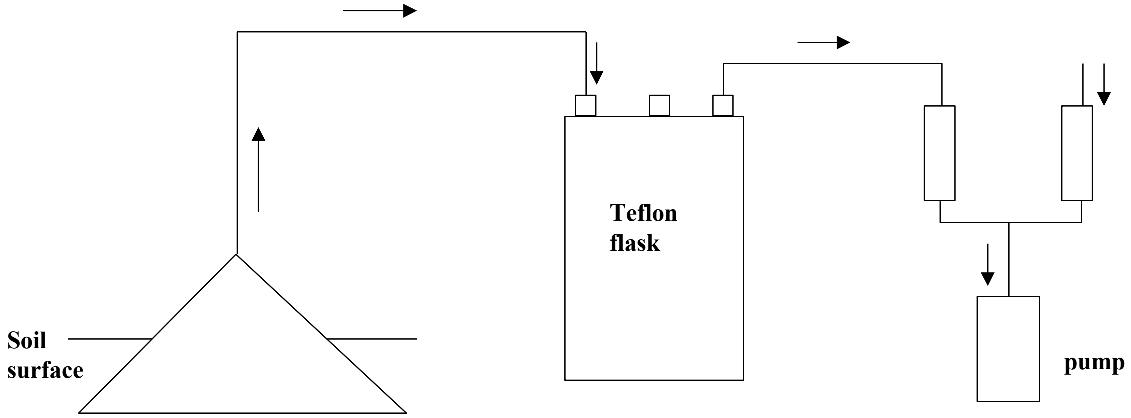

Figure A1: Schematic diagram of flask sampling design.

At the end of the 4-hour collection period, the stopcocks are closed and the tubing detached from the flask ports. The flask is then removed from the field to an instrument shelter, where it is connected to a mercury vapor analyzer (model 2537A, Tekran, Inc.) via a valve assembly (see Figure 3.1). The analyzer produces TGM concentrations integrated over five minutes. The valve assembly consists of three solenoid valves (Tekran, Inc.), each with three ports. The common ports on each valve, labeled as ‘c’ in Figure 3.1, ultimately connect the analyzer sample stream to a “zero” air canister by Teflon tubing. The zero air canister scrubs Hg from ambient air using an activated charcoal and iodine mesh. In the default mode (valves I-III not energized), the zero air by-passes the flask and enters the analyzer. When valve III is energized, the analyzer samples ambient air near the soil-air interface, and does so during the flask collection period. In order to analyze the TGM concentration inside the flask, the flask is first attached to ports 2 on valves I and II, and valve III is deactivated so that ambient air is no longer drawn into the analyzer. Valves I and II are then energized, the flask stopcocks are opened and the flask air is drawn into the analyzer using the zero air as carrier.

Even while sampling zero air, the analyzer will detect small blank, or baseline, levels of TGM (typically ≤ 0.1 ng m^{-3}). Accordingly, the flask should be flushed for three to four additional 5-minute cycles after the soil air sample is released into the analyzer, so that the blank concentration is determined. By recovering the blank, the sample concentration can be more accurately determined by subtracting the average blank from that of the detected sample concentration.

A2. Laboratory Tests

A2.1. Experimental procedure

Four laboratory experiments were conducted to test the reliability and accuracy of this system. The first experiment involved collection and recovery of zero air. The flask was connected to the valve assembly, flushed with zero air for 10-15 minutes, sealed with zero air trapped inside and sampled after a period of 2-12 hours. The second experiment involved collection and recovery of room air. The flask lid was opened for a period of 18-24 hours, allowing room air to enter by molecular diffusion, then sealed and sampled. The third experiment involved direct injection of known volumes of Hg vapor into the flask. A 50 μL syringe was used to draw known volumes (5 to 30 μL) of saturated Hg vapor from a bottle of pure liquid Hg placed in a water bath at a known temperature. The Hg vapor was injected through the septum in the central port of the flask. The mass of Hg in the injected sample was determined by multiplying the known concentration of the saturated Hg vapor by the syringe volume. The resultant concentration in the container is simply the injected mass divided by the analyzer sample volume of 7.5 L, noting that the analyzer produces 5-minute average concentrations at a flow rate of 1.5 L min^{-1}. This number must also be corrected for blank, as well as temperature and pressure since the analyzer samples at standard temperature and pressure (STP). For three of the injections, the flask was left sealed and undisturbed for 14, 19 and 24 hours before being attached to the valve assembly and sampled, testing for slow leakage. Since many injections were performed, the septum was periodically replaced in order to minimize contamination.

In the fourth experiment, the entire system (flask collection setup and valve assembly) was tested in the laboratory. Room air was pumped through the Teflon funnel and into the flask over a 4-hour period (Figure A1). At the same time, valve III was energized and room air TGM concentration was measured by the analyzer (see Figure 3.1). At the end of the collection period, the analyzer was switched to zero air (valve III energized) as the flask was attached. Several 5-minute cycles of zero air were obtained both before (see sudden drop in concentration in Figure A2) and after the flask air was sampled. The small spike in Figure A2 shows an apparent flask TGM concentration in ng m^{-3}. For meaningful comparison, this concentration was converted to a mass by multiplying by the analyzer sample volume (7.5 L), divided by the flask volume (1 L) and reconverted to ng m^{-3}. Unless desorption or absorption of Hg is occurring within the system, the converted flask concentration should equal the average room concentration during the collection period.

A3. Results

Average TGM concentrations recovered from the flask sample in the zero air tests were 0.05 ± 0.02 ng m^{-3} (number of observations = 4), not significantly different from those in standard, zero air samples whose concentrations were 0.02 ± 0.04 ng m^{-3}. When the separated flask was left undisturbed for a 12 hour period, the measured flask concentration (0.07 ng m^{-3}) was still representative of typical baseline concentrations (<0.1 ng m^{-3}). When the same test was performed with room air, TGM concentrations in

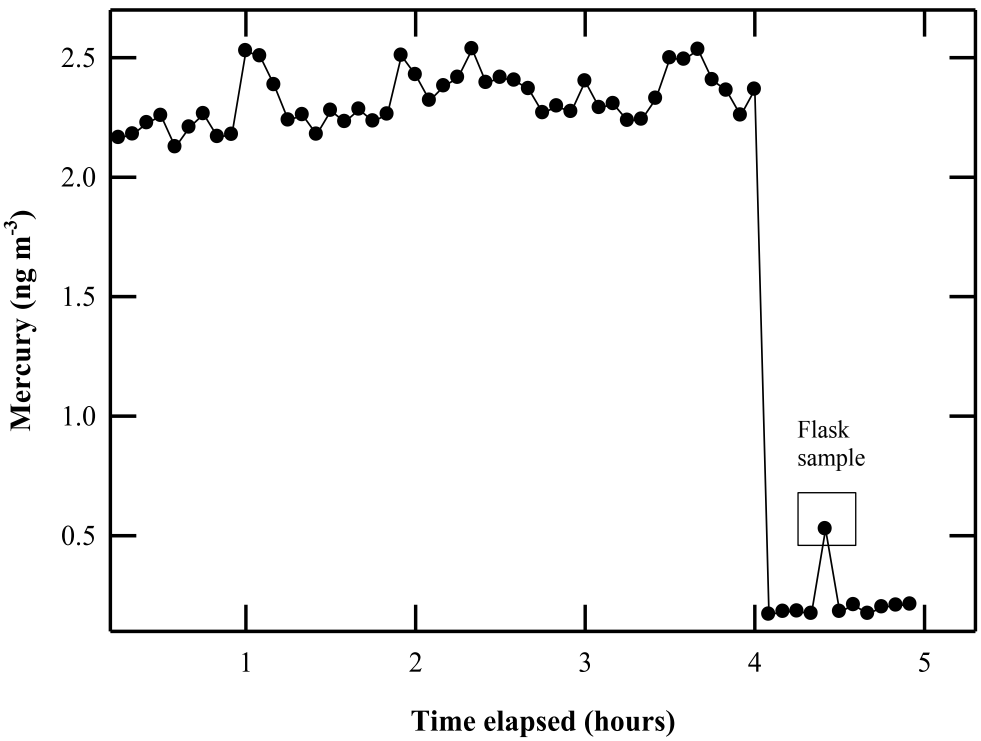

Figure A2: Example time series of the Hg analyzer output during a laboratory test. Room air TGM was measured over four hours and simultaneously pumped into the flask, which is analyzed at the end of the collection period. The sudden drop in Hg near the 4-hour mark indicates the manual switch from room to zero air. The small spike shortly after the switch indicates analysis of the flask sample.

the flask (2.09 ± 0.38 ng m^{-3}, n = 7) agreed with those of room air within 3% (2.15 ± 0.37 ng m^{-3}).

Results of the injection tests are shown in Figure A3. Over a total of 27 separate injections with concentrations ranging from 10 to 50 ng m^{-3}, strong correlation (R^2 = 0.97, $p<0.01$) between measured and injected TGM concentrations was achieved. Furthermore, no significant differences were observed when the flask was allowed to sit for 14 and 19 hours between injection and sampling (shown as open circles in Figure A3). One possible outlier (open circle farthest from the regression line in Figure A3) represents a 24-hour wait between injection and sampling and may suggest slow leakage from the container over time periods longer than 19 hours.

The results of the fourth laboratory experiment yielded generally good agreement between flask and direct sampling (see Figure 3.2). Two outliers are represented as open circles in Figure 3.2, one indicating under-recovery of TGM and the other indicating over-recovery. The latter case, which represents our first room air collection with the funnel setup (Figure A1), is explained by the use of a LDPE funnel, as a Teflon funnel was unavailable at that time (for all other collections, a Teflon funnel was used). The former case may be explained by the fact that the ambient concentration represents a 4-hour average and is biased high by unusually large room air concentrations early during the collection period. Use of the average concentration over the second half of the collection period (2.5 ng m^{-3}) would give a much better agreement.

The combined results of these four experiments support two important conclusions. First, neither the flask collection nor valve assembly experiences significant leakage over periods as long as 12 hours. A leak in the system would draw in room air

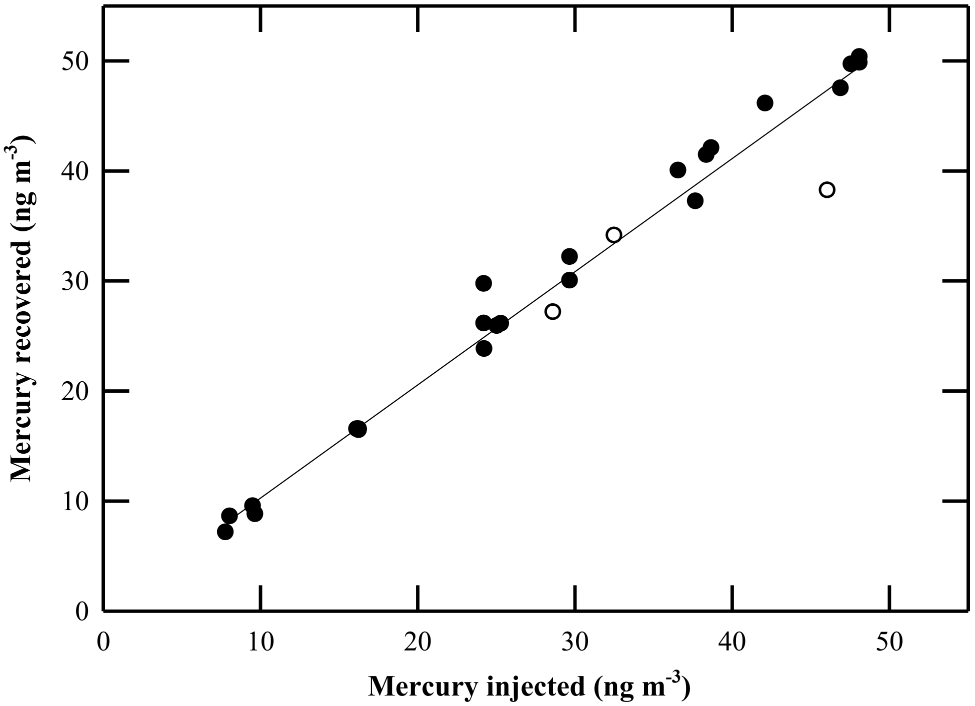

Figure A3: Comparison of recovered and injected mercury vapor in the flask. The solid line is the linear regression line ($y = 0.138 + 1.024x$; r = 0.99, $p<0.01$, $n = 27$). Open circles represent tests in which the sealed flask was allowed to sit undisturbed for 14-24 hours.

with TGM concentrations ~ 2.0 ng m^{-3}, resulting in a recovered concentration well above baseline in the zero air tests and well below the large concentrations considered in the injection experiment. Second, the system is able to accurately and fully recover known TGM concentrations. Results indicate no contamination within either the flask collection setup or valve assembly, or inability of the entire system to accurately analyze the air trapped within the flask. Taken together, these conclusions suggest that the system is not only robust for collecting and analyzing soil or ambient air samples in the field, but also creates the possibility of collecting a sample at a remote location and transporting it elsewhere within a 19-hour time frame for analysis.

A4. Field test

A collection of soil air was performed at Great Mountain Forest, a mixed coniferous/deciduous forest located near Norfolk, CT. [41°58′N, 73°14′W; *Lee and Hu*, 2002] on 3 June 2003. Soil temperature at 5-cm depth and ambient pressure at the site during the collection period were 15° C and 96 kPa, respectively. The funnel was installed in the litter/upper soil layer at a depth of 5 cm. The selection of this depth is arbitrary and there is no obvious limitation in terms of depth of funnel placement. Disturbed litter and soil were carefully repacked around the funnel. The flask was transported to the laboratory and sampled approximately two hours after the completion of the 4-hour collection period. The result of the analysis is shown in Figure A4, with the spike indicating an apparent TGM concentration of 1.04 ng m^{-3}. This concentration reduces to 0.88 ng m^{-3} when the baseline is subtracted. The baseline was determined as the average of the four data points following the flask sample in Figure A4. The system

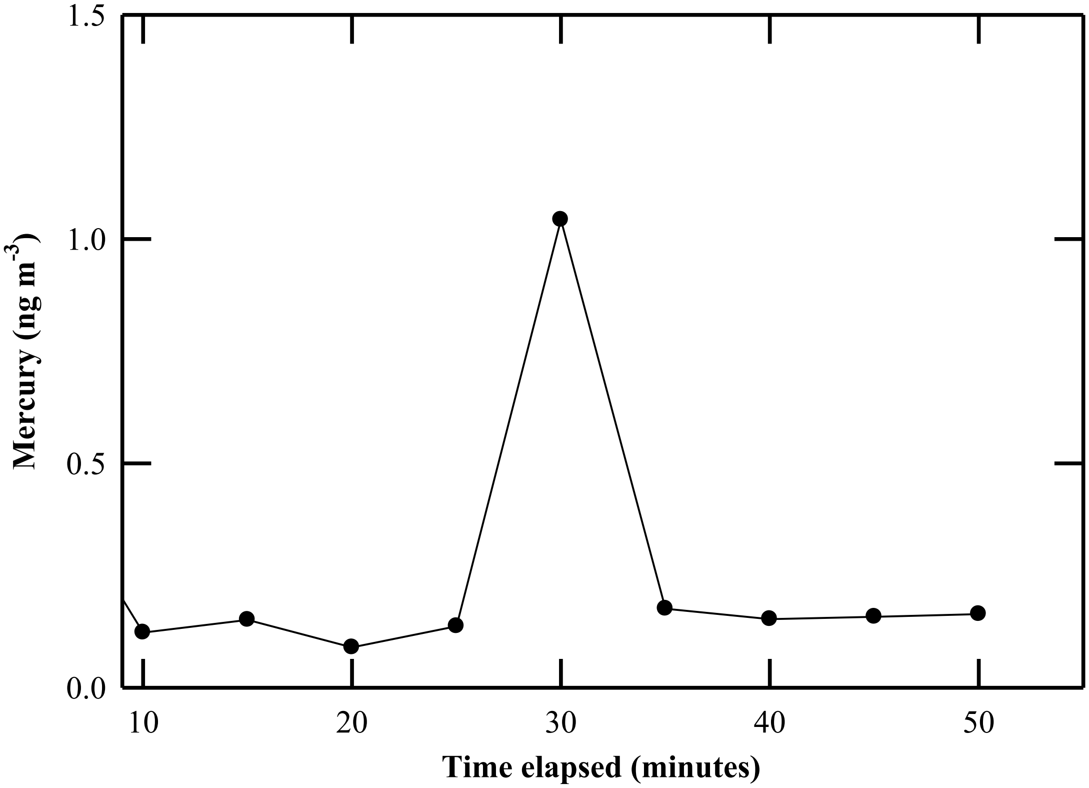

Figure A4: Time series of the Hg analyzer output during analysis of a soil air sample collected at Great Mountain. The spike at 30 minutes represents the flask air sample, and concentrations quickly return to baseline (blank) levels after one 5-minute flushing period.

clearly returns to baseline, or blank, levels after a single flushing of the flask. Accounting for the volume conversion and the STP correction, the flask yielded a soil TGM concentration of 5.95 ng m^{-3}, which was significantly higher than typical ambient concentrations (~2.0 ng m^{-3} [*Lee et al.*, 2001])

A5. Flow rate consideration

In a related study, *Wallschläger et al.* [2002] drew air directly via Teflon tubing (0.95 cm inner diameter) from the soil at 10 cm depth into their analyzer for analysis. They demonstrated a systematic dilution of measured soil TGM concentrations with increasing sample volume due to intrusion of ambient air under a very high pumping rate (1.5 L min^{-1}). In this design, the intrusion of ambient air is minimized by using a funnel with a large aperture and a small flow rate. The choice of the flow rate is based in part on the study of *Fang and Moncrieff* [1998], who showed that at a flow rate of 30 cc min^{-1}, the dilution effect on their soil CO_2 measurement was negligible. Additional guidance is found from theoretical studies of convective air motion in snow and soil [*Colbeck*, 1989; *Farrell et al.*, 1966]. These studies suggest that vertical air speed caused by wind pumping is in the range of 10^{-4} to 10^{-2} m s^{-1} in the top 10 cm soil. Air speed produced by the flask sampling should be smaller than this to minimize the artifact of ambient air intrusion. In this case, the vertical air speed across the funnel aperture is 9×10^{-5} m s^{-1}.

A6. Drawbacks

Preliminary field testing of the system indicates that a dry flask and zero air stream is desirable. Moist air within the flask or the valve assembly may result in high blanks and an inability to determine a flask TGM concentration significantly above baseline. This problem is minimized by operating in dry conditions as much as possible or by allowing the incoming air stream to pass through a container of Drierite before the zero air canister (Figure 3.1).

Another obvious drawback to the flask sampling system is its small temporal and spatial scales. Because of the long (>24 hours) time for equilibrium between soil and the funnel air space, frequent sampling is not desirable. Also, the system becomes more labor-intensive if multiple site or simultaneous depth collections are desired.

A7. References

Cerling, T.E., Solomon, D.K., Quade, J., and Bowman, J.R. (1991), On the isotopic composition of carbon in soil carbon dioxide, *Geochim. Cosmochim. Acta*, 55, 3402-3405.

Colbeck, S.C. (1989), Air movement in snow due to windpumping, *J. Glaciology*, 35, 209-213.

de Jong, E., and Schappert, H.J.V. (1972), Calculation of soil respiration and activity from CO_2 profiles in the soil, *Soil Science*, 113, 328-333.

Ehleringer, J.S., and Cook, C.S. (1998), Carbon and oxygen isotope ratios of ecosystem respiration along an Oregon conifer transect: preliminary observations based on small-flask sampling, *Tree Physiology*, 18, 513-519.

Fang, C., and Moncrieff, J.B. (1998), Simple and fast technique to measure CO_2 profiles in soil, *Soil Bio. Biochem.*, 30, 2107-2112.

Farrell, D.A., Graecen, E.L., and Gurr, C.G. (1966), Vapor transfer in soil due to air Turbulence, *Soil Science*, 102, 305-313.

Hersterberg, R., and Seigenthaler, U. (1991), Production and stable isotopic composition of CO_2 in a soil near Bern, Switzerland, *Tellus* 43B, 197-205.

Lee, X., Bullock, O.R., and Andres, R.J. (2001), Anthropogenic emission of mercury to the atmosphere in the northeast United States, *Geophys. Res. Lett.*, 28, 1231-1234.

Lee, X., and Hu, X. (2002), Forest-air fluxes of carbon, water and energy over non-flat Terrain, *Boundary-Layer Met.*, 103, 277-301.

Wallschläger, D., Kock, H.H., Schroeder, W.H., Lindberg, S.E., Ebinghaus, R., and Wilkin, R.-D. (2002), Estimating gaseous mercury emission from contaminated floodplain soils to the atmosphere with simple field measurement techniques, *Water Air Soil Poll.*, 135, 39-54.

Wood, B.D., Keller, C.K., and Johnstone, D.L. (1993), In situ measurement of microbial activity and controls on microbial CO_2 production in the unsaturated zone, *Water Resources Research*, 29, 647-659.

Appendix II:

Photos of flask sampling system

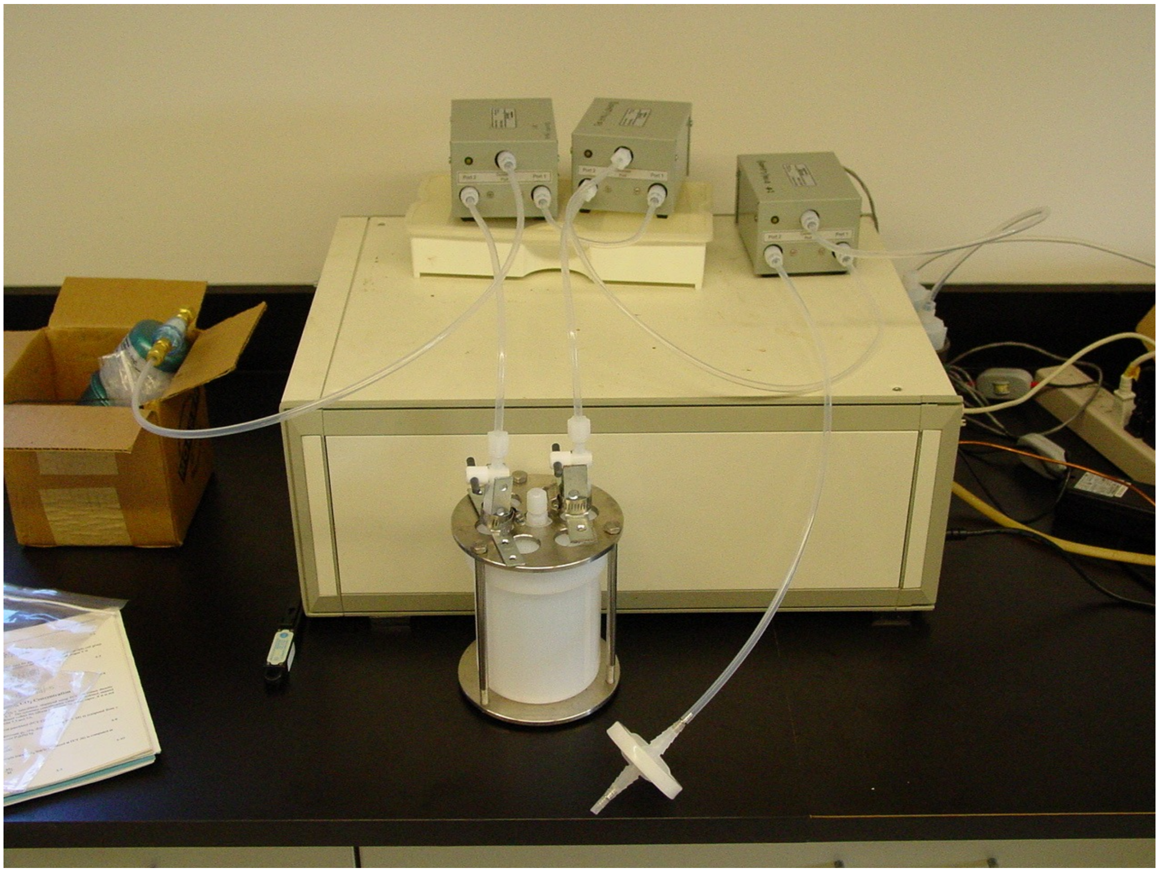

Figure A5: Flask sampling system in laboratory (represented in Figure 3.1).

Figure A6: Flask sampling system at Coventry forest site, central plot, August 2003 (as represented in Figure A1).

Figure A7: As in Figure A6.